

# UC Riverside

## UC Riverside Electronic Theses and Dissertations

### Title

Leveraging Zebrafish to Identify Chemicals Disrupting Early Embryonic Development

### Permalink

<https://escholarship.org/uc/item/22h2j1q8>

### Author

Vliet, Sara Michell

### Publication Date

2019

Peer reviewed|Thesis/dissertation

UNIVERSITY OF CALIFORNIA  
RIVERSIDE

Leveraging Zebrafish to Identify Chemicals Disrupting Early Embryonic Development

A Dissertation submitted in partial satisfaction  
of the requirements for the degree of

Doctor of Philosophy

in

Environmental Toxicology

by

Sara Michell Vliet

June 2019

Dissertation Committee:

Dr. David C. Volz, Chairperson

Dr. Daniel Schlenk

Dr. Prue Talbot

Copyright by  
Sara Michell Vliet  
2019

The Dissertation of Sara Michell Vliet is approved:

---

---

---

Committee Chairperson

University of California, Riverside

## **Acknowledgements**

The completion of this dissertation would not have been possible without the constant support of many people. First and foremost, my advisor, Dr. David Volz. During the past 4 years, Dr. Volz has been a constant source of guidance, mentorship, advice, and resources. He has endlessly supported my personal and professional goals and has provided me with the networking opportunities to achieve them. I will be forever grateful for the lessons he has taught me, the example he has set, and the knowledge he has shared. Without his time and effort, this dissertation would not be possible, and I would not be the scientist I am today. I would also like to thank my members that have served on my committee over the years for their support and advice; Dr. Daniel Schlenk, Dr. Prue Talbot, Dr. Nicole zur Nieden, Dr. Margarita Curras-Collazo, and Dr. David Eastmond.

There have been many past and present lab mates and collaborators who were essential in the completion of this dissertation. Dr. Luisa Becker Bertotto and Dr. Graciél Diamante were instrumental in making my transition to graduate school successful, training me in lab techniques, and patiently answering all of my questions. Trina Ho was instrumental in assisting with data analysis in Chapter 1. I would especially like to recognize Dr. Allison Kupsco, Dr. Subham Dasgupta, Constance Mitchell, Aalekhya Reddam, Victoria McGruer and Vanessa Cheng for the support they have provided me the past 4 years. Their friendship, advice, commiseration, and laughter has made our lab a collaborative and inviting place to work. Without them this truly would not have been possible.

Finally, I would like to acknowledge and thank my friends and family for their endless support during this journey. I have been incredibly lucky to have made many close friends during my time at UCR and I am grateful for their support, companionship, and the sense of family they have provided. I am forever grateful to my father, Donald, and sister, Chelsea, for endlessly supporting me in everything that I do, even though my pursuits have taken me far from home. I am also grateful for my parents-in-law, Brenda and LeRoy, as well as the entire Frie/Nohner family for their support. Finally, I would like to acknowledge my partner, Alex. His unwavering consistency and strength have never failed to lift me up, especially during the difficult times. I am incredibly grateful to have had him by my side during these past four years.

This research was supported by UCR's Graduate Division and the NRSA T32 Training Program (T32ES018827). Research support was provided by the USDA National Institute of Food and Agriculture Hatch Project (1009609) as well as a National Institutes of Health grant (R01ES027576). Funding for attendance to numerous conferences was provided by the UCR Graduate Student Association Travel Grants, Society of Toxicology Student Travel Award, Society of Environmental Toxicology and Chemistry North America Student Travel Award, The Teratology Society Student Travel Award, and the Federation of American Societies for Experimental Biology.

## Copyright Acknowledgements

The text and figures in Chapter 2, in part or in full, are a reprint of the material as it appears in “Behavioral screening of the LOPAC<sup>1280</sup> library in zebrafish embryos” published in *Toxicology and Applied Pharmacology*, Vol. 329, Pages 241-248, 2017. The co-author Trina C. Ho helped in setting up experiments and analyzing data. The co-author Dr. David Volz directed and supervised this research.

The text and figures in Chapter 3, in part or in full, are a reprint of the material as it appears in “Niclosamide Induces Epiboly Delay During Early Zebrafish Embryogenesis” published in *Toxicological Sciences*, Vol. 166, Issue 2, Pages 306-314, 2018. The co-author Dr. Subham Dasgupta helped in experimental design and data analysis and the co-author Dr. David Volz directed and supervised this research.

The text and figures in Chapter 4, in part or in full, are currently under review for publication as “Maternal-to-Zygotic Transition as a Potential Target for Niclosamide During Early Embryogenesis” in *Toxicology and Applied Pharmacology*. This work was submitted for publication on April 24<sup>th</sup>, 2019.

## **Dedication**

I would like to dedicate this dissertation to my father, Donald P. Vliet. Thank you for teaching me how to work hard, persevere through challenges, and keep my heart open to opportunities. All that I have accomplished, I owe to you.

## ABSTRACT OF THE DISSERTATION

Leveraging Zebrafish to Identify Chemicals Disrupting Early Embryonic Development

by

Sara Michell Vliet

Doctor of Philosophy, Graduate Program in Environmental Toxicology  
University of California, Riverside, June 2019  
Dr. David C. Volz, Chairperson

For many compounds currently used in commerce, there are minimal developmental toxicity data available. Additionally, current developmental toxicity testing guidelines require the use of rodents, making them expensive, time consuming, and inefficient to address existing data gaps. Therefore, alternatives to conventional animal testing – such as cell-free assays, cell-based assays, and non-protected stages of non-mammalian models – are needed to support the screening and prioritization of chemicals for developmental toxicity testing. Zebrafish offer one of the most promising alternative and cost-effective vertebrate models to support drug discovery and toxicity testing. Their small size, rapid development, and conservation of early developmental processes with mammals (including humans), make the zebrafish embryo an ideal model for the identification of compounds that disrupt the normal trajectory of early embryonic development. Therefore, the overall goal of this research is to leverage early, non-

protected life stages of zebrafish embryos to identify compounds that may be adversely impacting early development. For Aim 1, using high-content screening techniques, embryonic behavior was examined as a potential readout for detection of compounds adversely impacting the development and function of the nervous system. For Aim 2, the effects of niclosamide – a widely used anthelmintic that was identified from our high-content screen – on early embryonic development was assessed using a multipronged approach at multiple levels of biological organization. For Aim 3, based on our findings within Aim 2, the mechanism of niclosamide-induced developmental toxicity was further examined using a combination of whole-embryo assessments and human embryonic stem cell-based assays. Overall, our findings highlight the utility of embryonic zebrafish as a physiologically-intact, non-mammalian model for 1) rapid chemical screening and prioritization for developmental toxicity testing; 2) discovering biologically active yet understudied chemicals; and 3) investigating mechanisms of developmental toxicity.

## Table of Contents

### Chapter 1: Introduction

1.1 Toxicity Testing in the 21st century.....	1
1.2 Traditional Models of Toxicity Testing.....	5
1.3 The Use of Alternative Models in Toxicity Testing.....	7
1.4 Zebrafish as a Model for Toxicity Testing.....	10
1.5 Toxicity Tests Utilizing Zebrafish.....	11
1.6 Early Zebrafish Development: Zygote through Gastrulation.....	12
1.7 Zebrafish Neurodevelopment: Segmentation.....	14
1.8 Overview of Research Aims & Hypotheses.....	16

### Chapter 2: Behavioral Screening of Chemical Toxicity in Zebrafish Embryos

2.0 Abstract.....	18
2.1 Introduction.....	19
2.2 Materials and Methods.....	22
2.3 Results.....	27
2.2.1 Assay Variability.....	27
2.3.2 Assay Reproducibility.....	29
2.3.3 LOPAC <sup>1280</sup> Library Screen.....	32
2.3.4 Data Mining.....	35
2.4 Discussion.....	39

### **Chapter 3: Early Developmental Toxicity of Niclosamide in Zebrafish Embryos**

3.0 Abstract.....	46
3.1 Introduction.....	47
3.2 Materials and Methods.....	49
3.3 Results.....	56
3.3.1 Epiboly Progression.....	56
3.3.2 Oxygen Consumption.....	60
3.3.3 ATP Pre-Treatment Assay.....	61
3.3.4 mRNA-Sequencing and Differential Gene Expression.....	62
3.3.5 mRNA-Sequencing and the Maternal-to-Zygotic Transition.....	64
3.3.6 In-Vitro Tubulin Polymerization Assay.....	66
3.4 Discussion.....	67

### **Chapter 4: Potential Mechanism of Niclosamide Toxicity During Embryogenesis**

4.0 Abstract.....	71
4.1 Introduction.....	72
4.2 Materials and Methods.....	74
4.3 Results.....	82
4.3.1 Embryonic Yolk Sac Integrity, Cell Area, and Actin Networks.....	82
4.3.2 Human Embryonic Stem Cells.....	83
4.3.3 Whole-Embryo Metabolomics.....	83

4.3.4 Whole-Embryo mRNA Sequencing.....89  
4.3.5 Ribosomal and Transfer RNA.....91  
4.4 Discussion .....92

**Chapter 5: Conclusions**

5.0 Summary.....98  
5.1 Behavioral Screening in Embryonic Zebrafish.....99  
5.2 Niclosamide as a Potential Developmental Toxicant.....102  
5.3 The Embryonic Zebrafish Model: Further Directions and Considerations...108

**References.....111**

## List of Figures

### *Chapter 2*

Figure 1: Decision Tree for Behavioral Screening of the LOPAC <sup>1280</sup> library .....	26
Figure 2: High-Content Behavioral Screen: Temperature Variability.....	28
Figure 3: High-Content Behavioral Screen: Assay Variability.....	30
Figure 4: High-Content Behavioral Screen: Assay Reproducibility.....	31
Figure 5: High-Content Behavioral Screen: Positive Control.....	32
Figure 6: LOPAC <sup>1280</sup> Library Screen: Overview of Results. ....	34
Figure 7: LOPAC <sup>1280</sup> Library Screen: Tier I and Tier II Hits.....	35
Figure 8: LOPAC <sup>1280</sup> Library Screen: Results by LogP and Molecular Weight .....	37
Figure 9: LOPAC <sup>1280</sup> Library Screen: Results by Structure Clustering .....	38

### *Chapter 3*

Figure 10: Structure of Niclosamide.....	47
Figure 11: Niclosamide Induces Epiboly Delay.....	57
Figure 12: Niclosamide Recovery and Window of Sensitivity.....	58
Figure 13: Niclosamide Exposure and 24 hpf Body Area.....	59
Figure 14: Niclosamide Exposure and Oxygen Consumption.....	60
Figure 15: Niclosamide Exposure and ATP Pre-treatment.....	61
Figure 16: Niclosamide Exposure and Differential Gene Expression.....	63
Figure 17: Niclosamide Exposure and the Maternal-to-Zygotic Transition.....	64
Figure 18: Niclosamide Exposure and Tubulin Dynamics.....	66

*Chapter 4*

Figure 19: Niclosamide Exposure and Actin Dynamics.....84

Figure 20: Niclosamide Exposure and Human Embryonic Stem Cells.....85

Figure 21: Niclosamide Exposure and Non-Polar Metabolomics.....86

Figure 22: Niclosamide Exposure and Polar Metabolomics.....87

Figure 23: Niclosamide Exposure and the aminoacyl-tRNA pathway.....88

Figure 24: Niclosamide Exposure and Stage-Matched Transcriptomics.....89

Figure 25: Niclosamide Exposure and Stage-Matched Processes and Pathways.....90

Figure 26: Niclosamide Exposure, tRNA, and rRNA.....91

*Chapter 5*

Figure 27: Hypothesized Adverse Outcome Pathway for Niclosamide.....104

Figure 28: Current Hypothesis: A Conceptual Diagram.....105

Figure 29: Comparative timelines of zebrafish and human embryogenesis.....107

## List of Acronyms

2D-	Two-Dimensional
3D-	Three-Dimensional
AARS-	Aminoacyl tRNA Synthase
ADME-	Absorption, Distribution, Metabolism, Excretion
ANOVA-	Analysis of Variance
AOP-	Adverse Outcome Pathway
ATP-	Adenosine Triphosphate
CDER-	Center for Drug Evaluation and Research
CM-	Cell Mass
CNS-	Central Nervous System
CV-	Coefficient of Variation
DAPI-	4',6-diamidino-2-phenylindole
DAVID-	Database for Annotation, Visualization and Integrated Discovery
DMSO-	Dimethyl Sulfoxide
eGFP-	Enhanced Green Fluorescent Protein
EM-	Embryo Media
EPA-	Environmental Protection Agency
EU-	European Union
EVL-	Enveloping Layer
FDA-	Food and Drug Administration
FIFRA-	Federal Insecticide, Fungicide, and Rodenticide Act

FITC-	Fluorescein Isothiocyanate
GDP-	Guanosine Diphosphate
GLM-	General Linear Model
GTP-	Guanosine Triphosphate
h-	Hour
HCS-	High-Content Screening
hESC-	Human Embryonic Stem Cell
hpf-	Hours Post-Fertilization
HTS-	High-Throughput Screening
IPA-	Ingenuity Pathway Analysis
IND-	Investigational New Drug Process
IXM-	ImageExpress Micro
KEGG-	Kyoto Encyclopedia of Genes and Genomes
LogP-	Partition Coefficient
LOPAC <sup>1280</sup> -	Library of 1,280 Pharmacologically Active Compounds
LSCA-	Lautenberg Chemical Safety Act
Lyso-PC-	Lysophosphatidylcholine
MALDI -	Matrix-Assisted Laser Desorption Ionization
MIE-	Molecular Initiating Event
min-	Minute
mRNA-	Messenger Ribonucleic Acid
MS/MS-	Tandem Mass Spectrometry

MSI-	Mass Spectrometry Imaging
MTT-	4,5-dimethylthiazol-2-yl)-2,5-diphenyltetrazolium bromide
MZT-	Maternal-to-Zygotic Transition
NCBI-	National Center for Biotechnology Information
OXPHOS-	Oxidative Phosphorylation
PBS-	Phosphate Buffered Saline
PC-	Phosphatidylcholine
PMR-	Photomotor Response Assay
RNA-	Ribonucleic Acid
rpm-	Rotation Per Minute
rRNA-	Ribosomal Ribonucleic Acid
TG-	Triglyceride
tRNA-	Transfer Ribonucleic Acid
TSCA-	Toxic Substance Control Act
VC-	Vehicle Control
vs-	Versus
YS-	Yolk Sac
YSL-	Yolk Syncytial Layer

## **Chapter 1: Introduction**

### *1.1 Toxicity Testing in the 21<sup>st</sup> Century*

Globally, there are thousands of industrial chemicals produced and used every day. These include basic chemicals such as petrochemicals, specialty chemicals such as pesticides and paints, and consumer chemicals such as detergents, perfumes, and soaps (European Chemical Industry Council, 2018). As of 2017, global chemical turnover was valued at nearly \$4 trillion dollars, 4.6 times larger than 2016. Among this global market, China is by far the largest producer, contributing over 37% to the global market share. Aside from China, the European Union (EU) and North America – coming in second and third, respectively – make up 29% of the global market share combined (European Chemical Industry Council, 2018). The current distribution is in sharp contrast to chemical sales a decade ago (2007), where the EU and North America comprised 51% of the global share. These statistics demonstrate the shift in chemical markets to China and emerging economies, a trend that is expected to continue in years to come (European Chemical Industry Council, 2018).

In the United States, chemicals are regulated depending on their use. For example, the Toxic Substance Control Act (TSCA) regulates the production, use, and disposal of industrial chemicals, the Federal Insecticide, Fungicide, and Rodenticide Act (FIFRA) regulates the registration, distribution, sale, and use of pesticides (US EPA, 2013a, 2013b), and the Food and Drug Administration (FDA) regulates the safety, efficacy and security of human and veterinary drugs, biological products, medical devices, food supply, cosmetics, and products that emit radiation (FDA, 2018). Given that pesticides and drugs are designed

to be biologically active and cause harm to insects, plants or other living things, the requirements for FIFRA-based pesticide registrations and FDA-based drug registrations are generally much stricter than TSCA-based registration of industrial chemicals.

FIFRA was first enacted in 1947 and requires registering with the U.S. Environmental Protection Agency (EPA) (US EPA, 2013a). Prior to registering a pesticide, the registrant must demonstrate that using the pesticide according to the label “will not generally cause unreasonable adverse effects on the environment.” The EPA defines this as not having “any unreasonable risk to man or the environment, considering the economic, social, and environmental costs and benefits of the use of any pesticide” or “any human dietary risk from residues that result from use of a pesticide in or on any food”. Generally, this requires the registrant to conduct many studies to assess the safety of the chemical that often require a high number of animals, typically rodents, and are generally time-consuming and costly to perform (US EPA, 2013c). Since its establishment, FIFRA regulations have undergone many amendments to help strengthen FIFRA enforcement, broaden the legal emphasis, and extend their scope to cover intrastate regulations. Pesticides that have been registered for use under FIFRA are under continuous review by the EPA and go through a re-registration process every 15 years. This ensures that, if new concerns are raised based on the current state of the science, the pesticide will get reevaluated for use based on best available data and methods (US EPA, 2013a).

Within the FDA, the Center for Drug Evaluation and Research (CDER) is responsible for reviewing all data to ensure that a drug’s benefits outweigh any potential risks to the population (FDA, 2018). During the drug development processes, potential

drug candidates first undergo extensive research to determine parameters including; chemical ADME (Adsorption, Distribution, Metabolism, and Excretion), potential benefits and mechanisms of action, routes of exposure, dose levels, potential drug interactions, and potential side effects. Next, several pre-clinical toxicity studies are conducted in cell-free, cell-based, and animal models to provide detailed information on compound dosing, toxicity levels, and to determine if a given drug candidate is eligible for clinical trials within human subjects (FDA, 2015). Comprehensive in nature, these pre-clinical studies include single- and repeated-dose toxicity tests, immunotoxicity testing, genetic toxicity testing, and a general pharmacological evaluation (Center For Drug Evaluation and Research, 1997). If successful within pre-clinical trials, the compound will proceed into the Investigational New Drug Process (IND) and move towards human testing. Overall, the FDA regulatory processes ensure that drug candidates entering the market do not pose an unacceptable risk to human populations.

TSCA was written in 1976 and, at the time of its enactment, approximately 62,000 chemicals currently used in commerce were “grandfathered” in under this law. Under TSCA, these chemicals can remain in commerce unless the EPA is able to demonstrate an unreasonable risk. Chemicals regulated under TSCA that have been introduced into commerce for the first time after the act was passed, or existing chemicals that are being registered for a new use, require the manufacturer to test the chemical and determine whether the chemical poses a human or environmental health risk. Despite These requirements of the manufacturer, TSCA regulations do not require any specific toxicity testing requirements (Locke and Bruce Myers, 2010; US EPA, 2013b). Therefore, unlike

pesticides, even today most chemicals on the TSCA inventory have not been assessed for potential health and/or environmental impacts.

The continued rise in chemical production and the global redistribution of the market creates concern regarding the minimal safety data available for most compounds regulated under TSCA, as this data gap makes assessing the risk of these chemicals on human health and the environment impossible. In response to this concern, the Frank R. Lautenberg Chemical Safety for the 21<sup>st</sup> Century Act (LSCA) was passed in June 2016 following years of negotiation and input from industry, environment, public health, animal rights, and labor groups (US EPA, 2016). This law amends TSCA and includes improvements that require the EPA to evaluate existing chemicals with clear and enforceable deadlines, generate new risk-based safety standards, increase public transparency for chemical information, and provide a consistent source of funding for EPA to carry out these new responsibilities (US EPA, 2016). Although LSCA provides the structure necessary for TSCA reform, the reality of generating toxicity data for the approximately 85,000 chemicals currently regulated under TSCA will prove challenging, in part, due to limitations associated with the traditional toxicity methods used under FIFRA. In addition to these challenges, LSCA specifies that, when new toxicity data are needed for chemicals and mixtures, efforts should be made to “reduce and replace, to the extent practicable, scientifically justified, and consistent with the policies of this title, the use of vertebrate animals”. Given this language, it is clear that alternative toxicity testing and prioritization methods are increasingly necessary (US EPA, 2015a, 2016).

Since the passing of LSCA in 2016, the EPA has made progress on moving forward with TSCA reform implementation. In 2017, the EPA published a list of 10 chemicals that it was prioritizing for risk evaluations and has taken steps to complete the evaluation within a 3-5 year timespan (US EPA, 2017). Additionally, in June of 2017, the EPA established its “Procedures for Chemical Risk Evaluation Under the Amended Toxic Substances Control Act” as a guideline for prioritizing chemical substances for risk evaluation and determining if a chemical substance presents an unreasonable risk to human health or the environment. Although this guideline did not include costs or other non-scientific factors, it did incorporate the best-available science and relied on a weight-of evidence approach to determine chemical risk. As highlighted in a 2018 report, EPA is continuing to make steady progress in meeting the requirements of LSCA. Most notably, the EPA prioritized at 20 Low-Priority and 20 High-Priority candidates by the end of 2018 and completed a report to the United States Congress detailing the resources necessary to conduct risk evaluations. Moving forward, the EPA intends to designate 20 substances as Low-Priority and start risk evaluations on 20 High-Priority substances by December 2019 (US EPA, 2018).

### *1.2 Traditional Models of Toxicity Testing*

As mentioned in Section 1.1, much of toxicology currently relies on traditional whole-animal experiments, which are well accepted by the regulatory community. Although animal models can be useful in predicting human health effects and elucidating chemical mode-of-action, these models are not always the best choice for several reasons.

For chemicals regulated under FIFRA and TSCA, EPA toxicity testing guidelines for the identification of potentially toxic chemicals includes tests for acute toxicity, sub-chronic toxicity, chronic toxicity, genetic toxicity, neurotoxicity, and several special studies (US EPA, 2015b). Most of these tests specify the use of rodents, mice, or other mammalian models such as rabbits. These traditional testing strategies typically require a high number of animals (generally rodents) and are time-consuming to perform. In 2009 alone, the estimated number of animals used for experiments was over 1.1 million (Rusche, 2003).

From the perspective of the chemical manufacturer or registrant, whole-animal toxicity testing is also very costly to perform. In addition to the cost of the animal itself, study costs include manpower and space for animal housing and care. For example, a sub-chronic neurotoxicity study lasts for 90 days, requires 20 animals per treatment, and can cost up to \$280,000 per study (CEHTRA, 2012). For assessing developmental and reproductive toxicity, the limitations of mammalian models become magnified due to the long study duration required. For example, a reproductive and developmental toxicity study in rats is conducted for approximately 54 days, with chemical dosing occurring during 14 days of mating, 22 days of gestation, and 4 days of lactation. The high animal use associated with toxicity testing studies such as this has raised concerns among the public, animal rights groups, and various stakeholders.

Aside from the cost, study duration, and animal use, many additional uncertainties exist regarding the use of traditional whole-animal toxicity testing. Although it is commonly believed that mammalian systems are more like humans in terms of biological processes and genetic similarity, this is not necessarily true across all mammalian models.

The availability of different rodent strains with differing sensitivity to chemical exposures is a clear example of this. Therefore, regardless of species and strain, any toxicity study will be biased, in some way, towards a specific genetic background that may not be an accurate representation of a chemical's human hazard.

### *1.3 The Use of Alternative Models in Toxicity Testing*

As discussed above, the use of mammalian models for drug discovery and toxicity testing is costly, time-intensive, and requires millions of dollars per chemical (Kuhlmann, 1999, 2000; Zon and Peterson, 2005). Moreover, ethical concerns regarding high animal use have accelerated the development of alternative testing methods to reduce, refine, and ultimately replace animal use for chemical testing (Arora et al., 2011; Bal-Price et al., 2012; Crofton et al., 2011; National Academies Press, 2007; Richmond, 2002; Zon and Peterson, 2005). In response to the growing need for alternative testing methods to efficiently assess chemical toxicity, high-throughput screening (HTS) and high-content screening (HCS) assays have been developed over the last decade to screen more chemicals at a lower cost within a shorter period of time (Möller and Slack, 2010; Persson and Hornberg, 2016; Zhu et al., 2014). The vast majority of HTS and HCS assays used for drug discovery and toxicity testing utilize cell-free and cell-based methods that model key biological events across a wide range of pharmacologically- or toxicologically-relevant pathways (Fernandes et al., 2009; Zanella et al., 2010; Zhu et al., 2014). However, since these assays do not adequately reflect the complex physiology of an intact organism, the use of smaller, alternative non-mammalian animal models have been proposed as complementary models, as these models

are (1) suitable for high-content and high-throughput applications and (2) not protected by animal use regulations around the world (Coecke et al., 2007; Crofton et al., 2012).

Computational (or *in silico*) methods of evaluating chemical toxicity use computational resources to manage, visualize, simulate, and detect patterns and interactions in large biological and chemical data sets with the goal of predicting the toxicity of chemicals and their biological mechanism of action (Goodarzi, 2012; Rusyn and Daston, 2010; Wambaugh et al., 2018). *In silico* toxicology encompasses a wide variety of computational tools including chemical information databases, software, simulation tools, and modeling methods. These methods typically complement *in vitro* and *in vivo* toxicity tests and help improve toxicity prediction while minimizing the need for animal testing and reduce the cost and time of toxicity tests (Raies and Bajic, 2016). In addition, *in silico* methods are able, in theory, to estimate the toxicity of a compound before any exposure has occurred. Currently, many systems are available within online servers or as standalone applications for predicting and visualizing chemical toxicity (Raies and Bajic, 2016).

Cell culture is a technique used across many scientific disciplines and cell-based assays provide another alternative strategy to support drug discovery and toxicity testing (Jedrzejczak-Silicka, 2017; Rossini and Hartung, 2012; van Vliet, 2011). Cell-based models typically consist of a monolayer of cells grown in media and provide a means of examining morphological and biochemical signaling processes while avoiding many of the limitations of animal models. Cell-based imaging techniques can be combined with HTS and HCS assays, rapidly increasing the evaluation of compounds (Jedrzejczak-Silicka, 2017). Despite these advantages, cell-based assays are limited in their ability to predict

human toxicity, as the identity and behavior of cells is dependent on neighboring cells, molecular pathways, and biological processes occurring within the entire organism. Primary cell cultures isolated from either animal or human tissues represent the best attempt at recapitulating biological complexity and normal biology within a monolayer. These cell cultures can consist of mixed cell populations and are ideal for mechanistic studies. In addition, studies using human cells can avoid any species-specific differences in toxicity (van Vliet, 2011).

Emerging organ-on-a-chip models represent an *in vitro* model that is, theoretically, one step closer to the complexity of a whole-animal model. These methods attempt to narrow the gap between cell-based assays and animal models by growing cells within a three-dimensional (3D) structure. These models can be achieved by either culturing cells on specially-treated surface, or by using scaffolding to promote cell adherence and are designed to most accurately mimic the biochemistry that occurs within tissues by capturing cell-to-cell interactions (Jedrzejczak-Silicka, 2017; Pampaloni and Stelzer, 2010). These models are particularly useful in examining tumor growth, cell migration, and understanding drug efficacy and compound toxicity within single tissues (Jedrzejczak-Silicka, 2017). Taking this one step further, multi-organ-on-a-chip (MOC) models are designed to recapitulate interactions between organs and provide a means for assessing compound uptake, metabolism, and excretion (Bovard et al., 2017; Low and Tagle, 2017).

Despite the rapid advances in cell culture technology, no existing *in vitro* method can accurately capture the complexity of an intact organism and the complex interactions that lead to toxic responses. For this reason, non-mammalian animal models have become

a popular alternative. Non-mammalian models often share a high degree of genetic, biochemical, and physiological similarity to humans, and models such as *Drosophila*, *Caenorhabditis elegans*, *Xenopus*, and zebrafish (*Danio rerio*) have been shown to be useful models for understanding the biological targets of many compounds (Crofton et al., 2011; Peterson et al., 2008; Zon and Peterson, 2005). The use of alternative non-mammalian models provides an intact organism, that, in many cases, is amenable to HCS/HTS technologies and provides a means of addressing the high volume of chemicals currently lacking toxicity data (Crofton et al., 2011).

#### *1.4 Zebrafish as a Model for Toxicity Testing*

Zebrafish offer one of the most promising alternative and cost-effective vertebrate models to support drug discovery and toxicity testing. The use of zebrafish for research began when it was discovered that the zebrafish is highly suited to large-scale genetic screens due to their transparent *ex utero* development, high fecundity, and relatively simple husbandry (Grunwald and Eisen, 2002; Wolpert et al., 2015; Zon and Peterson, 2005). Soon after, the use of zebrafish for examining the function and structure of the nervous system became popular (Grunwald and Eisen, 2002). Over the last 15 years, the use of the zebrafish for research has grown rapidly and it has become an important model for studying some human genetic diseases (Wolpert et al., 2015). Beyond its use in genetics, zebrafish has become an important model within the field of toxicology, as it is well suited to HCS/HTS phenotypic screens (Zon and Peterson, 2005). By using zebrafish, efficiently assessing the toxicity of many compounds becomes a reality and, while their use does not

eliminate the need for mammalian testing, they do provide a means to prioritize compounds for further evaluation and ultimately reduce mammals used for safety testing.

### *1.5 Toxicity Tests Utilizing Zebrafish*

In recent decades, a repertoire of zebrafish-based assays for chemical screening and toxicity testing across multiple life-stages has been developed (Bang et al., 2002; Brockerhoff et al., 1995; Egan et al., 2009; Kokel et al., 2010; MacRae and Peterson, 2015; Persson and Hornberg, 2016; Zon and Peterson, 2005). Although a handful of studies have leveraged adult stages of zebrafish, the majority of zebrafish assays rely on larval and embryonic stages due to the extensive understanding of zebrafish genetics and developmental biology (Hill, 2005). Zebrafish embryos have been used extensively to study cardiotoxicity following drug exposure (Zakaria et al., 2018) or developmental alterations following exposure to chemically diverse environmental agents such as flame retardants (McGee et al., 2012), nanoparticles (K. Nasrallah et al., 2018), and dioxin (King-Heiden et al., 2012).

High-throughput phenotypic screens using zebrafish for small molecule discovery have been well received and have contributed significantly toward phenotype-based discovery of novel drug candidates (Zon and Peterson, 2005). More recently, this approach has also been applied to the development of whole-embryo, high-throughput behavioral screens to detect potential neurotoxicants (Peterson et al., 2008). For example, the photomotor response assay (PMR) uses an automated platform to analyze the effect of small molecules on behavioral responses in embryonic zebrafish. Using a high-intensity light stimulus to induce a series of stereotyped behaviors in embryonic zebrafish, the effect

of chemical exposure can be identified by assessing behavioral changes (Kokel et al., 2010). At the time of publication (2010), hundreds of behavior-modifying compounds had been discovered by the PMR, and the assay has received a great deal of interest among sectors. In addition to the complex “behavioral barcodes” induced by stimulated behavior, other assays leveraging non-stimulated behavioral responses have also been developed (Raftery et al., 2014).

#### *1.6 Early Zebrafish Development: Zygote through Gastrulation*

Zebrafish embryogenesis occurs rapidly, *ex utero*, and consists of seven distinct developmental stages: zygote (0-0.75 hours post fertilization, hpf), cleavage (0.75-2.25 hpf), blastula (2.25-5.25 hpf), gastrula (5.25-10 hpf), segmentation (10-24 hpf), pharyngula (24-48 hpf), and hatching (48-72 hpf) (Kimmel et al., 1995). When zebrafish eggs are laid, they consist of mixed cytoplasm and yolk surrounded by a chorion. Upon fertilization, when the sperm enters the egg through a single site located at the animal pole, the cytoplasm begins to separate from the yolk and stream towards the animal pole. At ~0.5 hpf, the zygote consists of a cytoplasmic blastodisc located on top of the large yolk mass (Kimmel et al., 1995; Solnica-Krezel, 2002).

At ~0.75 hpf, the zygote cytoplasm undergoes its first cleavage event, forming a two-cell embryo and entering the cleavage stage of development. The cleavage stage encompasses six cell divisions that occur synchronously. Early in cleavage, the cells are connected to the yolk through cytoplasmic bridges and the first cleavage events are vertical, until the end of the sixth cleavage event (~2 hpf) when the cells arrange horizontally

(Kimmel et al., 1995). Following the final cleavage cycle, the embryo consists of 64 cells present in a mound on top of the yolk sac.

The blastula stage of zebrafish embryogenesis begins at the 128-cell stage and continues until the onset of gastrulation. This period consists of continued cell division as well as the initiation of many important developmental events. Shortly after the beginning of the blastula stage (~3 hpf), the maternal-to-zygotic transition (MZT) commences. During the MZT, a suite of biological changes occur in the embryo including the activation of the zygotic genome, degradation of maternally-loaded mRNA transcripts, initiation of cell motility, and introduction of S and Gap phases to the cell cycle (Kane and Adams, 2002; Kimmel et al., 1995; Langley et al., 2014). The MZT also marks the loss of cell division synchronicity, has been shown to be required for the embryo to move into gastrulation, and coincides with the first appearance of different cell lineages resulting in three distinct cell types (Kane and Adams, 2002; Solnica-Krezel, 2002). At the onset of the MZT, the embryo consists of a blastoderm, or mass of cells sitting on top of the yolk sac. The cells present on the outside surface of the blastoderm form the enveloping layer (EVL), while the cell layer present between the blastoderm and the yolk sac forms the yolk syncytial layer (YSL). The cells in the center of the blastoderm form the “deep cells” that go on to form the zebrafish embryo (Kimmel et al., 1995; Lepage and Bruce, 2010; Solnica-Krezel, 2002).

Epiboly, or the thinning and spreading of the blastoderm around the yolk sac, is another important developmental event occurring within the blastula stage of development (Kimmel et al., 1995). Epiboly is the first morphogenic movement within zebrafish

embryos and is initiated by the yolk cell “doming” upward towards the bottom of the blastoderm, followed by the slow progression of the blastoderm towards the vegetal pole (Kane and Adams, 2002). Although the mechanism underlying epiboly is not completely understood, its progression in zebrafish embryos has been shown to rely on the presence of intact yolk sac microtubules and microfilaments, cell differentiation, and the initiation of zygotic gene transcription (Jesuthasan and Strähle, 1997; Lepage and Bruce, 2010).

During the next stage of zebrafish embryogenesis (the gastrula period), the blastoderm continues its progression towards the vegetal pole. In addition to movements of epiboly, new cell movements such as involution, convergence, and extension commence (Kimmel et al., 1995). At approximately 5 hpf, epiboly reaches the equator of the embryo and pauses, beginning the process of involution and resulting in the presence of a germ ring, which becomes mesodermal tissue (Kane and Adams, 2002; Kimmel et al., 1995). At the same time, cells deep in the blastoderm converge towards the dorsal side, forming the “embryonic shield” which acts as an organizer. During gastrulation, the germ ring slowly forms an inner and outer layer (the hypoblast and epiblast), positioning the mesoderm tissue inside the tissue that will become endoderm (Kimelman and Schier, 2002). By the end of gastrulation, the process of epiboly is complete, the tail bud has formed, and the mesodermal precursors for the notochord, somites, and blood cells are arranged along the dorsal-ventral axis (Kimelman and Schier, 2002; Kimmel et al., 1995)

### *1.7 Early Zebrafish Neurodevelopment: Segmentation*

Following gastrulation, the next developmental stage of the zebrafish embryo is

segmentation. During the segmentation period (10-24 hpf), the embryo elongates, somites appear, development of the neural tube and central nervous system (CNS) occurs, organ development begins, heart precursors are established, and the embryo first demonstrates movement (Kimmel et al., 1995). At the end of gastrulation, the neural plate is already localized and can be detected by its thickness and by the expression of neural patterning genes. During segmentation, the neural plate transforms into a neural tube and forms a distinct midline. The anterior neural tube then develops into distinct brain neuromeres while the posterior neural tube develops into the spinal cord (Kimmel et al., 1995).

Soon after development of the neural plate and throughout development of the nervous system, primary neurons begin to develop and begin to extend their axons from the spinal cord, innervating target axial muscles around 18 hpf. This innervation results in the initiation of weak, spontaneous muscle contractions within the developing embryo that represent the first sign of embryonic locomotion (Kimmel et al., 1995; Saint-Amant and Drapeau, 1998). These muscle contractions, termed spontaneous activity, are characterized by a series of trunk coils and are divided into early and late behaviors. Early spontaneous activity consists of single coils that are driven by periodic, non-chemically-mediated depolarizations, excitation spikes, and gap-junction-mediated electrical coupling within early spinal neurons (Saint-Amant and Drapeau, 2000, 2001). On the other hand, late spontaneous activity consists of side-to-side double coils that arise through the addition of chemically-mediated synapses to the existing electrical circuit and is regulated within the spinal cord as well as the hindbrain of embryonic zebrafish (Behra et al., 2002; Knogler et al., 2014; Raftery and Volz, 2015).

### *1.8 Overview of Research Aims & Hypotheses*

As discussed above, there is a need to generate toxicity data for many of the compounds used in commerce and the use of mammalian models is not adequate to address current data gaps. Zebrafish provide a promising alternative vertebrate model to support toxicity testing and, due to their small size, rapid development, and conservation of early developmental processes with mammals (including humans), zebrafish represent an ideal model for the identification of compounds that disrupt the normal trajectory of early embryonic development. Therefore, the overall goal of this research was to leverage early, non-protected life stages of zebrafish embryos to identify compounds that may be adversely impacting early development. Within Chapter 2, we hypothesize that embryonic behavior can be leveraged as a predictive readout to detect compounds adversely impacting the development and function of the nervous system. Within Chapter 3, the effects of niclosamide – a widely used anthelmintic that was identified from our high-content screen within Chapter 2 – on early embryonic development was assessed using a multipronged approach at multiple levels of biological organization. The overall hypothesis driving this work is that niclosamide exposure during early zebrafish development induces developmental toxicity through disruptions to oxidative phosphorylation. When data from Chapter 3 suggested that disruptions to oxidative phosphorylation were not the mechanism driving niclosamide-induced developmental delay, alternative hypotheses were investigated within the second half of Chapter 3 and within Chapter 4. As similar phenotypes have been observed following exposure to compounds disrupting the embryonic cytoskeleton, impairing lipid metabolism, and preventing the activation of the

zygotic genome, we hypothesized that niclosamide may be acting by one of these mechanisms. Within Chapter 4, these hypotheses were addressed using a combination of whole-embryo assessments and human embryonic stem cell-based assays. Overall, our findings highlight the potential utility of embryonic zebrafish as a model for screening and prioritization of chemicals for developmental toxicity.

## **Chapter 2: Behavioral Screening of Chemical Toxicity in Zebrafish Embryos**

### **2.0 Abstract**

Spontaneous activity represents an early, primitive form of motor activity within zebrafish embryos, providing a potential readout for identification of neuroactive compounds. However, despite use as an endpoint in chemical screens around the world, the predictive power and limitations of assays relying on spontaneous activity remain unclear. Using an improved high-content screening assay that increased throughput from 384 to 3,072 wells per week, we screened a well-characterized library of 1,280 pharmacologically active compounds (LOPAC<sup>1280</sup>) – 612 of which target neurotransmission – to identify which targets are detected using spontaneous activity as a readout. Results from this screen revealed that (1) 8% of the LOPAC<sup>1280</sup> library was biologically active; (2) spontaneous activity was affected by compounds spanning a broad array of targets; (3) only 4% of compounds targeting neurotransmission impacted spontaneous activity; and (4) hypoactivity was observed for 100% of hits detected, including those that exhibit opposing mechanisms of action for the same target. Therefore, while this assay was able to rapidly identify potent neuroactive chemicals, these data suggest that spontaneous activity may lack the ability to discriminate modes of action for compounds interfering with neurotransmission, an issue that may be due to systemic uptake following waterborne exposure, persistent control variation, and/or interference with non-neurotransmission-related mechanisms.

## 2.1 Introduction

The use of mammalian models for drug discovery and toxicity testing is costly, time-intensive, and requires millions of dollars per chemical (Kuhlmann, 1999, 2000; Zon and Peterson, 2005). Moreover, ethical concerns regarding high animal use have accelerated the development of alternative testing methods to reduce, refine, and ultimately replace animal use for chemical testing (Arora et al., 2011; Bal-Price et al., 2012; Crofton et al., 2011; National Academies Press, 2007; Richmond, 2002; Zon and Peterson, 2005). As a result, high-throughput screening (HTS) and high-content screening (HCS) assays have been developed over the last decade to screen more chemicals at a lower cost within a shorter period of time (Möller and Slack, 2010; Persson and Hornberg, 2016; Zhu et al., 2014). The vast majority of HTS and HCS assays used for drug discovery and toxicity testing utilize cell-free and cell-based methods that model key biological events across a wide range of pharmacologically- or toxicologically-relevant pathways (Fernandes et al., 2009; Zanella et al., 2010; Zhu et al., 2014). However, since these assays do not adequately reflect the complex physiology of an intact organism, the use of smaller, alternative non-mammalian animal models (such as nematodes and fish embryos) have been proposed as complementary models, as these models are (1) suitable for microplate-based assays and (2) not protected by animal use regulations around the world (Coecke et al., 2007; Crofton et al., 2012).

Zebrafish offer one of the most promising alternative and cost-effective vertebrate models to support drug discovery and toxicity testing (MacRae and Peterson, 2015; Persson and Hornberg, 2016; Zon and Peterson, 2005), particularly for identification of neuroactive

drugs and/or neurotoxic chemicals (Kokel et al., 2010; Lee and Freeman, 2014; Rihel and Schier, 2012). As such, a repertoire of zebrafish-based behavioral assays across multiple life-stages (including adulthood) have been developed over the last 10-15 years (Bang et al., 2002; Brockerhoff et al., 1995; Egan et al., 2009; Kokel et al., 2010). Although different forms of larval and adult zebrafish locomotion have been leveraged within behavioral assays, spontaneous activity (tail contraction) – a behavior that occurs from late-segmentation (~17-19 hours post-fertilization, hpf) through early-pharyngula (~27-29 hpf) – represents an early, primitive form of motor activity within zebrafish embryos, providing a potential readout for rapid identification of neuroactive chemicals (Kokel et al., 2010; Raftery et al., 2014; Reif et al., 2015; Truong et al., 2016). Although previous studies have explored the biological basis of this behavior (Knogler and Drapeau, 2014; Knogler et al., 2014; Saint-Amant and Drapeau, 2000, 2001), it remains unclear whether spontaneous activity is responsive only to certain compounds with specific mechanisms of action.

In 2014, we developed a high-content screening (HCS) assay that quantifies background (unstimulated) spontaneous activity within single zebrafish embryos after exposure to chemicals in 384-well plates (Raftery et al., 2014). Within this assay, 192 viable embryos were arrayed into a 384-well plate, resulting in one embryo per well and 16 initial embryos per treatment. Following static exposure from 5 to 25 hpf, automated image acquisition procedures and custom analysis protocols were then used to quantify spontaneous activity within live, non-malformed embryos using a 6-s video per well. Although survival and imaging success rates were >85% and the total assay duration was <30 hours, we observed a high degree of natural variability in the percent of control

embryos exhibiting spontaneous activity despite efforts to control for developmental stage, temperature, and light conditions (Raftery et al., 2014). Moreover, initial attempts to use 384 embryos per plate were unsuccessful due to prolonged image acquisition times, resulting in across-plate variation in spontaneous activity (Raftery et al., 2014).

To address these challenges, the objectives of the present study were to (1) decrease assay control variability by increasing video duration per well from 6 to 18 s; (2) increase assay throughput from 384 (one plate) to 3,072 wells (eight plates) per week by imaging four wells simultaneously (rather than one well at a time); (3) assess the reproducibility of our improved assay using negative and positive control wells across replicate plates; and (4) using our improved assay, reveal which targets are detected using spontaneous activity as an integrative behavioral readout. To accomplish the final objective, we screened the commercially available LOPAC<sup>1280</sup> (Library of Pharmacologically Active Compounds) library – a widely used library of 1,280 marketed drugs, failed development candidates, and well-characterized small molecules that (1) span a broad molecular weight range (36 to 1,485 g/mol), (2) represent multiple mechanisms of action, and (3) target a diverse set of biological receptors. In addition, nearly half of the LOPAC<sup>1280</sup> library targets neurotransmission, providing an ideal, commercially available resource for identifying which targets are detected using spontaneous activity while, at the same time, increasing our understanding of targets that may be involved in regulating this behavior during early zebrafish embryogenesis. For all assays, abamectin – an avermectin insecticide and potent anticonvulsant within zebrafish embryos (Raftery and Volz, 2015; Raftery et al., 2014) – was used as a positive control.

## 2.2 Materials and Methods

### 2.2.1 Animals

For this study, we used a transgenic (*flil:egfp*) strain of zebrafish that stably express enhanced green fluorescent (eGFP) protein within vascular endothelial cells (Lawson and Weinstein, 2002), as this strain begins expressing eGFP at ~14 hpf. Adult *flil:egfp* zebrafish were maintained on a recirculating system with UV sterilization and mechanical/biological filtration units (Aquaneering, San Diego, CA, USA), and were kept under a 14-h:10-h light:dark cycle at a water temperature of ~27-28°C, pH of ~7.2, and conductivity of ~900-950  $\mu$ S. Water quality was constantly monitored for pH, temperature, and conductivity using a real-time water quality monitoring and control system. Ammonia, nitrate, nitrite, alkalinity, and hardness levels were manually monitored weekly by test strip (Lifeguard Aquatics, Cerritos, CA). Zebrafish were fed twice per day with dry diet (Gemma Micro 300, Skretting, Fontaine-lès-Vervins, France). Adult males and females were bred directly on-system using in-tank breeding traps suspended within 3-L tanks. For all experiments described, newly fertilized eggs were collected within 30 min of spawning, rinsed, and reared in a temperature-controlled incubator (28°C) under a 14-h:10-h light:dark cycle. All embryos were sorted and staged according to previously described methods (Kimmel et al., 1995). All adult breeders were handled and treated in accordance with an Institutional Animal Care and Use Committee (IACUC)-approved animal use protocol (#20150035) at the University of California, Riverside.

### 2.2.2 Chemicals

Abamectin was purchased from ChemService, Inc. (West Chester, PA, USA), and a low-volume (25  $\mu$ l per compound) library of 1,280 pharmacologically active compounds (LOPAC<sup>1280</sup>) was purchased from Sigma-Aldrich (St. Louis, MO, USA). Stock solutions of abamectin (50 mM) were prepared by dissolving abamectin in high performance liquid chromatography (HPLC)-grade dimethyl sulfoxide (DMSO) and stored at room temperature within 2-ml amber glass vials containing polytetrafluoroethylene (PTFE)-lined caps. Stock solutions (25  $\mu$ l of 10 mM stock per compound) of the LOPAC<sup>1280</sup> library (16 96-well racks containing 80 compounds per rack) were prepared and provided in DMSO by Sigma-Aldrich and stored at -30°C upon arrival; except for partition coefficient (LogP) values, all compound-specific information was provided by Sigma-Aldrich within a Microsoft Excel spreadsheet following acquisition of the LOPAC<sup>1280</sup> library. For each individual plate, working solutions of all treatments were freshly prepared by diluting stock solutions 1:1000 into embryo media (EM) (10 mM NaCl, 0.17 mM KCL, 0.66 mM CaCl<sub>2</sub>, 0.66 mM MgSO<sub>4</sub>), resulting in 0.1% DMSO within all vehicle control and treatment groups.

### 2.2.3 Assay Design

Newly fertilized embryos were collected immediately following spawning and incubated in groups of approximately 50 per plastic petri dish until 5 hpf. Embryo media, vehicle control (0.1% DMSO), positive control (abamectin), or test solution (50  $\mu$ l/well) was loaded into a black 384-well microplate containing 0.17-mm glass-bottom wells (Matrical Bioscience, Spokane, WA, USA). For the LOPAC<sup>1280</sup> screens, vehicle (0.1% DMSO) and positive (6.25  $\mu$ M abamectin) control groups each occupied two columns (32

wells per group) flanking the left and right sides of the plate (0.1% DMSO: columns 1 and 24; 6.25  $\mu$ M abamectin: columns 2 and 23), whereas each LOPAC<sup>1280</sup> compound occupied one column (16 wells) on each plate. At 5 hpf, 384 viable *fli1:egfp* embryos were manually arrayed into each well of a 384-well plate over a 45-min time period, resulting in one embryo per well. The plate was then covered with a plate lid, wrapped with parafilm to minimize evaporation, and incubated at 28°C under a 14-h:10-h light:dark cycle until 24 hpf. At 24 hpf, the plate was placed in a second incubator at 25°C for 1 h to acclimate embryos to room temperature prior to imaging. At 25 hpf, the plate was then centrifuged for 2 min at 200 rpm to ensure all embryos were positioned at the well bottom.

#### *2.2.4 Image Acquisition and Analysis*

Using a time-lapsed image acquisition protocol optimized for our ImageXpress Micro (IXM) XLS Widefield High-Content Screening System equipped with MetaXpress 6.0.3.1658 (Molecular Devices, Sunnyvale, CA), four wells were simultaneously imaged every 0.3 s over an 18-s time period using a 2X objective and FITC filter cube, resulting in a total of 96 acquisitions per 384-well plate, 60 frames per acquisition, and 5,760 frames per 384-well plate. In addition, a 4X objective and FITC filter cube was used to acquire one frame per entire well for assessment of survival and quantification of total body area. During the entire ~30-min image acquisition period, internal temperature within the IXM system was maintained using previously described procedures (Raftery et al., 2014). Embryos were then euthanized by placing the plate at -30°C.

Using fully automated custom journal scripts, four-well frames were divided into individual quadrants and used to generate 18-s videos (.AVI files) representing individual wells. Videos (384 per plate) were manually checked to assess the presence or absence of spontaneous tail contractions and then analyzed within EthoVision XT 9.0 (Noldus Information Technology, Leesburg, VA) using previously described procedures (Raftery et al., 2014). Using images captured with a 4X objective, survival and total body area was also quantified using previously described procedures (Raftery et al., 2014). Treatments resulting in a significant decrease in total body area, <85% survival, or gross malformations were not analyzed for spontaneous activity.

#### *2.2.5 LOPAC<sup>1280</sup> Library Screen*

We relied on a two-tiered strategy to screen the LOPAC<sup>1280</sup> library. For Tier I, embryos were exposed from 5-25 hpf to each compound at a single limit concentration of 10  $\mu$ M. Compounds were identified as Tier-I hits if exposure resulted in a significant effect on survival, total body area, or spontaneous activity. Compounds resulting in autofluorescence, gross malformations (deformed axis, tail malformations, or underdeveloped head), or <85% survival were not analyzed for effects on total body area and spontaneous activity, and compounds resulting in a significant decrease in total body area were not analyzed for effects on spontaneous activity (Figure 1).

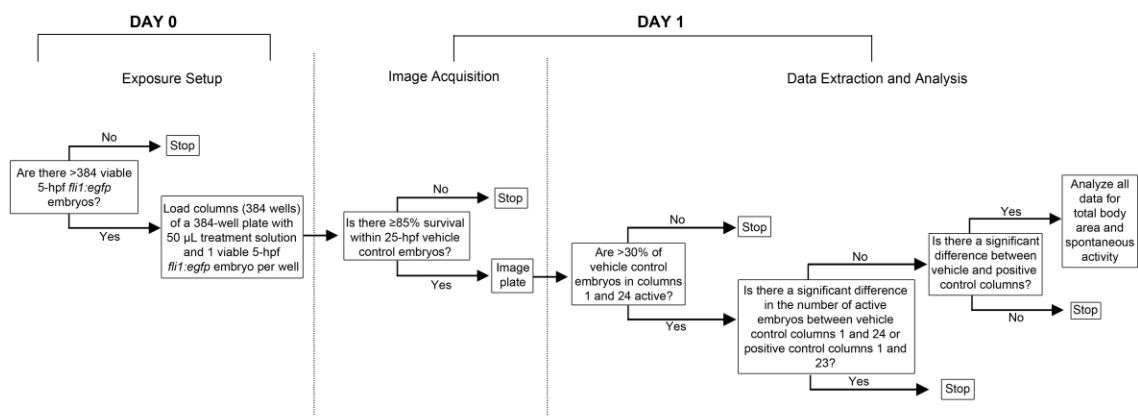


**Figure 1.** Decision tree for behavioral screening of the LOPAC1280 library. Assay/exposure setup occurred on Day 0, whereas image acquisition and data extraction/analysis both occurred on Day 1.

### 2.2.6 Statistical Analysis

All statistical analyses were performed using SPSS Statistics 23.0 (IBM, Chicago, IL, USA). Total body area was analyzed using a general linear model (GLM) analysis of variance (ANOVA) ( $\alpha = 0.05$ ), as these data did not meet the equal variance assumption for non-GLM ANOVAs. Pair-wise Tukey-based multiple comparisons of least-squares means were performed to identify significant treatment-related effects; treatments were only considered significant if total body area was statistically different from both vehicle control columns. Spontaneous activity data were analyzed using nonparametric tests, as these data were categorical and did not meet assumptions of normality. A Kruskal–Wallis test ( $\alpha = 0.05$ ) was used to test for main effect of treatment, and Mann-Whitney pairwise comparisons were used to test for differences between and among vehicle control, positive control, and treatment columns. For the LOPAC<sup>1280</sup> screens, plates were analyzed for differences between vehicle controls (columns 1 and 24) and positive controls (columns 2

and 23) as well as treatments (columns 3-22) relative to vehicle and positive controls ( $\alpha=0.05$ ); treatments were only considered significant if statistically different from both vehicle control columns and both positive control columns. If spontaneous activity between vehicle or positive control columns was statistically different based on the statistical tests described above, treatment columns were not analyzed, and the plate was repeated.

## **2.3 Results**

### *2.3.1 Assay Variability*

To determine whether differences in 1-h acclimation temperatures affected spontaneous activity, we reared and acclimated a total of 96 embryos across two independent plates at 23, 28, or 33°C from 24-25 hpf (following incubation from 5-24 hpf at 28°C) under normal light conditions. For all temperatures, percent survival was >85% for each column and total body area was consistent within and across acclimation temperatures (Figure 2A, 2B). Although there was a slight increase in the percent of embryos displaying spontaneous activity following acclimation at 33°C, no significant differences in spontaneous activity were observed among all three acclimation temperatures (Figure 2C).

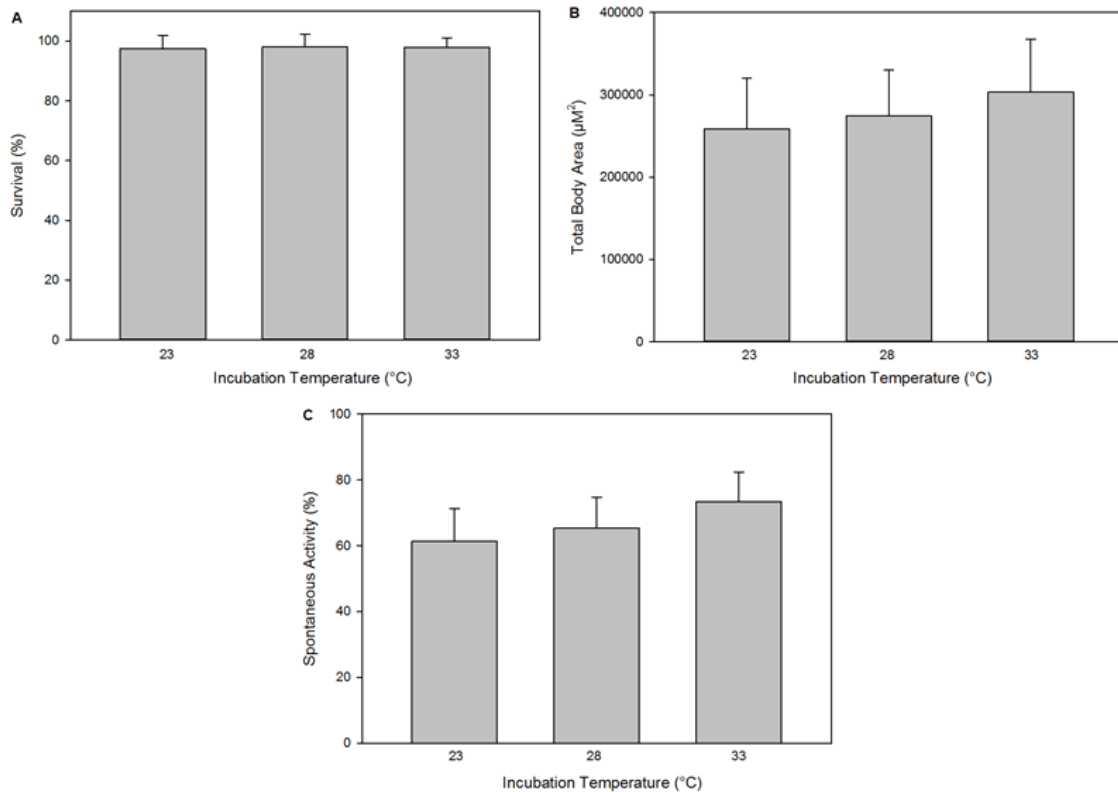


**Figure 2.** Embryos survival (A), total body area ( $\mu\text{M}^2$ ) (B), and spontaneous activity (C) are not significantly impacted by acclimation temperature from 24-25 hpf. Data collected following a 1-h acclimation from 24-25 hpf at 23, 28, or 33°C under normal light conditions. Data are presented as mean  $\pm$  standard deviation across two independent plates. N=96 initial embryos (six columns) per acclimation temperature.

After confirming that spontaneous activity was not significantly impacted by acclimation temperature, we reared and acclimated a total of 1,152 embryos across three independent negative control (embryo media only) plates from 5-24 hpf at 28°C and 24-25 hpf at 25°C; each plate was loaded on separate days to account for potential day-to-day variation. At 25 hpf, each plate was analyzed for survival, total body area, and spontaneous activity. For all control plates, embryo survival was >85% and there were no significant within-plate nor plate-to-plate differences in total body area (Figure 3A,3B). However, the

percent of embryos with spontaneous activity ranged from 30-93% per column across all three control plates, with most columns displaying 50-74% activity (Figure 3C, 3D).

### 2.3.2 Assay Reproducibility

Two replicate concentration-response curves for abamectin (0.09-50  $\mu\text{M}$ ) – a positive control within our assay – were screened on a single plate to identify the lowest concentration resulting in complete elimination of spontaneous activity in the absence of effects on survival or total body area (Figure 4). Based on these concentration-response curves, three independent plates were then screened using 6.25  $\mu\text{M}$  abamectin to confirm that effects on spontaneous activity were reproducible within and across plates (Figure 5). For all three plates, embryo survival was >85% and there were no significant within-plate nor plate-to-plate differences in total body area (Figure 5A,5B). Although vehicle controls were variable, there were no significant differences in spontaneous activity among vehicle control columns across all three plates. However, exposure to 6.25  $\mu\text{M}$  abamectin resulted in complete elimination of spontaneous activity within and across all three plates (Figure 5C).

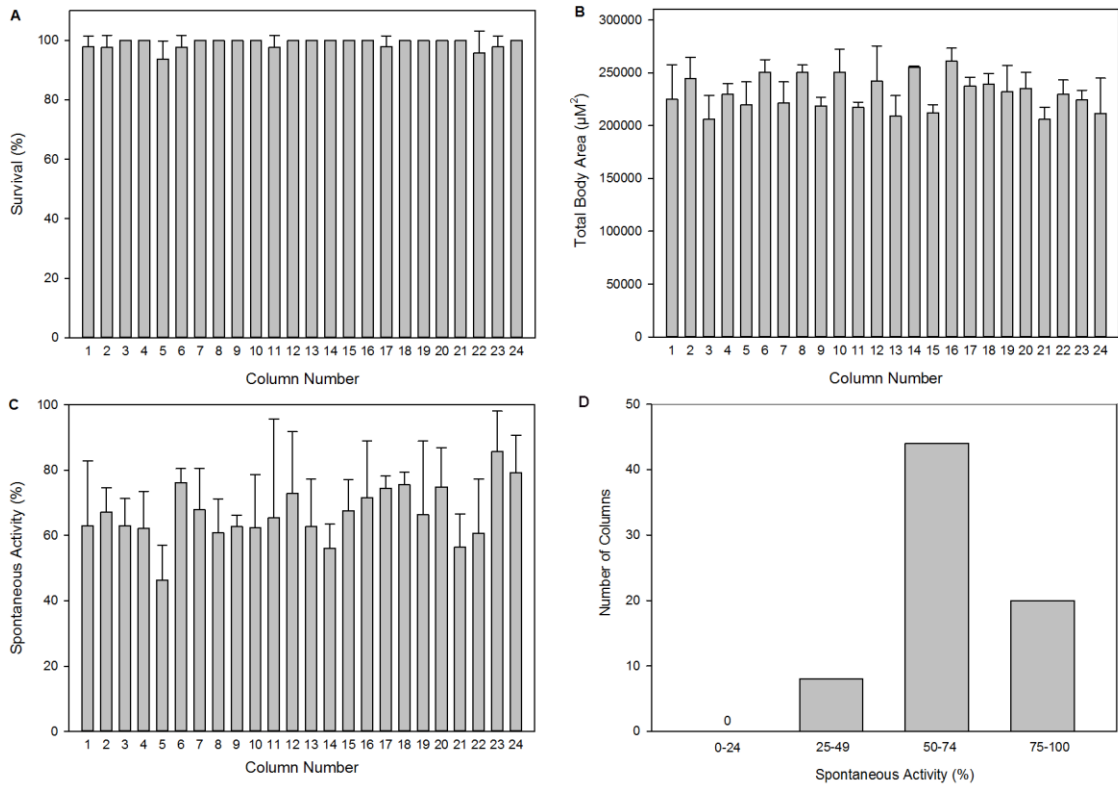


**Figure 3.** Embryo survival (%) (A), total body area ( $\mu\text{m}^2$ ) (B), and spontaneous activity (%) (C) are not significantly different within and across three independent negative control (embryo media-only) plates (N=48 initial embryos per column number). (D) Control spontaneous activity represented as bins. Data are presented as mean  $\pm$  standard deviation.

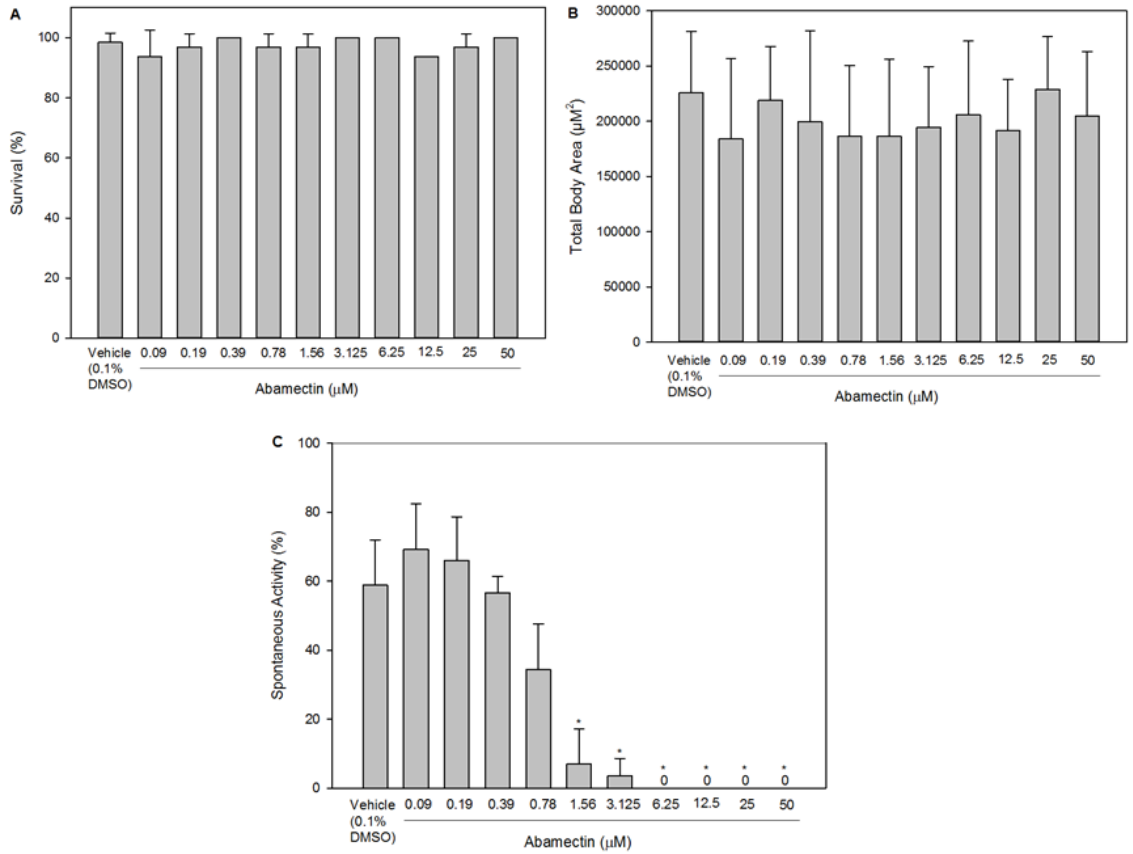


**Figure 4.** Abamectin induces a concentration-dependent decrease in spontaneous activity without affecting survival and growth. (A) Embryo survival (%), (B) total body area ( $\mu\text{m}^2$ ), and (C) spontaneous activity (%) following exposure to vehicle or abamectin. Spontaneous activity was completely abolished at 6.25  $\mu\text{M}$ . Data are presented as mean  $\pm$  standard deviation of two concentration-response curves within a single plate. Asterisk denotes significant difference from vehicle.



non-neurotransmission-related targets (Figure 7). Interestingly, all Tier-I spontaneous activity hits were driven by a significant decrease in spontaneous activity (hypoactivity), even for compounds that target the same receptor (e.g., dopamine receptor) but exhibit opposing modes of action (e.g., agonist vs. antagonist).

For Tier II, all Tier-I hits were screened at a 1- $\mu$ M limit concentration using a 23- to 25-hpf (2-h) exposure to eliminate false positives associated with adverse developmental effects prior to 23 hpf. Based on this secondary screen, there were no significant effects on survival or total body area, and approximately 15% (15 compounds) of the Tier-I hits were positive for significant impacts on spontaneous activity (Figure 7). Out of these 15 compounds, approximately 73% (11 compounds) resulted in significant impacts to spontaneous activity in both Tier I and II screens. Like Tier I, all 15 Tier-II spontaneous activity hits were driven by hypoactive effects relative to vehicle controls and spanned a wide range of neurotransmission- and non-neurotransmission-related targets with varying modes of action (Figure 7).

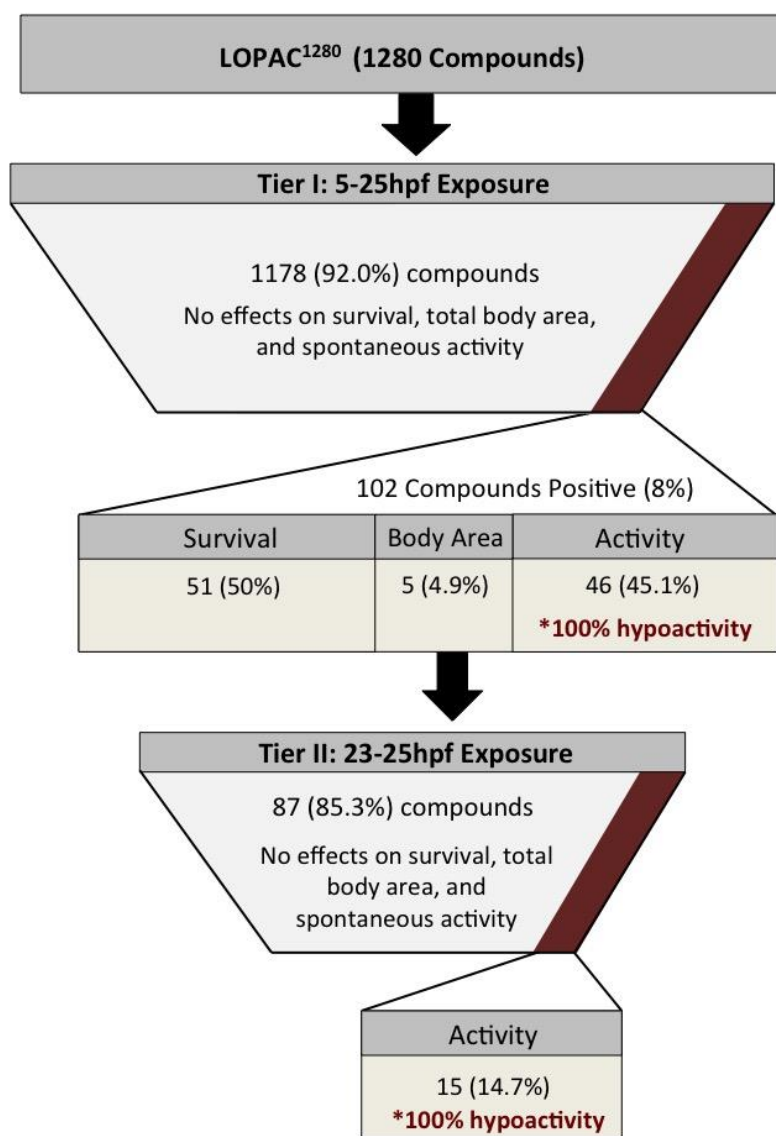


**Figure 6.** Summary of results from two-tiered behavioral screening of the Library of Pharmacologically Active Compounds (LOPAC1280).

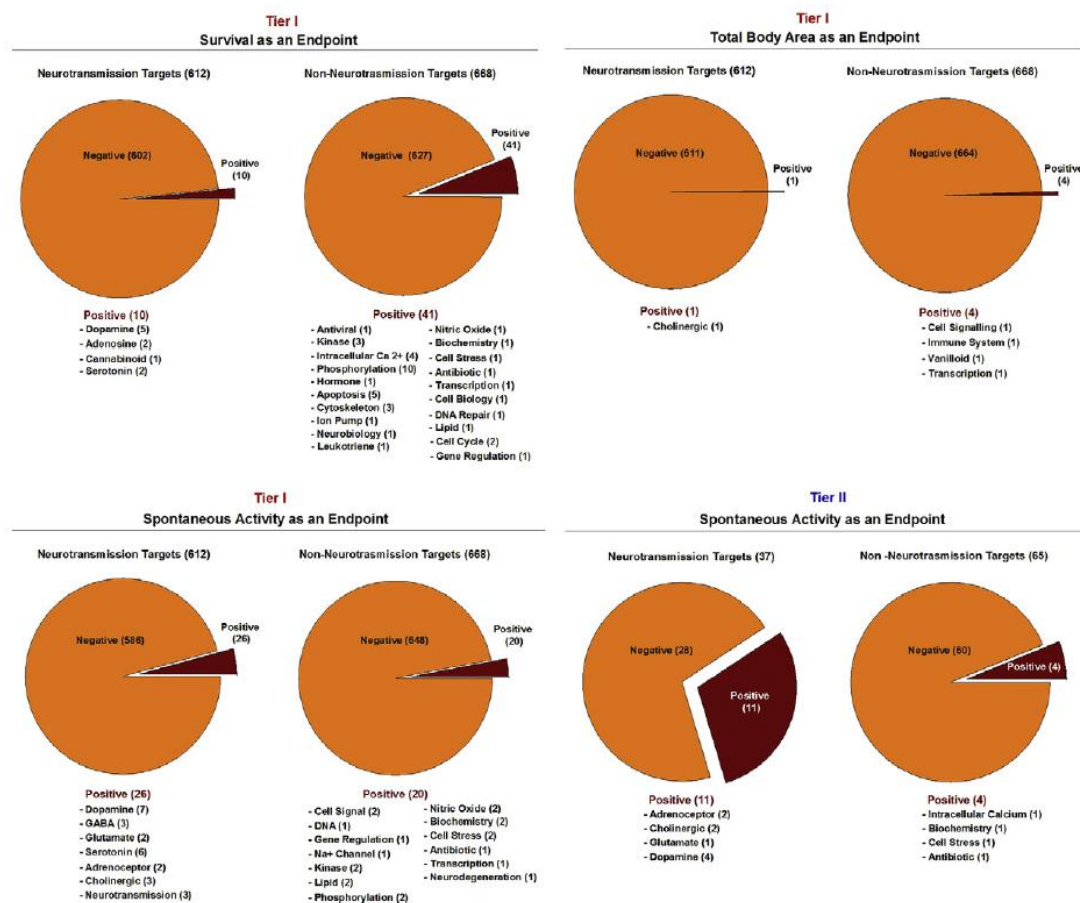


**Figure 7.** LOPAC<sup>1280</sup> Tier I and II hits are not associated with unique Sigma-Aldrich-defined classes of biological targets. LOPAC<sup>1280</sup> Tier I and II hits are presented as a function of 1) endpoint (survival, total body area, or spontaneous activity); 2) whether the compound targets neurotransmission; and 3) Sigma-Aldrich-defined biological class. Numbers within parentheses represent the total number of positive compounds within each group.

### 2.3.4 Data Mining

Partition coefficient (LogP) values were retrieved for all 1,280 compounds from the NCBI's PubChem database (<https://pubchem.ncbi.nlm.nih.gov>) and molecular weights for all compounds were correlated by endpoint to determine whether hydrophobicity and/or chemical size predicted the potential for a Tier-I or Tier-II hit within our assay. There was

no association between LogP and the potential for a Tier-I hit, with LogP values ranging from 0 to 10 for 98% of Tier-I hits (Figure 8A). Similarly, there was no association between molecular weight and the potential for a Tier-I hit, where molecular weights for all Tier-I hits ranged from 98 to 875 g/mol. Interestingly, while Tier-II spontaneous activity hits were not associated with molecular weights (180-875 g/mol), these hits clustered within a narrow range of LogP values (1.8-5.2) relative to Tier-I hits (Figure 8B).

Using NCBI's PubChem Chemical Structural Clustering Tool, the entire LOPAC<sup>1280</sup> library was clustered based on two-dimensional (2D) structural similarity using the Single Linkage algorithm (<https://pubchem.ncbi.nlm.nih.gov/assay/clustering>). Within this model, a Tanimoto Similarity score of 0.68 or higher denotes a statistically significant 2D structural similarity at the 95% confidence interval. Based on this analysis, the potential for a positive hit within Tier I – as well as impacts on survival, total body area, or spontaneous activity within both Tier I and II screens – were not associated with 2D compound structural similarity (Figure 9).

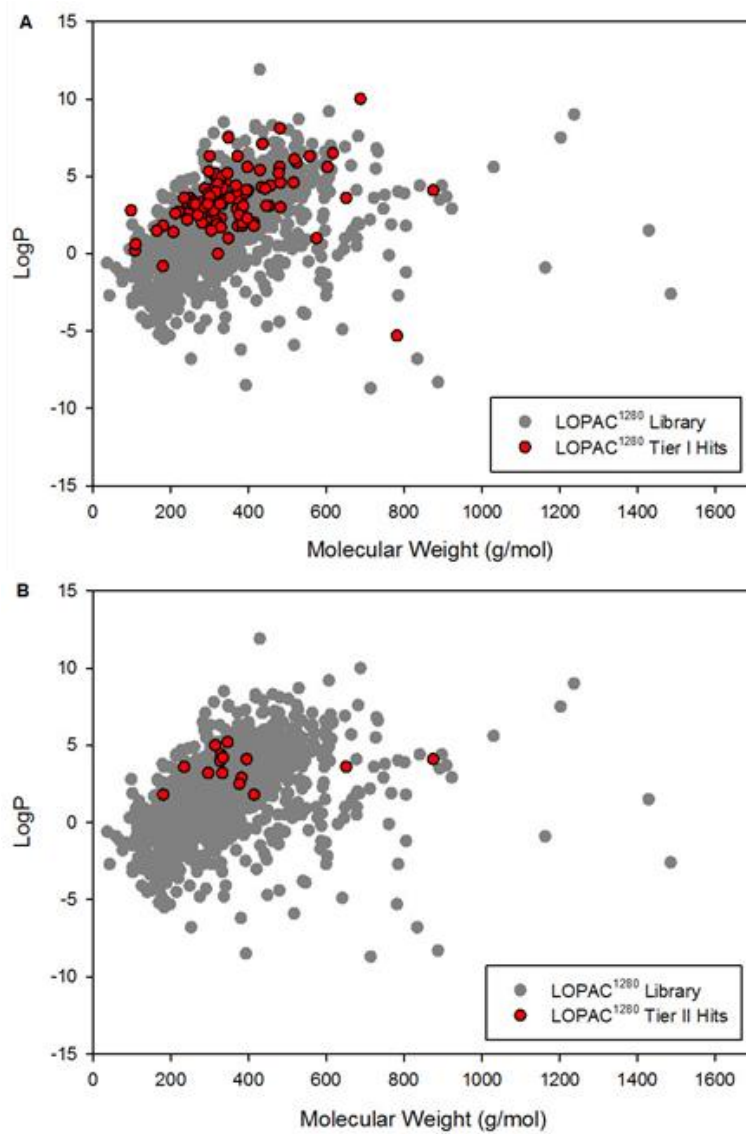


**Figure 8.** LOPAC<sup>1280</sup> hits are not associated with LogP and molecular weight. LogP values and molecular weights for all compounds were correlated to determine whether hydrophobicity and chemical size predicted the potential for a Tier I (A) or Tier II (B) hit within our assay.

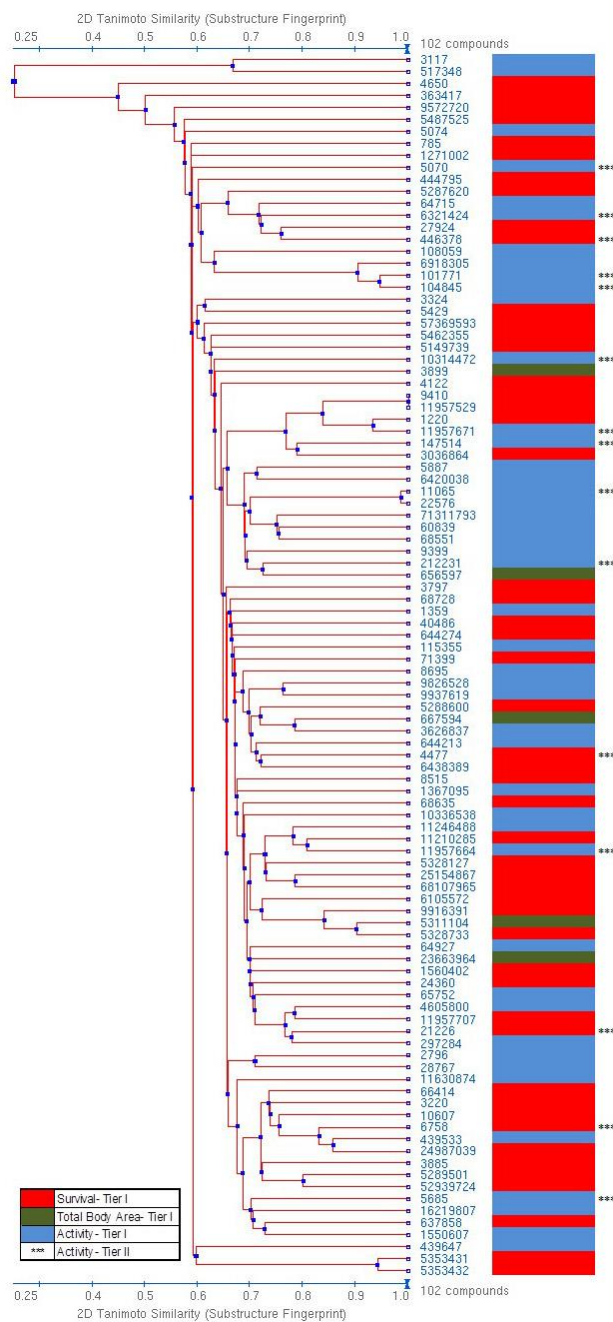


**Figure 9.** LOPAC<sup>1280</sup> hits are not associated with two-dimensional (2D) compound structural similarity. Compound structures for all Tier-I hits (102 compounds) were clustered using PubChem’s Chemical Structural Clustering Tool using the Single Linkage algorithm. Color map denotes which Tier-I endpoint was significantly affected. Triple-asterisk denotes Tier-II hits (15 compounds) driven by significant effects on spontaneous activity. A Tanimoto Similarity score of 0.68 or higher denotes a statistically significant 2D structural similarity.

## 2.4 Discussion

This study has revealed that (1) within the Tier-I screen, approximately 8% (102 compounds) of the LOPAC<sup>1280</sup> library was biologically active (at a 10- $\mu$ M limit concentration) based on significant effects on survival, body area, or spontaneous activity relative to vehicle controls; (2) within the Tier-I screen, only 4% (25 compounds) of 612 LOPAC<sup>1280</sup> compounds that interfere with neurotransmission impacted spontaneous activity; (3) within both screens, spontaneous activity was adversely affected by LOPAC<sup>1280</sup> compounds that spanned a broad array of non-neurotransmission and neurotransmission targets; and (4) within both screens, hypoactivity was observed for 100% of hits detected, including those that exhibit opposing mechanisms of action (e.g., agonist vs. antagonist) for the same target (e.g., dopamine receptor). Therefore, while our assay was able to identify potent neuroactive chemicals, these data suggest that spontaneous activity may lack the ability to discriminate modes of action (e.g., stimulants vs. sedatives) for compounds interfering with neurotransmission, an issue that may be a result of (1) systemic uptake following waterborne exposure; (2) persistent control variation despite negligible effects of temperature acclimation and assay improvements (increased video duration per well and assay throughput) relative to our previous study (Raftery et al., 2014); and/or (3) interference with non-neurotransmission-related mechanisms.

Within embryonic zebrafish, spontaneous activity is characterized by a series of trunk coils and represents the first sign of sensory-independent locomotion (Kimmel et al., 1995; Saint-Amant and Drapeau, 1998). Early spontaneous activity consists of single coils

that are driven by periodic, non-chemically-mediated depolarizations, excitation spikes, and gap-junction-mediated electrical coupling within early spinal neurons (Saint-Amant and Drapeau, 2000, 2001). On the other hand, late spontaneous activity consists of side-to-side double coils that arise through the addition of chemically-mediated synapses to the existing electrical circuit and is regulated within the spinal cord as well as the hindbrain of embryonic zebrafish (Behra et al., 2002; Knogler et al., 2014; Raftery and Volz, 2015). As such, late spontaneous activity represents an intermediate form of behavior that precedes secondary motorneuron development and bridges early spontaneous activity with stimuli-induced responses observed during later stages of embryonic and larval development (Knogler et al., 2014).

As image acquisition within our assay occurred during the peak frequency of spontaneous tail contractions (25-26 hpf when reared at 28°C) (Yozzo et al., 2013), LOPAC<sup>1280</sup> compounds that interfere with electrical coupling and/or chemically-mediated neurotransmission may have the potential to adversely affect late spontaneous activity following a 5-25 hpf exposure. Based on results from both screens, spontaneous activity was similarly impacted by LOPAC<sup>1280</sup> compounds targeting neurotransmission- and non-neurotransmission-related processes, where the magnitude of effect following a 10-µM exposure was, in several cases, equivalent for both groups of compounds. After eliminating the potential for false positive hits associated with systemic toxicity (based on survival and total body area), LOPAC<sup>1280</sup> hits for spontaneous activity were not limited to compounds targeting neurotransmission, raising the possibility that, at least for our Tier-I screen (exposure from 5-25 hpf), non-neurotransmission-related compounds that impact electrical

coupling during early spontaneous activity may lead to downstream effects on late spontaneous activity. However, even following a 2-h exposure from 23-25 hpf (Tier-II screen), four out of 15 hits for spontaneous activity were not classified as targeting neurotransmission, suggesting that other variables or mechanisms of action such as impaired muscle function and/or energy metabolism may influence spontaneous activity within our assay.

Interestingly, our results demonstrate that spontaneous activity may lack the ability to discriminate opposing modes of action (e.g., stimulants vs. sedatives) for neurotransmission-interfering compounds. Indeed, hypoactivity was observed for all compounds affecting spontaneous activity – even for compounds with opposing mechanisms of action for the same target. For example, within our Tier-I screen, exposure to seven different dopaminergic drugs with varying mechanisms of action (e.g., agonist, antagonist, or inhibitor) all resulted in a significant decrease in spontaneous activity. In contrast, Irons et al. (2013) examined the effect of six different dopaminergic drugs – all of which were present within the LOPAC<sup>1280</sup> library – on larval zebrafish locomotion, and demonstrated that exposure to dopaminergic agonists and antagonists induce hyperactivity and hypoactivity, respectively (Irons et al., 2013). Interestingly, dopaminergic drugs that resulted in changes to larval locomotion did not significantly alter embryonic spontaneous activity within our Tier-II screen. This discrepancy between life-stages may be due to differences in the presence and function of dopamine receptors within embryonic vs. larval zebrafish, as the expression of dopamine receptor genes is not initiated until ~24 hpf (Boehmler et al., 2004, 2007; Li et al., 2007). Therefore, given that other receptors and

targets for neurotransmission-related LOPAC<sup>1280</sup> compounds are likely absent or minimally functional at 25-26 hpf, our data suggest that compounds may be acting through other pathways and that, regardless of whether the receptor or target is present and functional, other variables such as compound uptake, distribution, and exposure concentration may be influencing behavior within our assay.

Similar to our findings within embryonic zebrafish, a recently published study demonstrates that, even within larval zebrafish harboring a more complex nervous system, the observed behavioral response is not always consistent with the expected behavioral response based on the known mechanism and mode of action within mammals (Kirla et al., 2016). Within this study, the authors relied on cocaine as a model compound, as cocaine acts on the monoaminergic neurotransmitter systems and is a stimulant within mammals. However, contrary to the expected outcome (hyperactivity), acute exposure to non-teratogenic concentrations of cocaine resulted in a concentration-dependent decrease in locomotion (hypoactivity) within both dark and light conditions following a waterborne exposure of cocaine (Kirla et al., 2016). Importantly, the authors also quantified cocaine uptake and distribution using matrix-assisted laser desorption ionization mass spectrometry imaging (MALDI MSI), and observed significant accumulation within the brain, eyes, and trunk of larval zebrafish. Therefore, the authors concluded that cocaine-induced hypoactivity was as a result of systemic (rather than targeted) cocaine uptake across the skin of larval zebrafish, leading to an anesthetic effect on the peripheral nervous system that suppressed stimulatory targets present in the central nervous system (Kirla et al., 2016). Likewise, within our assay, there is a strong possibility that, for compounds expected to

act as stimulants, waterborne exposure may have led to non-targeted, systemic uptake and distribution that overwhelmed the intended target and significantly biased behavior (spontaneous activity) toward a unidirectional hypoactive response.

Finally, the ability of our assay to identify and classify negative vs. positive hits was likely influenced by a complex interaction among exposure duration, compound potency (at a single limit concentration of 10  $\mu\text{M}$ ), and toxicokinetics (compound uptake over time) – variables that are dependent on assay design and physicochemical attributes. Clearly, exposure duration relative to the timing of key developmental landmarks is an essential consideration for assay design, as 87 of 102 Tier-I (5-25 hpf) hits for survival, total body area, or spontaneous activity were negative for all three endpoints within our Tier-II (23-25 hpf) screen. However, a more significant challenge is related to uncertainties about the influence of compound partitioning from water into zebrafish embryos following a 5-25 hpf exposure. Since we did not quantify internal doses, we were unable to determine if negative hits within our Tier-I screen were a result of (1) insufficient compound uptake over a 20-h exposure (for compounds that may otherwise have been potent) or (2) sufficient compound uptake over a 20-h exposure, but minimal potency at the limit concentration (10  $\mu\text{M}$ ) tested. Importantly, our data suggests that physicochemical attributes do not have the potential to predict Tier-I hits within our assay, as negative and positive hits spanned a broad range of LogP values and molecular weights. On the other hand, most Tier-I hits (98%) had LogP values favoring water-to-embryo partitioning (LogP>0) and Tier-II hits clustered within a narrower range of LogP values relative to Tier-I hits, suggesting that a short (2-h) exposure biased hits to hydrophobic compounds within an optimal LogP range

(LogP = ~2-5). Therefore, these results are consistent with other studies showing that compound bioactivity is not associated with compound size (for compounds  $\leq 3000$  g/mol) but, rather, tends to be dependent on compound hydrophobicity (LogP>0) and partitioning from water into zebrafish embryos (whether chorionated or not) over a specific exposure duration (Gustafson et al., 2012; de Koning et al., 2015; Pelka et al., 2017; Sachidanandan et al., 2008). Finally, the lack of structural similarity suggests that, like LogPs and molecular weights, 2D chemical structures do not have the potential to predict hits within our assay; however, it is important to note that this lack of predictability may be driven by the inherent chemical diversity of the LOPAC<sup>1280</sup> library.

In conclusion, results from this study suggest that, despite the seemingly simple biological basis of spontaneous activity (relative to more complex behaviors later in development), this primitive form of locomotion was affected by a wide range of pharmacologically and structurally diverse compounds. As a result, although the use of background (unstimulated) spontaneous activity was able to identify neuroactive compounds, this behavioral readout (as used in our assay) was unable to predict biological targets and discriminate chemical modes of action. This lack of specificity was likely due to a complex set of uncertainties associated with the underlying biology of embryonic zebrafish, persistent control variability (despite our efforts to control for developmental stage, temperature, and light conditions, and increase video duration per well), decisions about assay design, and toxicokinetics (i.e., the rate and magnitude of water-to-embryo partitioning). Despite limitations highlighted in this study, spontaneous activity may still hold utility as a readout within other behavioral assays, such as the photomotor response

(PMR) assay, which relies on a high-intensity light stimulus to generate more robust “behavioral barcodes” to identify compounds that interfere with startle-response and habituation (Kokel et al., 2010, 2013). However, to our knowledge, the LOPAC<sup>1280</sup> library has not been screened using the PMR assay, so it’s currently unclear whether the PMR assay will also suffer from similar uncertainties and limitations.

## **Chapter 3: Early Developmental Toxicity of Niclosamide in Zebrafish Embryos**

### **3.0 Abstract**

Niclosamide is an anthelmintic drug used worldwide for the treatment of tapeworm infections. Recent drug repurposing screens have revealed that niclosamide exhibits diverse mechanisms of action and, as a result, demonstrates promise for several applications, including the treatment of cancer, bacterial infections, and Zika virus. As new applications of niclosamide will require non-oral delivery routes that may lead to exposure in utero, the objective of this study was to investigate the mechanism of niclosamide toxicity during early stages of embryonic development. Using zebrafish as a model, we found that niclosamide induced a concentration-dependent delay in epiboly progression during late-blastula and early-gastrula, an effect that was dependent on exposure during the maternal-to-zygotic transition – a period characterized by degradation of maternally-derived transcripts, zygotic genome activation, and initiation of cell motility. Moreover, we found that niclosamide did not affect embryonic oxygen consumption, suggesting that oxidative phosphorylation – a well-established target for niclosamide within intestinal parasites – may not play a role in niclosamide-induced epiboly delay. However, mRNA-sequencing revealed that niclosamide exposure during blastula and early-gastrula significantly impacted the timing of zygotic genome activation as well as the abundance of cytoskeleton- and cell cycle regulation-specific transcripts. In addition, we found that niclosamide inhibited tubulin polymerization in vitro, suggesting that niclosamide-induced

delays in epiboly progression may be driven by disruption of microtubule formation and cell motility within the developing embryo.

### 3.1 Introduction

Niclosamide (2',5-dichloro-4-nitrosalicylanilide) is an oral anthelmintic drug that is approved by the U.S. Food and Drug Administration and has been used since the 1960s for treatment of tapeworm infections in

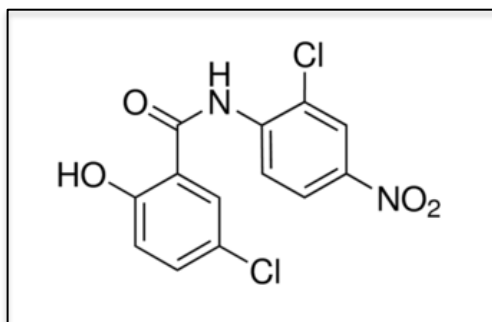


**Figure 10.** Structure of Niclosamide

humans and animals (Al-Hadiya, 2005; Andrews et al., 1982; Imperi et al., 2013).

Oral doses of niclosamide are well-tolerated and result in minimal side effects, an outcome that is due to low niclosamide absorption from the gastrointestinal tract to systemic circulation as well as rapid elimination and minimal bioaccumulation of any absorbed niclosamide (Andrews et al., 1982). Based on studies conducted to date, niclosamide is not suspected to result in birth defects or cause developmental toxicity, teratogenicity, mutagenicity, or carcinogenicity, although most animal studies supporting these conclusions relied on the use of oral doses of a niclosamide formulation that limits absorption within the gastrointestinal tract (WHO, 2002). Nevertheless, niclosamide should only be used by pregnant women when justified and use in the first trimester of pregnancy should only occur when necessary (Andrews et al., 1982; WHO, 2002).

The antiparasitic activity of niclosamide was first reported to be mediated through inhibition of mitochondrial oxidative phosphorylation (OXPHOS) and ATP production

(Weinbach and Garbus, 1969). This hypothesis was based on studies demonstrating that niclosamide exhibited uncoupling activity in isolated mitochondria (Tao et al., 2014; Yorke and Turton, 1974) as well as in vivo uncoupling measured by increased oxygen consumption in mice and invertebrates (Raheem et al., 1980; Tao et al., 2014). Niclosamide has also been reported to inhibit the conversion of NADH to NAD<sup>+</sup> within tapeworms (Park and Fioravanti, 2006) and increase intracellular reactive oxygen species and apoptosis in cell-based assays (Jin et al., 2010; Lee et al., 2014).

Recent drug repurposing screens have shown that niclosamide may be effective for treating a broad range of illnesses such as cancer (Chen et al., 2017; Li et al., 2014; Pan et al., 2012), bacterial infections (Gwisai et al., 2017; Imperi et al., 2013; Rajamuthiah et al., 2015; Tharmalingam et al., 2018), and Zika Virus (Cairns et al., 2018; Li et al., 2017; Xu et al., 2016). Although the mechanisms underlying these potential off-label uses remain largely unknown, these studies have reported that niclosamide has the potential to disrupt multiple signaling pathways including NF- $\kappa$ B, Wnt/ $\beta$ -catenin, STAT3, mTORC1, and Notch (Balgı et al., 2009; Chen et al., 2009; Jin et al., 2010; Ren et al., 2010; Suliman et al., 2016). Overall, the diversity of literature and observed effects of niclosamide exposure suggest that the mechanisms responsible for many therapeutic (as well as toxic) effects are likely complex and may not be directly related to niclosamide's activity as an inhibitor of mitochondrial function.

The low systemic bioavailability of niclosamide through oral administration – although key to its success as an anthelmintic – may prove to be a challenge for many of the proposed off-label uses. Therefore, new routes of exposure with increased absorption

will be essential for the future success of niclosamide in treating various conditions within humans (Li et al., 2014; Lu et al., 2016). Additionally, the broad range of uses for niclosamide currently being discussed introduces the possibility for in utero exposure within human populations. Therefore, there is a need to reevaluate the toxicity of niclosamide within a developmental context. In 2017, we carried out a high-content screen of the LOPAC<sup>1280</sup> (Library of Pharmacologically Active Compounds) library – a commercially available library of 1,280 marketed drugs, failed development candidates, and well-characterized small molecules widely used for validation of high-throughput screening assays. Based on this screen, niclosamide was one of the most potent developmental toxicants within zebrafish embryos during the first 25 h of development (Vliet et al., 2017), with exposure to 10  $\mu$ M niclosamide from 5-25 h post-fertilization (hpf) resulting in 100% embryo mortality (Vliet et al., 2017). Therefore, the overall objective of this study was to investigate the mechanism of toxicity of niclosamide at lower, non-lethal concentrations during early stages of zebrafish development.

## **3.2 Materials and Methods**

### *3.2.1 Animals*

Adult *fli1:egfp* zebrafish were maintained and bred on a recirculating system using previously described procedures (Vliet et al., 2017). We relied on *fli1:egfp* zebrafish for this study, as we originally identified niclosamide as a potential developmental toxicant using this strain (Vliet et al., 2017). For all experiments, newly fertilized eggs were collected within 30 min of spawning, rinsed, and reared in a temperature-controlled

incubator at 28°C under a 14:10-h light-dark cycle. All embryos were sorted and staged according to previously described methods (Kimmel et al., 1995). Adult breeders were handled and treated in accordance with an Institutional Animal Care and Use Committee (IACUC)-approved animal protocol (20150035) at the University of California, Riverside.

### *3.2.2 Chemicals*

Niclosamide ( $\geq 98\%$ ) was purchased from Sigma-Aldrich. Stock solutions were prepared in high performance liquid chromatography (HPLC)-grade dimethyl sulfoxide (DMSO) and stored within 2-mL amber glass vials with polytetrafluoroethylene-lined caps. Working solutions were prepared in embryo media (5 mM NaCl, 0.17 mM KCl, 0.33 mM CaCl<sub>2</sub>, 0.33 mM MgSO<sub>4</sub>, pH 7) immediately prior to each experiment.

### *3.2.3 Phenotypic Assessments*

The magnitude of epiboly delay within zebrafish embryos was assessed by exposing embryos (10 embryos per petri dish; three replicate petri dishes per treatment) from 2-6 hpf under static conditions at 28°C to 3 ml of vehicle (0.1% DMSO) or niclosamide concentrations (0.078-0.625  $\mu\text{M}$ ) that resulted in epiboly delay in the absence of mortality. At 6 hpf, embryos were removed from treatment solution, arranged laterally in an agarose mold, and imaged using a Leica MZ10 F stereomicroscope equipped with a DMC2900 camera. The height of the cell mass and percent epiboly – calculated as (cell mass progression over yolk sac)/yolk sac height\*100 – were measured for each embryo using ImageJ (v1.51m9).

To assess embryo recovery and identify potential sensitive windows of exposure, embryos (10 embryos per petri dish; three replicate petri dishes per treatment) were exposed under static conditions at 28°C to 3 ml of vehicle (0.1% DMSO) or niclosamide (0.156, 0.313, and 0.625  $\mu$ M) beginning at 2 hpf. Every hour until 6 hpf, embryos were removed from the exposure dish by aspirating treatment solution and transferring to clean embryo media. At 6 hpf, all embryos were imaged using procedures described above. To identify possible sensitive windows of exposure, exposures were carried out under similar conditions as the recovery assay, with exposures beginning every hour until 5 hpf.

To investigate the effect of early developmental niclosamide exposure on later stages of development, the effect of niclosamide-induced epiboly delay on 24-hpf embryos was assessed by exposing embryos (10 embryos per petri dish; three replicate petri dishes per treatment) statically at 28°C to 3 ml of vehicle (0.1% DMSO) or niclosamide (0.313  $\mu$ M) at time points equivalent to recovery and sensitive window assays. At 6 hpf, embryos were transferred to replicate petri dishes containing clean embryo media and incubated at 28°C until 24 hpf. At 24 hpf, viable embryos were arrayed into a 384-well plate, resulting in one embryo per well and 16 embryos per treatment. At 25 hpf, the plate was centrifuged for 2 min at 200 rpm to ensure all embryos were positioned at the well bottom. Using previously described procedures (Vliet et al., 2017), embryos were imaged on our ImageXpress Micro XLS Widefield High-Content Screening System and total body area was analyzed within MetaXpress 6.0.3.1658 (Molecular Devices, Sunnyvale, CA).

#### *3.2.4 Oxygen Consumption Assay*

We used 2-ml glass vials containing oxygen-sensitive sensors to monitor the oxygen concentration within the surrounding embryo media using an SDR SensorDish Reader (PreSens Precision Sensing GmbH, Regensburg, Germany). Zebrafish embryos were exposed to vehicle (0.1% DMSO) or niclosamide (0.156-0.625  $\mu\text{M}$ ) in groups of 10 embryos per petri dish from 2-6 hpf under static conditions at 28°C. At 6 hpf, embryos were rinsed three times with clean embryo media and placed into equilibrated sensor vials containing clean embryo media at a density of 20 embryos per vial, with four independent replicate vials per treatment. Oxygen concentrations were then measured at 28°C in a dark incubator over the course of 400 min. Oxygen consumption data were analyzed by comparing the slope of each time-dependent oxygen profile that excluded the initial 30-min lag necessary for vial equilibration. For all oxygen consumption experiments, a blank sample without embryos and a negative control (embryos exposed to embryo media alone) were included. All samples were tested using a linear regression and the blank slope was subtracted from the slope of each treatment.

#### *3.2.5 ATP Pre-Treatment Assay*

Embryos (10 embryos per well) were exposed to 100  $\mu\text{l}$  of vehicle (embryo media, as ATP is soluble in water) or ATP (5 or 10 mM) from 0.75-2 hpf within clear 96-well plates (Corning Incorporated, Corning, NY, USA). At 2 hpf, embryos were removed from wells and transferred to petri dishes (10 embryos per petri dish; three replicate petri dishes per treatment) containing vehicle (0.1% DMSO) or 0.313  $\mu\text{M}$  niclosamide. At 6 hpf,

embryos were removed from treatment solution and assessed for epiboly progression as described above.

### *3.2.6 mRNA-Sequencing*

Embryos (10 embryos per petri dish; nine petri dishes per treatment) were exposed under static conditions at 28°C to 10 ml of vehicle (0.1% DMSO) or 0.313 µM niclosamide from 1) 2-6 hpf or 4-6 hpf and 2) 2-3, 2-4, 2-5, or 2-6 hpf. Surviving embryos (30 per replicate pool; triplicate pools per treatment) were snap-frozen in liquid nitrogen at the end of each exposure, and then stored at -80°C until RNA extraction. Triplicate pools of 30 embryos per pool were homogenized in 2-ml cryovials using a PowerGen Homogenizer (Thermo Fisher Scientific, Waltham, MA, USA), resulting in a total of 36 samples. Following homogenization, an SV Total RNA Isolation System (Promega, Madison, WI, USA) was used to extract total RNA from each replicate sample per manufacturer's instructions.

Libraries were prepared using a QuantSeq 3' mRNA-Seq Library Prep Kit FWD (Lexogen, Vienna, Austria) and indexed by treatment replicate per manufacturer's instructions. Library quality and quantity were confirmed using our Qubit 3.0 Fluorometer and 2100 Bioanalyzer system, respectively. Libraries from two exposure scenarios were then pooled (12 libraries per pool), diluted to a concentration of 1.3 pM (with 1% PhiX control), and single-read (1X75) sequenced on our Illumina MiniSeq Sequencing System (San Diego, California, USA) using three separate 75-cycle High-Output Reagent Kits. All sequencing data were uploaded to Illumina's BaseSpace in real-time for downstream

analysis of quality control. Raw Illumina (fastq.gz) sequencing files (36 files totaling 8.24 GB) are available via NCBI's BioProject database under BioProject ID PRJNA454154, and a summary of sequencing run metrics are provided in Table S1 ( $\geq 92.41\%$  of reads were  $\geq Q30$ ). All 36 raw and indexed Illumina (fastq.gz) sequencing files were downloaded from BaseSpace and uploaded to Bluebee's genomics analysis platform (<https://www.bluebee.com>). Quality trimming of reads was performed within Bluebee using BBDuk (v35.92). Trimmed reads were aligned against the current zebrafish genome assembly (GRCz10) using STAR Aligner (v2.5.2a) with modified ENCODE settings. Aligned reads were then indexed, counted, and mapped using Samtools (v1.3), HTSeq-count (v0.6.0), and RSeQC (v2.6.4), respectively.

For 2-6 hpf and 4-6 hpf exposures, a DESeq2 application within Bluebee (Lexogen Quantseq DE 1.2) was used to identify significant treatment-related effects on transcript abundance (relative to vehicle controls) based on a false discovery rate (FDR) p-adjusted value  $< 0.05$ . Using DESeq2-identified transcripts, downstream analyses were run using Qiagen's Ingenuity Pathway Analysis (IPA). Statistically significant transcripts were uploaded to IPA, and human, rat, and mouse homologs were automatically identified within IPA using NCBI's HomoloGene. An Expression Analysis was then performed using a Fisher's Exact Test p-value threshold of 0.05 as the basis for identifying statistically significant pathways; the algorithm considered both direct and indirect relationships using Ingenuity Knowledge Base (genes only) as the reference set. To identify potential effects on maternal transcript degradation and zygotic genome activation, vehicle (0.1% DMSO) and niclosamide (0.313  $\mu\text{M}$ ) libraries from 2-3, 2-4, 2-5, and 2-6 hpf exposures were

normalized in Bluebee's DESeq2 application (Lexogen Quantseq DE 1.2). A list of zebrafish-specific maternal and zygotic transcripts was obtained from the literature (Harvey et al., 2013), and the sum of DESeq2-normalized read counts was calculated for zygotic and maternal transcripts within each library.

### *3.2.7 Whole-mount Immunohistochemistry*

Embryos (10 embryos per petri dish; nine replicate petri dishes per treatment) were exposed under static conditions 28°C from 2-6 hpf or 4-6 hpf to 3 ml of vehicle (0.1% DMSO) or niclosamide (0.313  $\mu$ M). At 6 hpf, embryos were removed from treatment solution, dechorionated by incubating in 10 mg/ml pronase for 10 min, pooled (30 per pool; three replicate pools) and fixed overnight in 4% paraformaldehyde/1X phosphate-buffered saline (PBS). Fixed embryos were labeled using a 1:100 dilution of zebrafish-reactive anti-acetylated  $\alpha$ -tubulin (Sigma) antibody and 1:500 dilution of Alexa Fluor 555-conjugated goat anti-mouse IgG2b (ThermoFisher Scientific). Stained embryos were imaged using a Leica MZ10 F stereomicroscope equipped with a DMC2900 camera. Tubulin fluorescence in the yolk sac, cell mass, and whole embryo was quantified using the Corrected Total Cell Fluorescence method for ImageJ (v1.51m9) (McCloy et al., 2014).

### *3.2.8 In-Vitro Tubulin Polymerization Assay*

A fluorescence-based porcine brain tubulin polymerization assay (Cytoskeleton, Inc.) was used to determine whether niclosamide interferes with polymerization of tubulin into microtubules in vitro. The rate of polymerization in the presence of vehicle (0.1%

DMSO), 3  $\mu\text{M}$  nocodazole (a known inhibitor of tubulin polymerization), or niclosamide (1.56-200  $\mu\text{M}$ ) was quantified in kinetic mode using a GloMax Multiplus Plate Reader (Promega) per manufacturer's instructions.

### *3.2.9 Statistical Analysis*

For all data, a general linear model (GLM) analysis of variance (ANOVA) ( $\alpha=0.05$ ) was performed using SPSS Statistics 24, as these data did not meet the equal variance assumption for non-GLM ANOVAs. Treatment groups were compared with vehicle controls, and time-points for recovery and sensitivity window assays were compared to 2-6 hpf exposures using pair-wise Tukey-based multiple comparisons of least square means to identify significant differences.

## **3.3 Results**

### *3.3.1 Epiboly Progression*

We first exposed embryos to a range of niclosamide concentrations (0.078-10  $\mu\text{M}$ ) from 2-6 hpf and determined that exposure to niclosamide resulted in a concentration-dependent arrest in epiboly at 6 hpf and increase in mortality at 24 hpf; at concentrations 2.5  $\mu\text{M}$  or higher, 100% mortality was observed at 24 hpf (data not shown). Exposure to lower niclosamide concentrations resulted in a concentration-dependent delay in epiboly progression, with a significant ( $\sim 0.8$  hr) delay starting at 0.156  $\mu\text{M}$  (Figure 11A and 11B). Moreover, we found that niclosamide-induced effects on epiboly at 6 hpf were dependent on niclosamide concentration and exposure duration.

When exposed to 0.156 and 0.313  $\mu\text{M}$  niclosamide, partial to full recovery occurred in the 2- to 4-hpf and 2- to 3-hpf exposure groups, respectively, relative to 2- to 6-hpf exposures (Figure 12A and 12C). In addition, after initiating exposure every hour to identify sensitive windows of niclosamide exposure, we found that initiation of niclosamide exposure at 2 or 3 hpf resulted in a higher magnitude of epiboly delay at 6 hpf (Figure 12B and 12D).

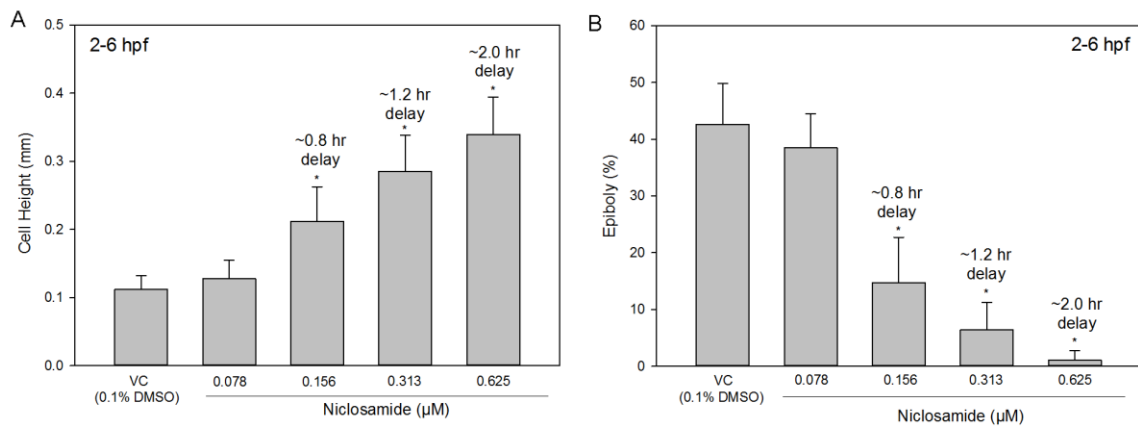


**Figure 11.** Initiation of exposure to niclosamide at 2 hpf results in epiboly delay at 6 hpf. Epiboly progression was quantified as cell height (mm) above yolk sac (A) and cell progression over yolk sac/total yolk height\*100 (or percent epiboly) (B). Data represent three independent replicate treatments (10 embryos per replicate) and are presented as mean  $\pm$  standard deviation. Asterisk denotes significant ( $p < 0.05$ ) difference relative to vehicle control.

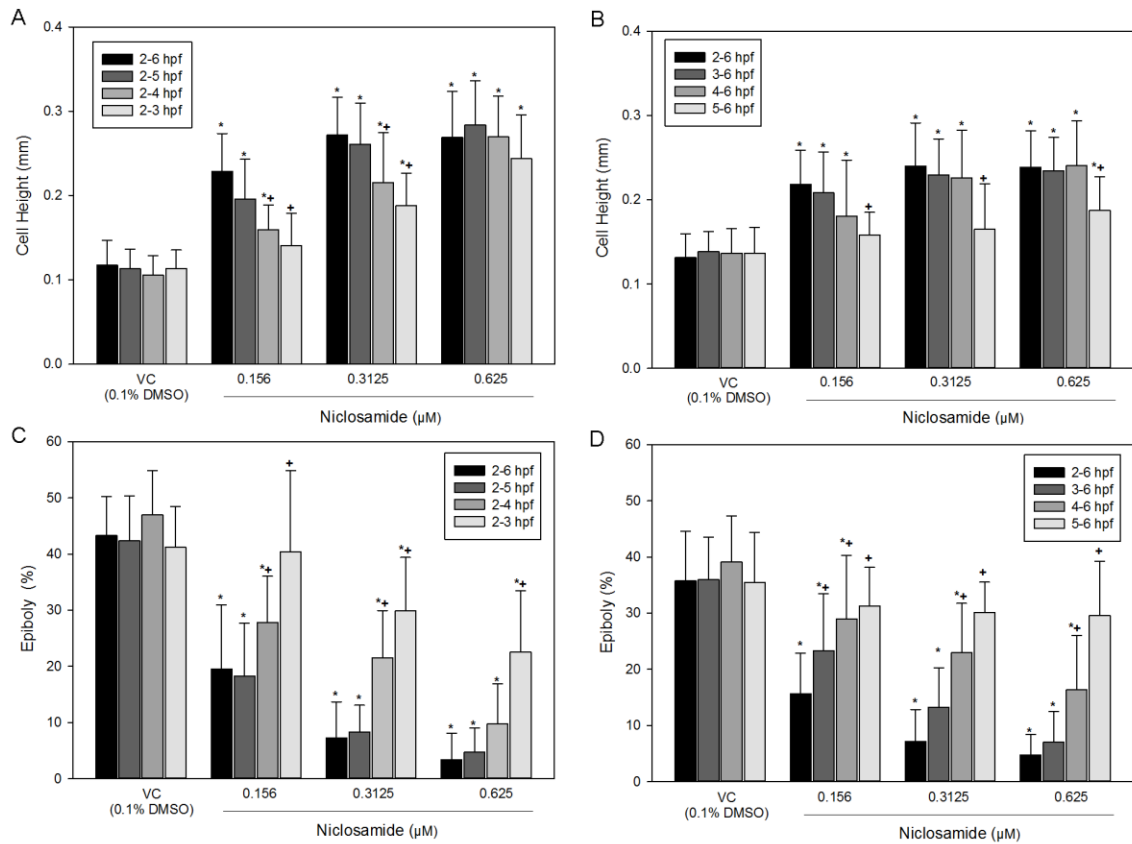


**Figure 12.** Niclosamide induces a delay in epiboly progression – an effect that increases in severity with longer exposure duration (A-B) and earlier exposure initiation (C-D). Epiboly progression was quantified as cell height (mm) above yolk sac and percent epiboly (cell progression over yolk sac/total yolk length). Data represent three independent replicate treatments (10 embryos per replicate) and are presented as mean  $\pm$  standard deviation.

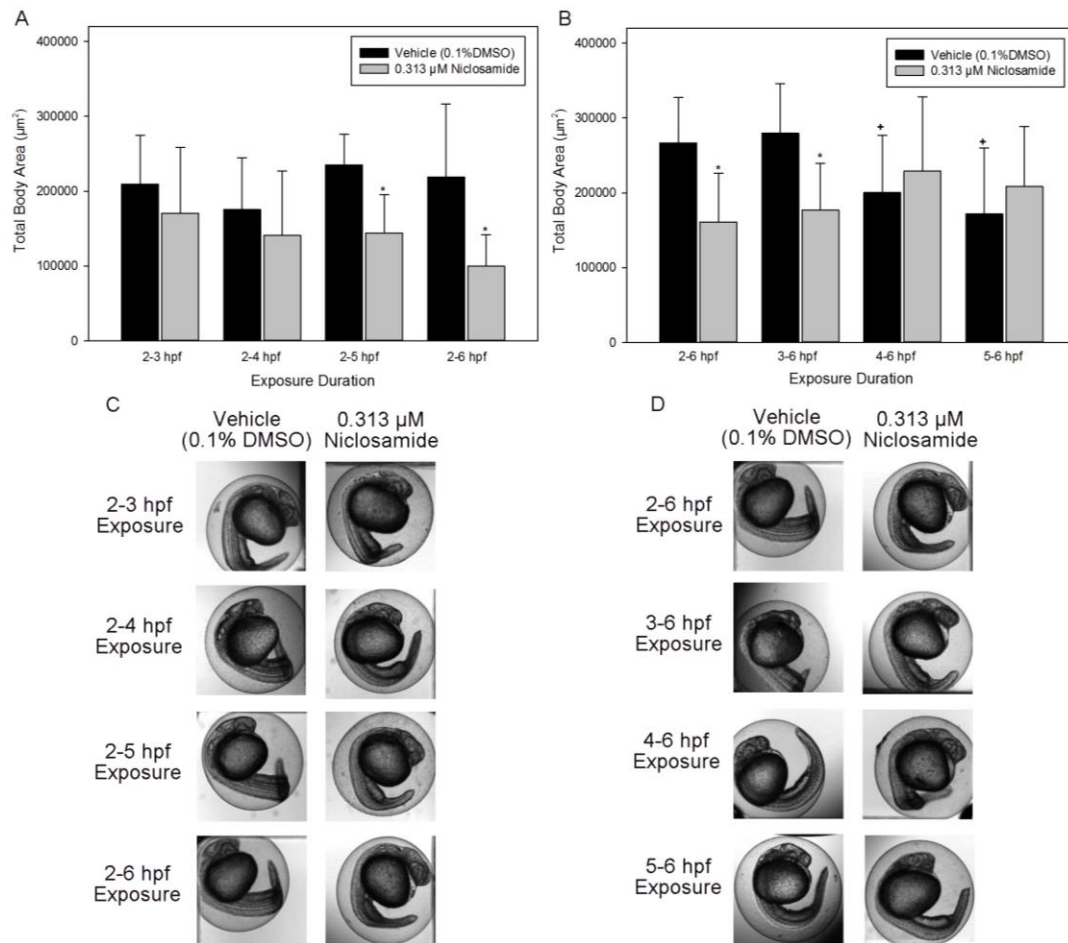


**Figure 13.** Exposure to 0.313 µM niclosamide from 2-6, 3-6, and 2-5 hpf results in a significant decrease in total body at 24 hpf. Panels A and B are based on a sample size of 16 embryos per treatment. Data are presented as mean ± standard deviation. Asterisk denotes significant ( $p < 0.05$ ) difference relative to vehicle control for the same time point. Cross (+) denotes significant difference relative to 2-6 hpf vehicle control. Representative images of 24-hpf embryos for each exposure scenario are shown in Panels C and D.

When embryos were exposed to niclosamide from 2-5 hpf, 2-6 hpf, or 3-6 hpf followed by incubation in clean media until 24 hpf, we found that total body area was significantly decreased within 24-hpf embryos, whereas total body area was not significantly decreased in embryos exposed from 4-6 hpf or 5-6 hpf (Figure 13). Collectively, these phenotypic assessments demonstrate that niclosamide exposure results

in epiboly delay in a concentration- and exposure duration-dependent manner, and that the susceptible window of niclosamide exposure is within blastula.

### 3.3.2 Oxygen Consumption

To test the hypothesis that niclosamide-induced epiboly delay may be due to effects on OXPHOS, we assessed the ability of niclosamide to interfere with oxygen consumption at early stages of embryonic development using vials containing oxygen-sensitive sensors. A density of 20 embryos per vial was identified as optimal based on preliminary experiments comparing oxygen consumption rates using 10, 20, and 30 embryos per vial (Figure 14A). Embryos exposed to 0.313  $\mu\text{M}$  from 2-6 hpf did not significantly alter oxygen consumption rates over a 400-min period following exposure (Figure 14B). Overall, these data suggest that niclosamide-induced epiboly delay may not be associated with uncoupling of OXPHOS.

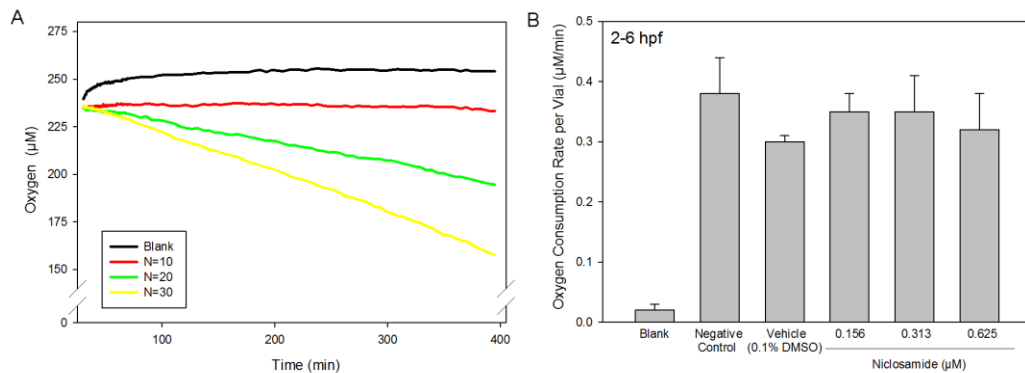


**Figure 14.** Exposure to niclosamide from 2-6 hpf does not significantly alter oxygen consumption rates over a 400-min period following exposure. In Panel A, data are presented as oxygen consumption profiles of vials containing either embryo media alone (blank), or groups of 10, 20, or 30 embryos per vial. In Panel B, data are presented as mean oxygen consumption rate  $\pm$  standard deviation across four independent replicates containing either embryo media alone (blanks) or 20 embryos per vial.

### 3.3.3 ATP Pre-Treatment Assay

We then tested the hypothesis that niclosamide-induced epiboly delay may be due to decreased ATP production. We first exposed embryos to a range of ATP concentrations (5-50 mM) from 0.75-2 hpf and determined that the maximum tolerated ATP concentration was <25 mM based on the absence of gross malformations and embryo mortality at 6 hpf (data not shown). Therefore, embryos were pre-treated to 5- or 10-mM ATP from 0.75-2 hpf and then treated with vehicle (0.1% DMSO) or 0.313  $\mu$ M niclosamide from 2-6 hpf. We found that pre-treatment with ATP did not block nor mitigate niclosamide-induced epiboly delay (Figure 15A and 15B), suggesting that niclosamide-induced epiboly delay may not be associated with a decrease in embryonic ATP concentrations following niclosamide exposure.

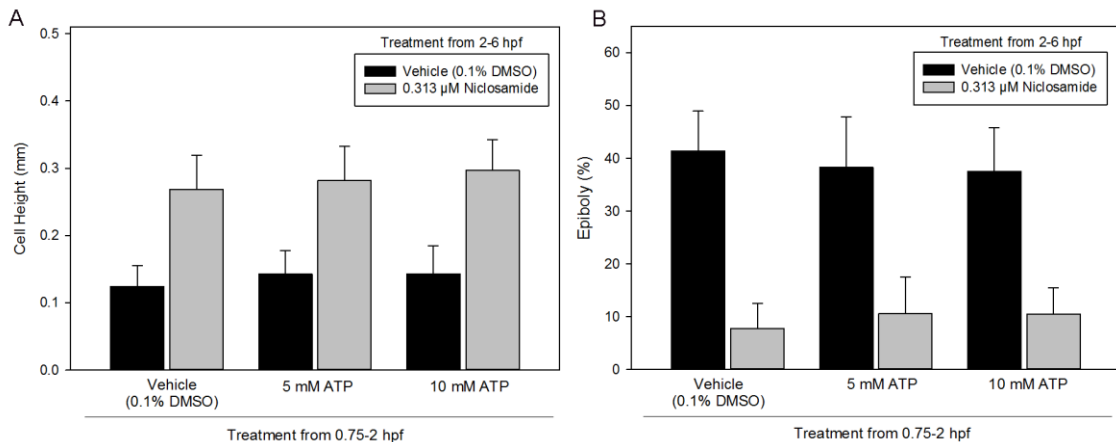


**Figure 15.** Pre-treatment with 5- or 10-mM ATP from 0.75-2 hpf does not significantly mitigate epiboly delay following exposure to 0.313  $\mu$ M niclosamide from 2-6 hpf. Epiboly progression represented as (A) cell height above yolk sac and (B) percent epiboly (cell progression over yolk sac/total yolk length\*100). Data represent the mean  $\pm$  standard deviation of three independent replicates, with a sample size of 10 embryos per replicate.

### *3.3.4 mRNA-Sequencing and Differential Gene Expression*

Exposure of embryos to 0.313  $\mu$ M niclosamide from 2-6 hpf significantly affected the abundance of 4,993 transcripts (relative to vehicle controls) at 6 hpf, where the abundance of 2,932 and 2,061 transcripts were significantly decreased and increased, respectively (Figure 16A). Following a two-hour exposure from 4-6 hpf, 1,959 transcripts were significantly affected (relative to vehicle controls) at 6 hpf, where 1,171 and 788 transcripts were significantly decreased and increased, respectively (Figure 16B). Interestingly, nearly 92% of significantly altered transcripts (1,795 total) in the 4- to 6-hpf exposure were also significantly affected in the 2- to 6-hpf exposure (Figure 16D).

Following automated identification of human, rat, or mouse homologs within IPA, approximately 64% (3,209 out of 4,993) and 66% (1,287 out of 1,959) of statistically significant transcripts from the 2- to 6-hpf and 2- to 4-hpf exposures, respectively, were included in IPA's analysis; the remaining statistically significant transcripts were excluded by IPA's analysis due to the absence of human, rat, and/or mouse orthologs within NCBI's Homologene database. Interestingly, based on IPA's canonical pathways, both exposure scenarios resulted in significant effects on pathways involved in protein synthesis (Figure 16C). At the transcript-level, the most significantly decreased transcripts were related to the cytoskeleton as well as gastrulation/epiboly and embryonic patterning (Table 1), whereas the most significantly increased transcripts were related to GTP/GDP binding, signal transduction, and cell cycle regulation (Table 1).

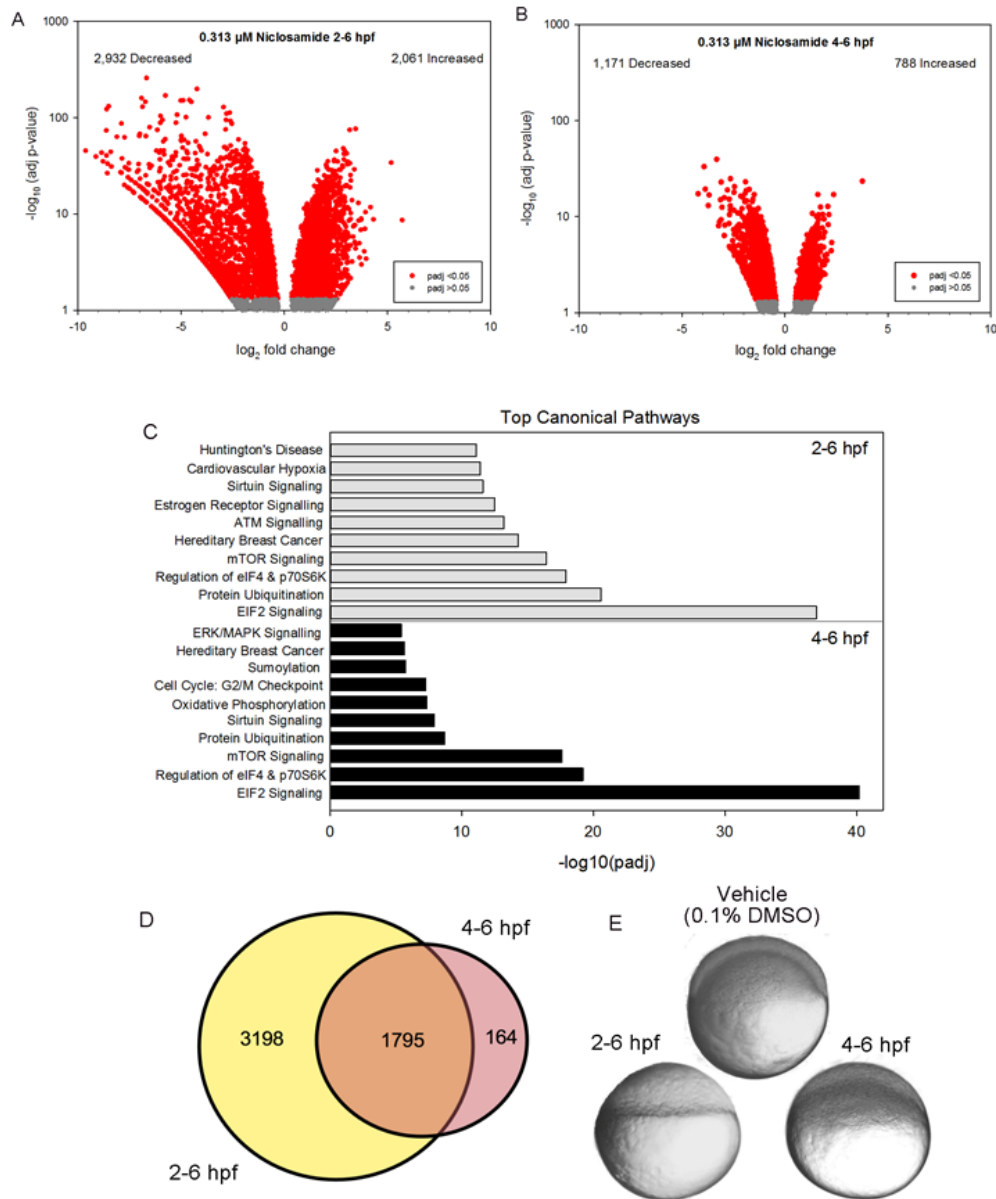


**Figure 16.** Exposure to 0.313  $\mu\text{M}$  niclosamide from 2-6 hpf and 4-6 hpf results in significant effects on transcript abundance (A-B) and pathways related to protein synthesis, cell cycle regulation, and various signaling pathways (C). Volcano plots showing the number of significantly different transcripts (red circles) within embryos exposed to 0.313  $\mu\text{M}$  niclosamide from 2-6 and 4-6 hpf (A-B), with the log<sub>2</sub>-transformed fold change on the x-axis and the -log<sub>10</sub>-transformed p-adjusted value on the y-axis. 1,795 significantly altered transcripts were common to both exposure durations (D). Canonical Pathways (C) affected by niclosamide exposure were identified by IPA's Expression-Analysis using a Fisher's exact p-value <0.05. Panel E shows representative images of embryos exposed to 0.313  $\mu\text{M}$  niclosamide from 2-6 and 4-6 hpf.

### 3.3.5 mRNA-Sequencing and the Maternal-to-Zygotic Transition

Exposure to 0.313  $\mu\text{M}$  niclosamide from 2-5 hpf resulted in significantly higher levels of maternal transcripts and significantly lower levels of zygotic transcripts (Figure 17). However, exposure from 2-6 hpf did not result in significant differences in maternal and zygotic transcripts despite a  $\sim 1.2\text{-h}$  delay in epiboly. These data suggest that niclosamide delays maternal transcript degradation and zygotic genome activation, an effect that may decrease in severity as embryos enter gastrula.

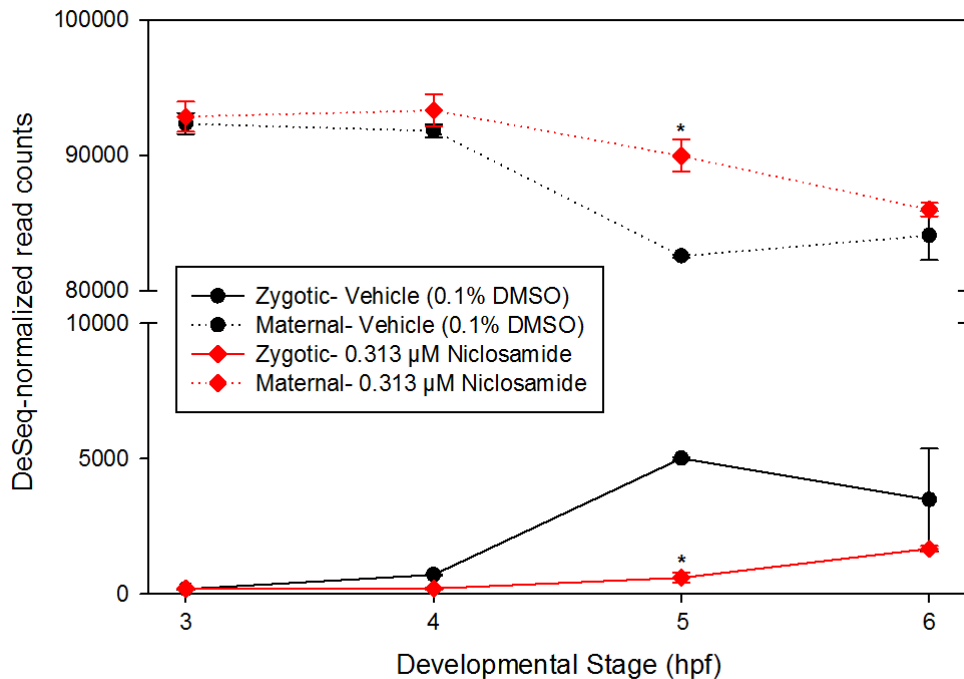


**Figure 17.** Exposure to 0.313  $\mu\text{M}$  niclosamide from 2-5 hpf results in a significant delay in degradation of maternal transcripts and initiation of zygotic genome activation. Data represent the mean  $\pm$  standard deviation of total DESeq-normalized read counts across three replicate libraries per treatment. Asterisk denotes significant ( $p < 0.05$ ) difference relative to stage-matched vehicle controls.

2-6 hpf Top 25 Decreased Transcripts					4-6 hpf Top 25 Decreased Transcripts							
Category	Gene	Shared	log2FoldChange	(- log10(FDR)	GO Terms	Category	Gene	Shared	log2FoldChange	(- log10(FDR)	GO Terms	
Cytoskeleton	krt92	Y	-9.63	45.32	Cytoskeletal filament	Cytoskeleton	krt17	N	-4.22	17.31	Cytoskeletal filament	
	krt4	N	-8.86	43.21	Cytoskeletal filament		zgc:110712	N	-3.69	16.78	Cytoskeletal filament	
	krt18	N	-8.11	63.26	Cytoskeletal filament		krt5	N	-3.10	22.85	Cytoskeletal filament	
	cyt11	N	-7.59	18.85	Cytoskeletal filament		krt96	Y	-2.95	15.78	Cytoskeletal filament	
	add3b	N	-7.56	28.89	Cytoskeleton		zgc:110333	N	-2.93	8.15	Structural Activity	
	evpla	Y	-7.53	28.79	Intermediate filament binding		evpla	Y	-2.79	18.91	Intermediate filament binding	
	krt97	N	-7.34	17.09	Cytoskeletal filament		krt92	Y	-2.65	24.74	Cytoskeletal filament	
	krt96	Y	-7.23	21.14	Cytoskeletal filament		tmsb1	N	-2.63	12.13	Actin filament organization	
Epiboly/Gastrulation	cldne	N	-8.41	44.12	Epiboly involved in gastrulation	Epiboly/Gastrulation	cyt1	Y	-3.93	33.12	Cell migration involved in gastrulation	
	cyt1	Y	-7.72	30.44	Cell migration involved in gastrulation		apoc1	N	-3.32	39.45	Cell migration involved in gastrulation	
Lipid & Membrane	atp4	N	-7.89	26.73	Lipid catabolism	Lipid & Membrane	zgc:101640	N	-2.69	10.47	Phospholipid transport	
	mtp	N	-7.20	20.86	Lipid Metabolism		mal2	N	-3.23	8.04	Membrane Integrity	
Development	asb11	N	-8.57	33.32	Notch Signalling, protein ubiquitination	Development	zgc:91849	N	-2.50	7.32	Membrane Integrity	
	tbx16	N	-8.51	131.29	Left/right symmetry		her7	N	-3.73	13.03	Anterior/posterior patterning	
	szl	N	-7.29	16.56	dorsal/ventral signalling		efnb2a	N	-2.72	8.45	Anterior/posterior patterning	
Transcription	vgll4l	N	-8.58	26.49	Transcription	Other	mespab	N	-2.66	4.70	Somite rostral/caudal axis specification	
	polr3gla	N	-7.90	26.78	Transcription		cd44a	N	-2.49	4.96	Cell adhesion	
	sb.cb81	N	-7.53	33.56	UTR-mediated mRNA destabilization		hk1	N	-2.52	4.39	Glycolysis	
Other	aldob	N	-8.63	73.66	Glycolysis	rabgap1l2	N	-2.65	11.77	Intracellular protein transport		
	fb06f03	N	-8.62	40.44	Fin regeneration	anxa1c	N	-2.68	4.77	Calcium ion binding		
	stm	N	-8.61	122.52	Otic placode formation	lut9d	N	-2.69	4.83	Protein glycosylation		
	lye	N	-8.38	31.03	Cellular adhesion and signaling	sox2	N	-2.70	4.88	Fin regeneration		
	sox11a	N	-7.51	18.32	Brain development	hsd17b14	N	-2.71	15.13	Oxoreductase activity		
	zic2b	N	-7.94	27.11	Regulation of retinoic acid receptor signaling	znf750	N	-2.95	6.35	Cell differentiation		
	dnase114.1	N	-7.58	24.00	DNA catabolism	im:7150988	N	-3.19	8.81	Cellular response to xenobiotics		
2-6 hpf Top 25 Increased Transcripts					4-6 hpf Top 25 Increased Transcripts							
Category	Gene	Shared	log2FoldChange	(- log10(FDR)	GO Terms	Category	Gene	Shared	log2FoldChange	(- log10(FDR)	GO Terms	
GTP/GDP	zgc:162879	N	3.13	11.28	GTP binding	GTP/GDP	ar4aa	Y	1.95	2.50	GTPase mediated signal transduction	
	ar4aa	Y	3.08	34.78	GTPase mediated signal transduction		btg4	N	2.10	8.25	Cell proliferation	
Cell Cycle	moto	N	3.70	6.83	Meiotic cell cycle	Cell Cycle	cdca9	N	1.73	2.73	Cell division	
	mtus1a	N	2.9	42.0	Cell cycle		zw10	N	1.70	4.58	Mitotic cell cycle	
	cdc45	N	2.9	36.7	Cell Cycle		zgc:113425	N	2.14	10.47	Membrane component	
Metabolism	hbegfa	N	3.39	28.95	Cell proliferation	Lipid & Membrane	slch211157b11.12	N	1.86	6.05	Membrane component	
	ppp	N	4.32	8.78	Metabolic process		vps9d1	N	1.84	3.38	Membrane component	
	lpg	N	3.05	33.86	Metabolic process		zgc:152977	Y	1.74	12.55	Cytoskeletal anchoring	
Phosphorylation	zgc:73340	N	3.02	19.81	Metabolic process	Cytoskeleton	zgc:56231	N	1.94	3.92	Microtubule-based movement	
	ulk1a	Y	3.59	13.00	Phosphorylation		Protein Transport	srx10a	N	1.90	9.43	Protein transport
	mos	N	3.21	25.35	Phosphorylation			stx11a	N	1.77	2.42	Protein transport
	ctdsp1	N	2.95	11.27	Phosphatase			egln3	N	3.77	23.38	REDOX processes
arhgap32a	N	2.9	45.4	Phosphorylation	sl.rp71-45k5.2	N		2.37	16.97	Transcription		
DNA Repair	apex2	N	3.28	13.87	DNA repair	Other	codc15	Y	2.28	5.36	Unfolded protein binding	
	erc4	N	3.0	19.6	DNA repair		igfbp1a	N	2.26	4.42	Response to hypoxia	
Other	dcun1d4	Y	5.18	34.02	Ubiquitin-protein transferase	dcun1d4	Y	2.09	12.76	Ubiquitin-protein transferase		
	alg13	N	3.61	8.51	Dorsal/ventral pattern formation	cbx8b	N	2.05	4.05	Hematopoietic progenitor cell differentiation		
	codc115	Y	3.42	7.64	Unfolded protein binding	ulk1a	Y	2.04	3.50	Phosphorylation		
	sytl4	N	3.35	7.41	Intracellular protein transport	gford2	N	1.88	4.80	Oxoreductase activity		
	dig5a	N	3.22	22.17	Apoptosis	mier3b	N	1.87	6.12	DNA binding		
	trim35-29	N	3.18	33.56	Carbonate dehydrogenase	mical2b	N	1.84	10.51	Endocytic recycling		
	bmb	N	3.17	74.62	Pronuclear fusion	cyp1b1	N	1.83	7.63	Xenobiotic metabolic process		
	osbp3a	N	3.12	5.78	Lipid transport	pim2	N	1.74	4.93	Apoptosis		
	asf1bb	N	3.06	32.67	Transcription	jost2	N	1.71	2.66	CNS morphogenesis		
	zgc:152977	Y	2.9	12.0	Cytoskeleton	tbpl2	N	1.71	2.46	Embryo pattern specification		

**Table 1.** Top 25 significantly decreased or increased transcripts ranked by fold change for each exposure duration. Gene Ontology (GO) terms were retrieved from The Zebrafish Information Network (<http://zfin.org>).

### 3.3.6 In-Vitro Tubulin Polymerization Assay

Zebrafish embryos exposed to 0.313  $\mu\text{M}$  niclosamide from 2-6 hpf or 4-6 hpf did not result in a significant effect on tubulin (based on total fluorescence) within the embryo yolk sac, cell mass, or whole embryo (Figure 18A). These results suggest that niclosamide does not alter the abundance nor localization of tubulin within the zebrafish embryo. However, within an in vitro tubulin polymerization assay, niclosamide resulted in a concentration-dependent decrease in tubulin polymerization starting at 12.5  $\mu\text{M}$  niclosamide (Figure 18B), suggesting that niclosamide may be inhibiting the formation of microtubule networks in vitro.

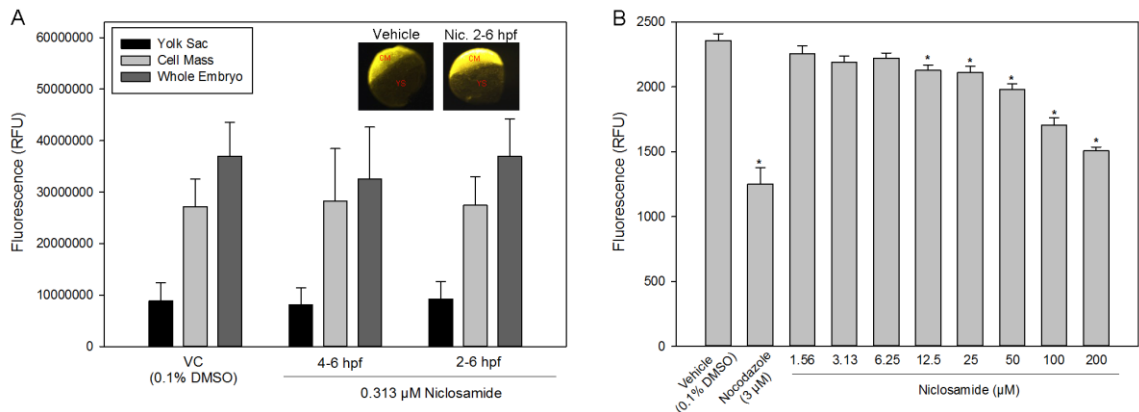


**Figure 18.** Niclosamide exposure from 2-6 or 4-6 hpf does not significantly affect tubulin abundance nor localization in the yolk sac, cell mass, or whole embryo (A), whereas niclosamide results in a significant, concentration-dependent decrease in tubulin polymerization in vitro (B). Fluorescence data within Panel A are presented as mean fluorescence (relative fluorescence units, or RFU)  $\pm$  standard deviation across 20 embryos. In vitro polymerization data within Panel B are presented as mean fluorescence (RFU)  $\pm$  standard deviation across four independent replicates. Nocodazole was used as a positive control for the inhibition of tubulin polymerization. CM denotes cell mass and YS denotes yolk sac.

### 3.4 Discussion

Epiboly is characterized by spreading of the cell mass over the yolk sac – an important process that plays a prominent role in embryo gastrulation and specification of the dorsoventral axis (Kimmel et al., 1995; Lepage and Bruce, 2010). Epiboly is a process that is shared among vertebrates (Solnica-Krezel, 2005), and epiboly delay is an adverse outcome that has been observed in response to a wide range of compounds, many of which are thought to target the mitochondrial electron transport chain (Lai et al., 2013; Legradi et al., 2014; Mendelsohn and Gitlin, 2008). In this study, we demonstrated that exposure to niclosamide during early zebrafish embryogenesis resulted in a concentration-dependent delay in epiboly progression ranging from ~0.8 to 2.0 h relative to vehicle controls, an effect that was more severe with increasing exposure duration and increasingly early exposure initiation.

Given that mitochondrial OXPHOS is responsible for the majority of oxygen metabolism and ATP production within complex organisms and oxygen consumption directly reflects OXPHOS (Stackley et al., 2011), we first leveraged oxygen consumption as a simple, non-invasive readout to evaluate potential OXPHOS dysfunction (Legradi et al., 2014; Raheem et al., 1980; Tao et al., 2014; Wilson et al., 1983). While niclosamide-induced epiboly delay may be indicative of OXPHOS uncoupling, embryos exposed to 0.313  $\mu$ M niclosamide from 2-6 hpf did not significantly alter oxygen consumption rates over a 400-min period within clean media from 6-13 hpf. Additionally, ATP pretreatment prior to niclosamide exposure did not mitigate niclosamide-induced epiboly delay. As increased oxygen consumption and inhibition of ATP production are downstream

consequences of OXPHOS uncoupling, our data suggest that niclosamide-induced epiboly delay may not be a result of OXPHOS disruption but, rather, may be acting through an alternative mechanism (Bestman et al., 2015).

The maternal-to-zygotic transition (MZT) within an embryo represents the transition from reliance on maternally-derived transcripts to de novo transcription of the zygotic genome. The MZT occurs in all animals and involves a host of changes in the developing embryo, including initiation of cell motility (Kimmel et al., 1990; Langley et al., 2014; Yartseva and Giraldez, 2015). In zebrafish, this transition occurs from ~2-3 hpf and is required for epiboly progression (Kane et al., 1996; Kimmel et al., 1995; Langley et al., 2014). In our study, exposure to niclosamide from 2-5 hpf or 2-6 hpf resulted in a more severe effect on epiboly progression relative to niclosamide exposure from 2-3 hpf or 2-4 hpf. In addition, initiation of niclosamide exposure at 2 or 3 hpf resulted in a more severe effect on epiboly progression and embryonic development by 24 hpf relative to exposures initiated at 4 or 5 hpf. Collectively, these data suggest the sensitive window of niclosamide exposure is within blastula, a period of development that encompasses the MZT. Indeed, niclosamide exposure resulted in significant increases in transcripts specific to transcriptional processes, suggesting that niclosamide may be targeting processes involved in the initiation of the MZT.

We then tested the hypothesis that niclosamide exposure blastula and early-gastrula leads to effects on maternal transcript degradation and zygotic genome activation. Indeed, exposure to niclosamide at the initiation of the MZT (2 hpf) resulted in an increased abundance of maternal transcripts and decreased abundance of zygotic transcripts at 5 hpf

relative to time-matched vehicle controls, suggesting that niclosamide may delay maternal transcript degradation and zygotic genome activation. However, maternal and zygotic transcripts were not significantly different at 6 hpf, suggesting that impacts to both sets of transcripts may decrease in severity as embryos progress through early-gastrula. As zygotic transcription is essential for epiboly initiation and progression (Kane et al., 1996; Lepage and Bruce, 2010), niclosamide-induced delays in zygotic genome activation may be responsible for downstream delays in epiboly – effects that may be due to delays in maternal transcript degradation. Among the most abundant maternal transcription factors present within developing embryos are *nanog*, *sox19b* and *pou5f1*, all of which have been shown to regulate zygotic genome activation in zebrafish (Lee et al., 2013). Indeed, niclosamide exposure resulted in significant impacts on *nanog*, *sox19b*, and *pou5f1* transcripts following a 2-6 hpf exposure, suggesting that niclosamide may disrupt transcript levels of key maternal transcription factors involved in zygotic genome activation and epiboly progression.

In addition to delays in maternal transcript degradation and zygotic genome activation, our mRNA-sequencing data demonstrated that numerous cytoskeleton-related transcripts were significantly altered following niclosamide exposure, including beta (*tubb2b*) and alpha (*tuba1a*, *tuba1b*, *tuba8l4*, and *tuba4l*) tubulin transcripts, suggesting that the cytoskeleton may be affected within epiboly-delayed embryos exposed to niclosamide. Prior studies have demonstrated that movement of the blastoderm around the yolk sac occurs through interactions with microtubules present in the yolk sac (Solnica-Krezel and Driever, 1994; Strahle and Jesuthasan, 1993), and epiboly progression in zebrafish

embryos is dependent on the presence of intact yolk sac microtubules that shorten as epiboly progresses (Jesuthasan and Strähle, 1997). Our whole-mount immunohistochemistry data suggest that niclosamide does not impact the abundance nor localization of tubulin from the yolk sac or embryonic blastodisc (cell mass). However, our *in vitro* tubulin polymerization data suggest that niclosamide inhibits polymerization of tubulin dimers into microtubules.

In conclusion, this study demonstrated that (1) niclosamide exposure during early zebrafish embryogenesis results in a concentration-dependent delay in epiboly that may be independent of OXPPOS disruption; (2) the window of sensitivity for niclosamide exposure is within blastula and coincides with the timing of the MZT; (3) niclosamide delays degradation of maternal transcripts and initiation of zygotic genome activation; and (4) niclosamide results in a concentration-dependent decrease in tubulin polymerization *in vitro*. Overall, our data suggest that niclosamide may be preventing the progression of epiboly by disrupting the timing of zygotic genome activation, an effect that may be mediated through disruption of maternal transcription factors and/or microtubule polymerization. Therefore, future studies are needed to 1) confirm the potential target and mechanism of action for niclosamide within zebrafish embryos and 2) determine whether similar effects on epiboly occur *in utero* within mammalian models following non-oral routes of niclosamide exposure.

## **Chapter 4: Potential Mechanism of Niclosamide Toxicity During Early Embryogenesis**

### **4.0 Abstract**

Niclosamide is an anthelmintic drug used worldwide for the treatment of tapeworm infections. Recent drug repurposing screens have highlighted the broad bioactivity of niclosamide across diverse mechanisms of action. As a result, niclosamide is being evaluated for a range of alternative drug-repurposing applications, including the treatment of cancer, bacterial infections, and Zika virus. As new applications of niclosamide will require non-oral delivery routes that may lead to exposure in utero, it is important to understand the mechanism of niclosamide toxicity during early stages of embryonic development. Previously, we showed that niclosamide induces a concentration-dependent delay in epiboly progression in the absence of effects on oxidative phosphorylation – a well-established target for niclosamide. Therefore, the overall objective of this study was to further examine the mechanism of niclosamide-induced epiboly delay during zebrafish embryogenesis. Based on this study, we found that (1) niclosamide exposure during blastulation resulted in disruption of yolk sac integrity and actin networks as well as an increase in cell size within the blastomere; (2) zebrafish embryos were more sensitive to niclosamide exposure than human embryonic stem cells (hESCs); (3) niclosamide exposure significantly altered amino acids and polar metabolites related to aminoacyl-tRNA biosynthesis in the absence of effects on lipid metabolism; and (4) niclosamide significantly altered transcripts related to translation, transcription, and mRNA processing. Overall, our findings suggest that niclosamide exposure during

blastulation alters the normal trajectory of embryogenesis through interference with maternal mRNA translation and zygotic genome transcription.

#### **4.1 Introduction**

Niclosamide (2',5-dichloro-4-nitro salicylanilide) is an oral anthelmintic drug that is approved by the U.S. Food and Drug Administration and has been used since the 1960s for the treatment of intestinal parasites, such as tapeworm, in humans and animals (Andrews et al., 1982). The antiparasitic activity of niclosamide is thought to be mediated through disruption of mitochondrial oxidative phosphorylation (OXPHOS) and inhibition of ATP production (Weinbach and Garbus, 1969), a hypothesis based on several studies that identified uncoupling activity of niclosamide in isolated mitochondria and invertebrates (Raheem et al., 1980; Tao et al., 2014; Yorke and Turton, 1974).

Beyond its traditional use in public health and veterinary medicine, niclosamide has recently received attention as a promising drug repurposing candidate for the potential treatment of a broad range of conditions including cancer (Chen et al., 2017; Pan et al., 2012), bacterial infections (Imperi et al., 2013; Tharmalingam et al., 2018), endometriosis (Prather et al., 2016), and Zika virus (Cairns et al., 2018; Li et al., 2017; Xu et al., 2016). Although the mechanisms underlying many of these alternative uses remains unclear, these studies have reported that niclosamide can interact with a wide range of signaling pathways including NF- $\kappa$ B, Wnt/ $\beta$ -catenin, NLRP3, STAT3, mTORC1, Notch, and LC3 lipidation (Balgi et al., 2009; Chen et al., 2009; Domalaon et al., 2019; Jin et al., 2010; Mook et al., 2019; Newton, 2019; Ren et al., 2010; Suliman et al., 2016; Tran and Kitami, 2019). The

broad bioactivity of niclosamide across diverse mechanisms of action raises questions about its specificity as an OXPHOS uncoupler and suggests that mechanisms underlying potential therapeutic effects may be complex.

As an anthelmintic drug, niclosamide is administered orally and is generally well-tolerated, demonstrating very low toxicity and minimal side effects (WHO, 2002). This is due, in part, to niclosamide's low oral bioavailability and rapid metabolism within the gastrointestinal tract (Espinosa-Aguirre et al., 1991), a chemical feature that makes it ideal for treatment of intestinal parasites but, on the other hand, may prove challenging within many of the proposed off-label uses. To address this challenge, new formulations of niclosamide or non-oral routes of exposure will likely be required to maintain efficacy within the context of unconventional uses (Li et al., 2014). Considering this need for alternative drug delivery along with the wide range of observed bioactivity, a further understanding of the potential toxicity of niclosamide is necessary.

Previous work in our lab has highlighted the potential for developmental toxicity following niclosamide exposure during early embryogenesis (Vliet et al., 2018). Using embryonic stages of zebrafish as a model for early development, we demonstrated that exposure to low micromolar concentrations of niclosamide results in a concentration-dependent delay in epiboly during gastrulation, a key developmental process that involves spreading of the embryonic cell mass around the yolk sac. Moreover, we found that niclosamide did not affect embryonic oxygen consumption, suggesting that oxidative phosphorylation may not play a role in niclosamide-induced epiboly delay. However, mRNA-sequencing revealed that niclosamide may be preventing the progression of epiboly

by disrupting the timing of zygotic genome activation, an effect that may be mediated through disruption of maternal transcriptional processes and/or the formation of cytoskeletal actin networks (Vliet et al., 2018).

Activation of the zygotic genome – and subsequent degradation of maternally-supplied mRNA – is a key developmental landmark that is conserved across vertebrate species, although the precise timing of this transition varies by species (Sha et al.; Yartseva and Giraldez, 2015). Regardless of when it occurs, the maternal-to-zygotic transition (MZT) is critical for normal embryonic development (Duffié and Bourc’his, 2013; Langley et al., 2014; Li et al., 2013). In addition to the MZT, the presence of an intact cytoskeleton network is also required for proper cell division, cell migration, and progression of embryonic development (Cheng et al., 2004; Gallicano, 2001; Solnica-Krezel, 2005; Solnica-Krezel and Driever, 1994). Given the importance of the MZT and cytoskeletal networks in embryonic development across species, additional studies are needed to understand how niclosamide may disrupt these early developmental processes. Therefore, using zebrafish embryos and human embryonic stem cells as model systems, the overall objective of this study was to investigate the mechanism of toxicity of niclosamide.

## **4.2 Materials and Methods**

### *4.2.1 Animals*

Adult wildtype (strain 5D) zebrafish were maintained and bred on a recirculating system using previously described procedures (Vliet et al., 2017). For all experiments, newly fertilized eggs were collected within 30 min of spawning, rinsed, and reared in a temperature-controlled incubator at 28°C under a 14:10-h light-dark cycle. All embryos

were sorted and staged according to previously described methods (Kimmel et al., 1995). All adult breeders were handled and treated in accordance with an Institutional Animal Care and Use Committee (IACUC)-approved animal use protocols (#20150035 and #20180063) at the University of California, Riverside.

#### *4.2.2 Chemicals*

Niclosamide ( $\geq 98\%$  purity) was purchased from Sigma-Aldrich (St. Louis, MO, USA). Stock solutions were prepared in high performance liquid chromatography (HPLC)-grade dimethyl sulfoxide (DMSO) and stored within 2-mL amber glass vials with polytetrafluoroethylene-lined caps. Working solutions were prepared in particulate-free water from our recirculating system (pH and conductivity of  $\sim 7.2$  and  $\sim 950 \mu\text{S}$ , respectively) immediately prior to each experiment, resulting in 0.1% DMSO within all vehicle control and treatment groups.

#### *4.2.3 Whole-mount Immunohistochemistry*

Embryos (10 embryos per petri dish; three replicate petri dishes per treatment) were exposed under static conditions at  $28^\circ\text{C}$  from 2 to 5 hpf to either vehicle (0.1% DMSO) or niclosamide ( $0.313 \mu\text{M}$ ) – a concentration that reliably induces epiboly delay in zebrafish (Vliet et al., 2018). At 5 hpf, embryos were removed from treatment solution, individual treatment dishes pooled (30 per pool; three replicate pools) and fixed overnight in 4% paraformaldehyde/1X phosphate buffered saline (PBS). Following fixation, embryos were manually dechorionated, rinsed, and incubated overnight in a 1:200 dilution of fluorescein-

labelled phalloidin (ThermoFisher Scientific, Waltham, MA, USA). Stained embryos were imaged using a Leica MZ10 F stereomicroscope equipped with a DMC2900 camera. Actin fluorescence localized within the yolk sac was quantified within Adobe Photoshop. The yolk sac was selected manually – from immediately below the cell mass boundary to the vegetal pole – for each embryo and a color mask was created by selecting the stained area in control embryos. Average cell area was determined by manually tracing 10 randomly selected cells on each embryo (50 total embryos), resulting in a total of 500 measurements.

#### *4.2.4 Whole-Embryo Metabolomics*

To extract metabolites from zebrafish embryos, 500  $\mu\text{L}$  of ice-cold solvent (30:30:20:20 MeOH:ACN:IPA:water) was added to pools of 30 embryos. Samples were then sonicated 15 min, vortexed 15 min, sonicated 15 min, then centrifuged at 16,000  $\times g$  at 4°C for 15 min. Supernatant was transferred to glass HPLC vials for LC-MS analysis.

Untargeted non-polar metabolomics was performed on a Xevo G2-XS quadrupole time-of-flight mass spectrometer (Waters, Milford, MA, USA) coupled to an H-class UPLC system (Waters, Milford, MA, USA). Separations were carried out on a CSH C18 column (2.1  $\times$  100 mm, 1.7  $\mu\text{M}$ ) (Waters, Milford, MA, USA). The mobile phases were (A) 60:40 acetonitrile:water with 10 mM ammonium formate and 0.1% formic acid and (B) 90:10 isopropanol:acetonitrile with 10 mM ammonium formate and 0.1% formic acid. The flow rate was 350  $\mu\text{L}/\text{min}$  and the column was held at 50°C. The injection volume was 1  $\mu\text{L}$ . The following gradient program (with respect to mobile phase B) was used: 0-1 min, 10% B; 1-3 min, 20%, 3-5 min, 40% B; 5-16 min, 80% B; 16-20 min 99% B; 20-20.5 min,

10% B. Prior to LC-MS analysis, samples were diluted 40-fold to prevent detector saturation. The MS was operated in positive ion mode (50 to 1200 m/z) with a 100 ms scan time. Source and desolvation temperatures were 120° C and 500°C, respectively. Desolvation and cone gas were set to 1000 and 150 L/hr., respectively. All gases were nitrogen except the collision gas (argon). Capillary voltage was 1 kV. A quality control sample, generated by pooling equal aliquots of each sample, was analyzed every 4-5 injections to monitor system stability and performance. Samples were analyzed in random order. Leucine enkephalin was infused and used for mass correction.

Targeted polar metabolomics was performed on a TQ-XS triple quadrupole mass spectrometer (Waters, Milford, MA, USA) coupled to an I-class UPLC system (Waters, Milford, MA, USA). Separations were carried out on a ZIC-pHILIC column (2.1 x 150 mm, 5 µM) (EMD Millipore). The mobile phases were (A) water with 15 mM ammonium bicarbonate adjusted to pH 9.6 with ammonium hydroxide and (B) acetonitrile. The flow rate was 200 µL/min and the column was held at 50°C. The injection volume was 1 µL. The following gradient program (with respect to mobile phase B) was used: 0-16 min, 90% B; 16-18 min, 20% B; 18-28 min, 90% B. The MS was operated in selected reaction monitoring mode. Source and desolvation temperatures were 150°C and 500°C, respectively. Desolvation and cone gases were set to 1000 and 150 L/hr., respectively. Collision gas was set to 0.15 mL/min. All gases were nitrogen except the collision gas (argon). Capillary voltage was 1 kV in positive ion mode and 2 kV in negative ion mode. A quality control sample, generated by pooling equal aliquots of each sample, was analyzed

every 4-5 injections to monitor system stability and performance. Samples were analyzed in random order.

Data processing (peak picking, alignment, deconvolution, integration, normalization, and spectral matching) for untargeted non-polar metabolomics was performed in Progenesis Qi software (Nonlinear Dynamics, Durham, NC, USA). Data were normalized to total ion abundance. Features with a coefficient of variation (CV) greater than 20% or with an average abundance less than 200 in the quality control injections were removed (Dunn et al., 2011). To help identify features that belong to a single metabolite, features were assigned a cluster ID using RAMClust (Broeckling et al., 2014). An extension of the metabolomics standard initiative guidelines was used to assign annotation level confidence (Schymanski et al., 2014; Sumner et al., 2007). Several MS/MS metabolite databases were searched against including Metlin, Mass Bank of North America, Lipidblast, and an in-house database. Data for targeted polar metabolomics were processed and peaks integrated with the open source software Skyline (<https://skyline.ms>) (MacLean et al., 2010). Q values were generated by performing the Benjamini-Hochberg correction of p-values generated from an Analysis of Variance (ANOVA) in R using the aov function.

#### *4.2.5 Whole-Embryo mRNA Sequencing*

Data from our prior mRNA-sequencing experiments (Vliet et al., 2018) were used to determine potential effects on the transcriptome within zebrafish embryos treated with 0.313  $\mu$ M niclosamide from 2-3 and 2-5 hpf, as differential expression analysis was not

previously conducted, and prior data were solely used for read-count analysis. Raw Illumina (fastq.gz) sequencing files (36 files totaling 8.24 GB) are available via NCBI's BioProject database under BioProject ID PRJNA454154, and all data were processed as previously described (Vliet et al., 2018). A DESeq2 application within Bluebee (Lexogen Quantseq DE 1.2) was used to identify significant treatment-related effects on transcript abundance (relative to vehicle controls) based on a false discovery rate (FDR) p-adjusted value  $< 0.05$ . Using DESeq2-identified transcripts, significantly altered genes were examined for enrichment of known biological processes and KEGG pathways using DAVID v6.8 (Dennis et al., 2003; Huang et al., 2009a, 2009b).

#### *4.2.6 Ribosomal and Transfer RNA*

To determine the relative contribution of ribosomal RNA (rRNA) and transfer RNA (tRNA), total RNA samples from embryos exposed to either niclosamide (0.313  $\mu\text{M}$ ) or vehicle control (0.1% DMSO) from 2-3 and 2-5 hpf were analyzed on an Agilent 2100 Bioanalyzer system (Santa Clara, CA). Peaks corresponding to 5.0S, 5.8S, 18S, 28S, and tRNA were integrated to determine rRNA concentration. tRNA and rRNA concentrations were then normalized to total RNA concentrations to determine percent contribution.

#### *4.2.7 Human Embryonic Stem Cell Exposure and Immunocytochemistry*

Human embryonic stem cells (hESCs) of the H9 line were acquired from WiCell Research Institute (Madison, WI, USA), cultured on Matrigel-treated dishes (BD Biosciences, La Jolla, CA, USA), and maintained as feeder-free cultures in mTeSR media

(Stem Cell Technologies, Vancouver, Canada) in 5% CO<sub>2</sub> at 37°C. Pluripotent colonies were passaged every five days upon reaching 70% confluency by dissociating cells with Accutase and a cell scraper. Differentiation was induced from confluent hESC cultures by switching to spontaneous differentiation medium consisting of Dulbeccos Modified Eagles Medium (ThermoFisher Scientific, Waltham, MA, USA), 15% fetal bovine serum (Atlanta Biologicals, Flowery Branch, GA, USA), 1% non-essential amino acids (ThermoFisher Scientific, Waltham, MA, USA), 1:200 penicillin/ streptomycin (ThermoFisher Scientific, Waltham, MA, USA), and 0.1 mM  $\beta$ -mercaptoethanol (Sigma-Aldrich, St. Louis, MO, USA). Niclosamide exposures were performed for the first 24 or 48 h of differentiation with nine concentrations ranging from 0.01 to 10  $\mu$ M. A solvent control containing 0.1% DMSO was included to control for non-chemical specific effects.

Cellular survival in response to niclosamide treatment was determined with 3-[4,5-dimethylthiazol-2-yl]-2,5-diphenylterazolium bromide (MTT) (Spectrum Chemicals, Gardena, CA, USA). Briefly, MTT solution was added to cell media to a final concentration of 0.5 mg/ml and incubated at 37°C. After 2 h, the medium/MTT mix was replaced with pre-warmed MTT desorption solution (0.7% sodium dodecyl sulfate, SDS) in 2-propanol and cells were gently rocked for 15 min. The change in absorbance was read at 570 nm using an iMark microplate reader (Bio-Rad, Hercules, CA, USA). As the generation of blue formazan product is proportional to dehydrogenase activity, a decrease in absorbance at 570 nm provided a direct measurement of the number of viable cells.

For concentrations of niclosamide that did not result in significant effects on cell viability across both time-points ( $\leq 1.0 \mu$ M), hESCs were fixed by incubating in 4% PFA

for 20 min at 4°C. Following incubation, cells were washed 3 times in 1X PBS for 5 min. Cells were then stored at 4°C in 1X PBS until staining. Fixed cells were permeabilized by incubation in 150 µL of 0.1% Triton X-100 in 1X PBS for 15 min at room temperature. Cells were then washed three times for 5 minutes in 150 µL 1X PBS and incubated overnight at 4°C in a 1:150 dilution of fluorescein-labelled phalloidin (ThermoFisher Scientific, Waltham, MA, USA). Cells were then counterstained with DAPI by incubating in a 1:3 dilution of Fluoromount-G (SouthernBiotech, Birmingham, AL, USA). Cells were then washed three times for 5 min in 200 µL 1X PBS and stored in 300 µL 1X PBS at 4°C until imaged. Cells were imaged on our ImageXpress Micro XLS Widefield High-Content Screening System (Molecular Devices, Sunnyvale, CA, USA). Briefly, a 10X objective and DAPI/FITC filter cubes were used to acquire a z-stack (10 steps, 5 µM per step) of 56 sites per each well. Z-stack slices were used to generate a two-dimensional projection of each site, and sites were then stitched together within MetaXpress 6.0.3.1658 (Molecular Devices, Sunnyvale, CA, USA) to generate an image of the entire well. Actin networks within each well were quantified by measuring total FITC fluorescence per well within ImageJ (v1.51m9).

#### *4.2.8 Statistical Analysis*

All statistical analyses were performed using Prism 8 (GraphPad, San Diego, CA, USA). For all data not specified otherwise, main effects of treatment were identified using a one-way ANOVA ( $\alpha=0.05$ ). Treatment groups were compared with either time-matched or stage-matched (based on embryo phenotype) vehicle controls using pair-wise Tukey-

based multiple comparisons of least square means to identify significant differences among treatment groups ( $\alpha=0.05$ ).

## **4.3 Results**

### *4.3.1 Embryonic Yolk Sac Integrity, Cell Area, and Actin Networks*

To determine if niclosamide-induced developmental delays were due to abnormal formation of embryonic actin networks, we exposed embryos to 0.313  $\mu\text{M}$  niclosamide from 2-5 hpf followed by fluorescent labeling of actin networks. Interestingly, niclosamide-exposed embryos displayed a loss of yolk sac integrity and, even following fixation, were significantly more fragile relative to vehicle controls (Figure 19A). Moreover, actin fluorescence localized to the embryonic yolk sac was significantly decreased within niclosamide-exposed embryos relative to vehicle controls, suggesting that niclosamide may be delaying the progression of yolk sac cortical actin networks (Figure 19B). Finally, niclosamide exposure resulted in a significant increase in average cell area in the blastomere (Figure 19C). As progressive reductions in cell size is associated with successive cell divisions, these data suggest that niclosamide exposure may also delay proliferation of cells within the embryonic blastomere.

### *4.3.2 Human Embryonic Stem Cells*

As the developmental toxicity of niclosamide is a potential concern for human populations, we assessed the potential effects of niclosamide to human embryonic stem cells (hESCs). Exposure to niclosamide significantly affected the viability of hESCs at concentrations 10  $\mu\text{M}$  and  $\geq 3$   $\mu\text{M}$  following 24- and 48-h exposures relative to time-

matched vehicle controls, respectively (Figure 20A and 20B) – nominal concentrations that were above the maximum tolerated concentration within zebrafish embryos. Additionally, niclosamide did not affect the formation of cellular actin networks within hESCs (Figure 20C), suggesting that factors not present in hESCs may be driving the decrease in yolk sac actin networks within zebrafish.

#### *4.3.3 Whole-Embryo Metabolomics*

As early embryonic development in zebrafish is dependent, in part, on nutrient uptake from maternally deposited nutrients in the yolk as well as the metabolism of cellular lipid droplets (Dutta and Sinha, 2017), we investigated the metabolomic profiles of zebrafish embryos following niclosamide exposure. The abundance nor distribution of non-polar metabolites and lipids were not significantly affected within embryos exposed to 0.313  $\mu$ M niclosamide from 2-5 hpf (Figures 21A and 21B).

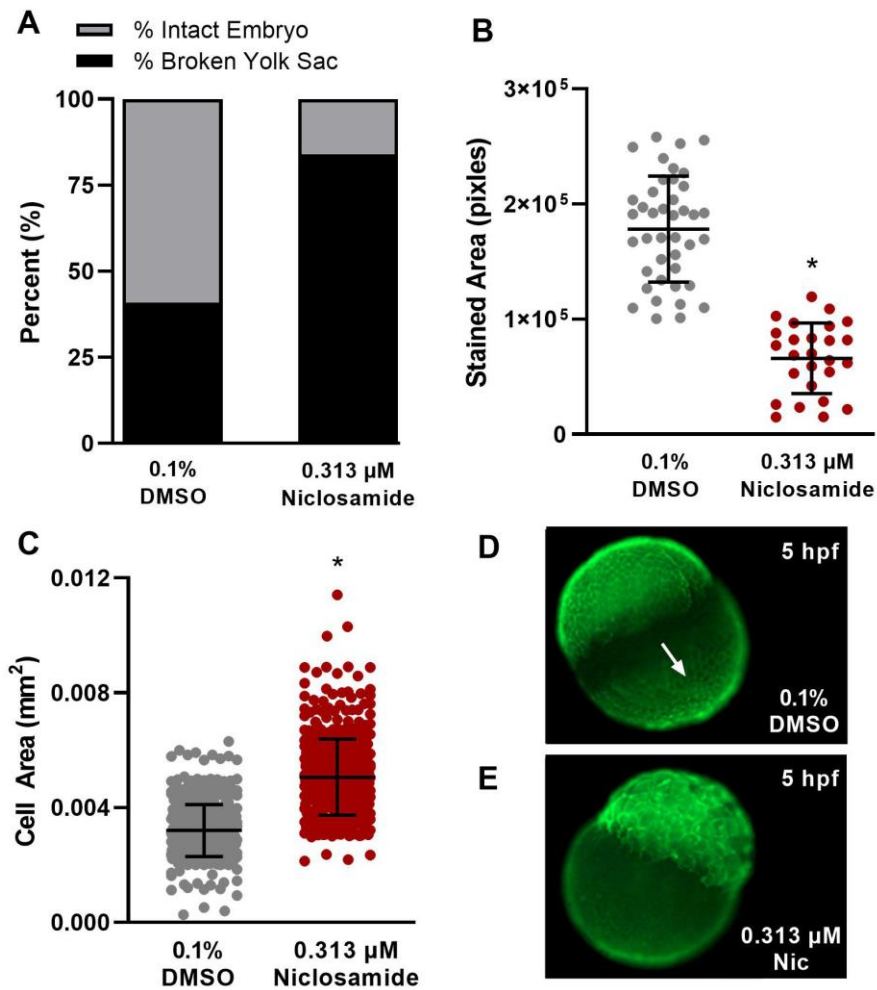


**Figure 19.** Niclosamide exposure alters yolk sac integrity, the presence of yolk sac cortical actin networks, and cell size in the embryonic blastodisc within 5-hpf embryos. Niclosamide exposure decreases embryonic yolk sac integrity in 5-hpf embryos (A), actin present in the embryonic yolk sac of intact embryos (B), and the size of cells present in the embryonic blastodisc in 5 hpf embryos (C). Representative images of vehicle- (0.1% DMSO) and niclosamide-treated (0.313  $\mu$ M) embryos stained with phalloidin (D, E). The cortical actin network is visible in the vegetal half of the embryonic yolk sac and is indicated by the white arrow in panel D. Asterisk denotes  $p < 0.05$ .

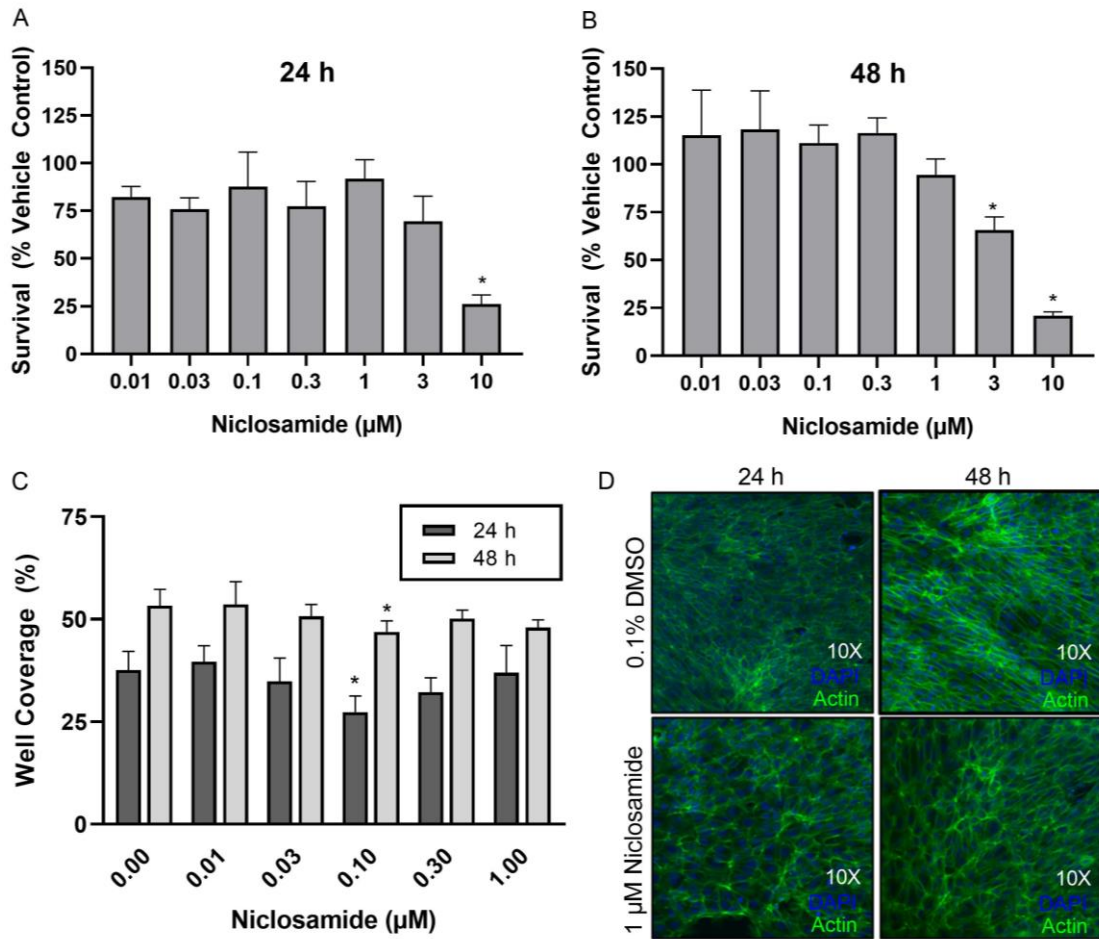


**Figure 20.** Niclosamide affects the viability of hESCs but does not affect cellular actin networks. Cell viability following a 24 h (A) and 48 h (B) exposure to niclosamide. Actin networks measured as percent of well area (C), and representative images of DAPI- and phalloidin-stained hESCs acquired at 10X magnification (D).

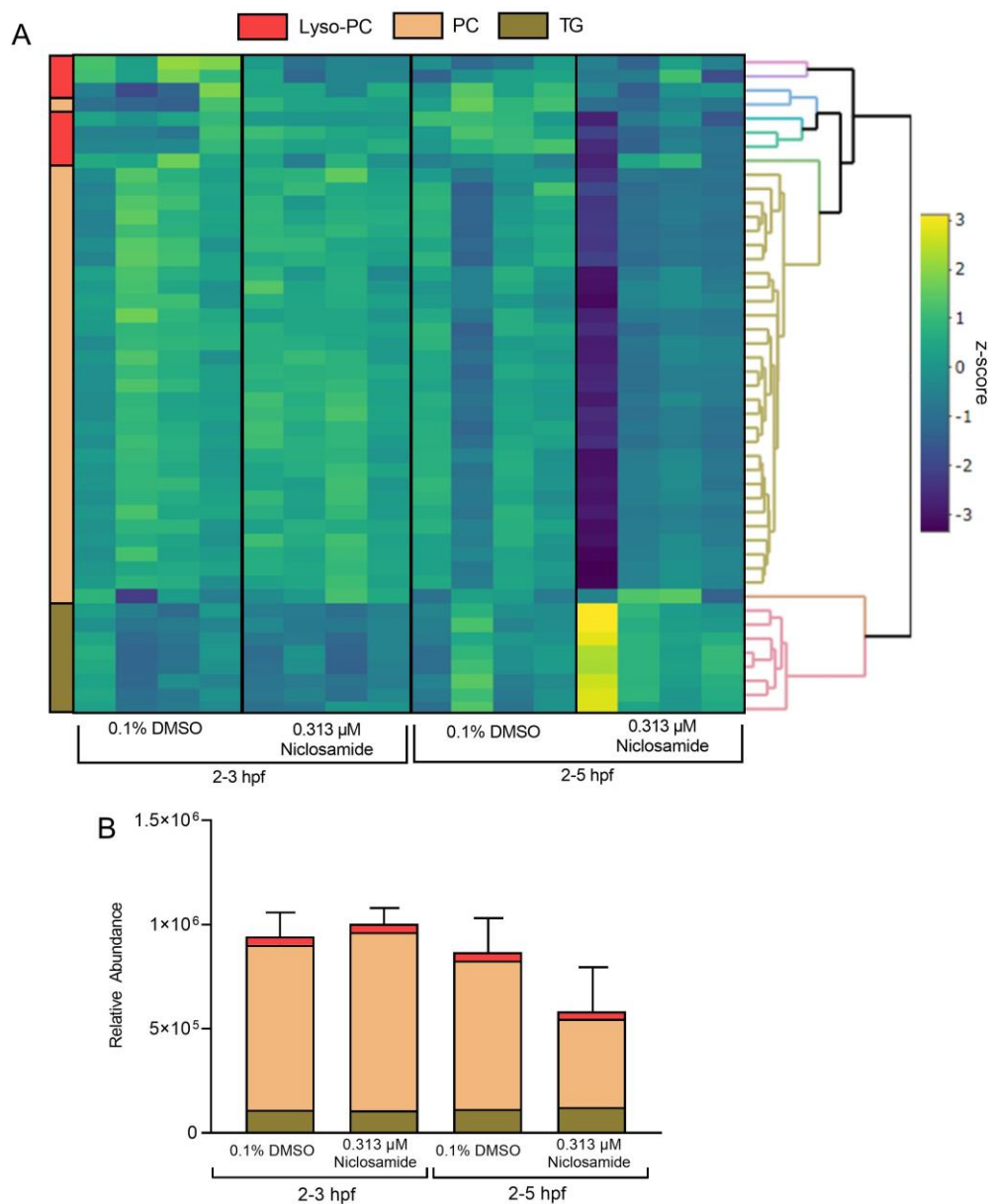


**Figure 21.** Niclosamide exposure does not result in significant effects on the distribution and abundance of non-polar metabolites. (A) No significant differences ( $p > 0.05$ ) were observed among the 47 identified non-polar metabolites following niclosamide exposure. (B) Following niclosamide treatment, there were no significant differences ( $p > 0.05$ ) in the abundance of identified lipid species nor the proportion of different lipid classes relative to vehicle controls. Lyso-PC = Lysophosphatidylcholine; PC = Phosphatidylcholine; and TG = Triglycerides. Heatmap indicates z-score.

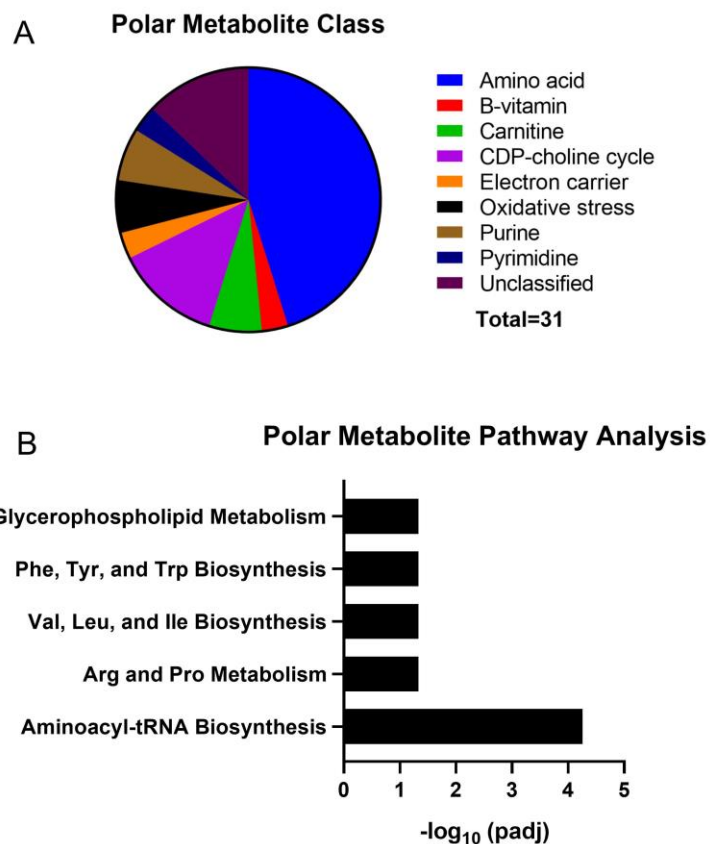


**Figure 22.** Thirty-one polar metabolites were significantly altered by niclosamide exposure. (A) Of the 31 significantly altered polar metabolites, the majority were annotated within the “amino acids” group. (B) Pathways significantly affected by niclosamide exposure were identified within MetaboAnalyst using a Fisher’s Exact p-value < 0.05.

Niclosamide exposure resulted in significant alterations on polar metabolites, where the majority of significantly altered metabolites were amino acids involved in the aminoacyl-tRNA biosynthesis pathway (Figures 22A and 22B; Figure 23). These results suggest that, within embryos exposed from 2-5 hpf, niclosamide affected the abundance and distribution of amino acids in the absence of effects of non-polar metabolites and lipids.

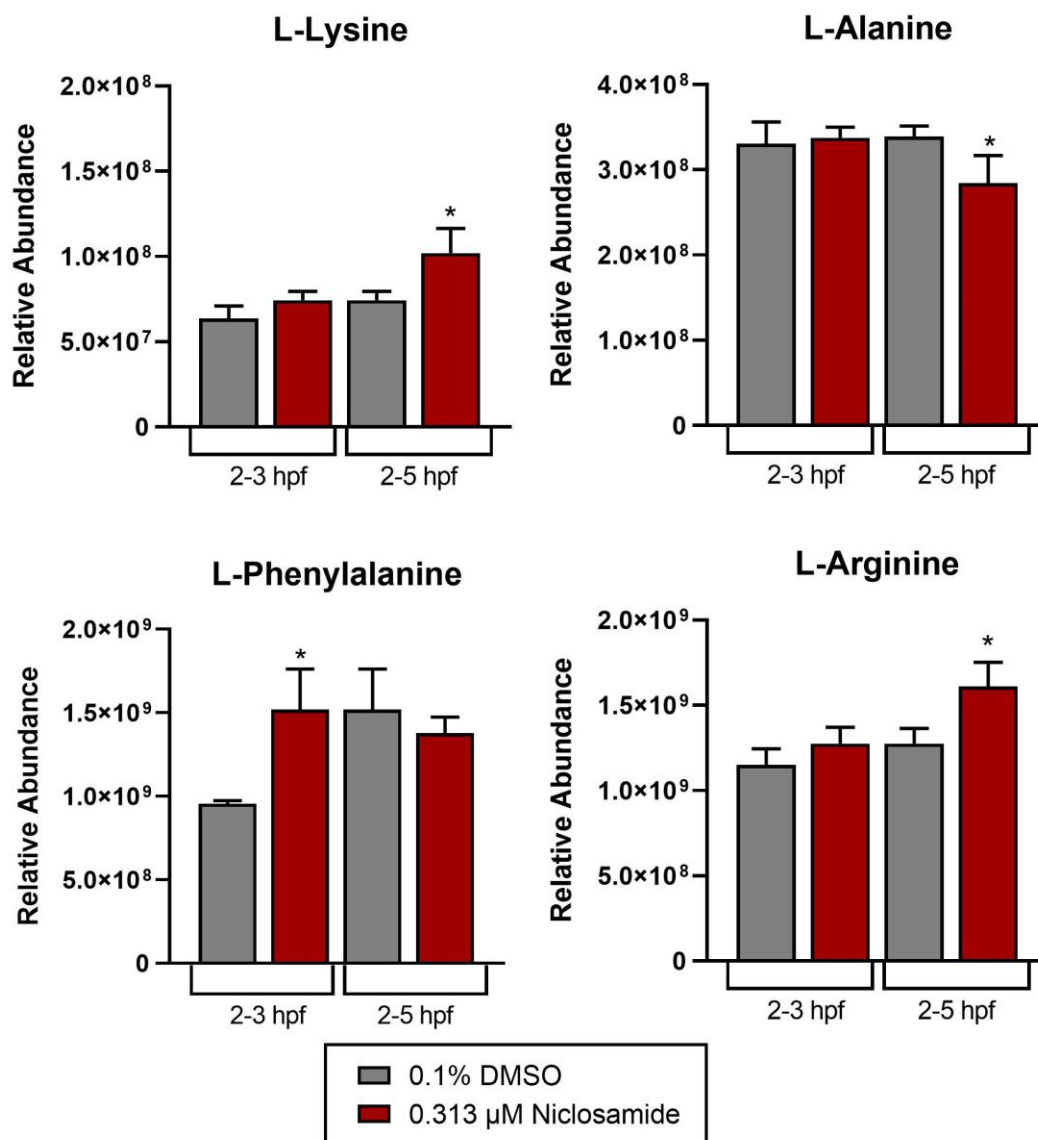


**Figure 23.** Among the significantly altered metabolites making up the aminoacyl-tRNA biosynthesis pathway, there were significant treatment-related effects on the relative abundance of L-amino acids (L-phenylalanine, L-lysine, L-alanine, and L-arginine) following niclosamide exposure relative to time-matched vehicle controls. Asterisk denotes  $p < 0.05$ .

#### 4.3.4 Whole-Embryo mRNA-Sequencing

To further understand the mechanism of niclosamide-induced epiboly delay during early zebrafish embryogenesis, we leveraged prior mRNA-sequencing data generated from zebrafish exposed to niclosamide from 2-3 and 2-5 hpf, and then analyzed these data to identify potential transcriptome-wide differences, an analysis that was not conducted in our prior study (Vliet et al., 2018). Exposure to niclosamide from 2-5 hpf resulted in significant alterations to 1) 1,526 transcripts relative to time-matched (2-5 hpf) vehicle controls (Figure 24A) and 2) 98 transcripts relative to stage-matched (2-3 hpf) vehicle controls (Figure 24B).

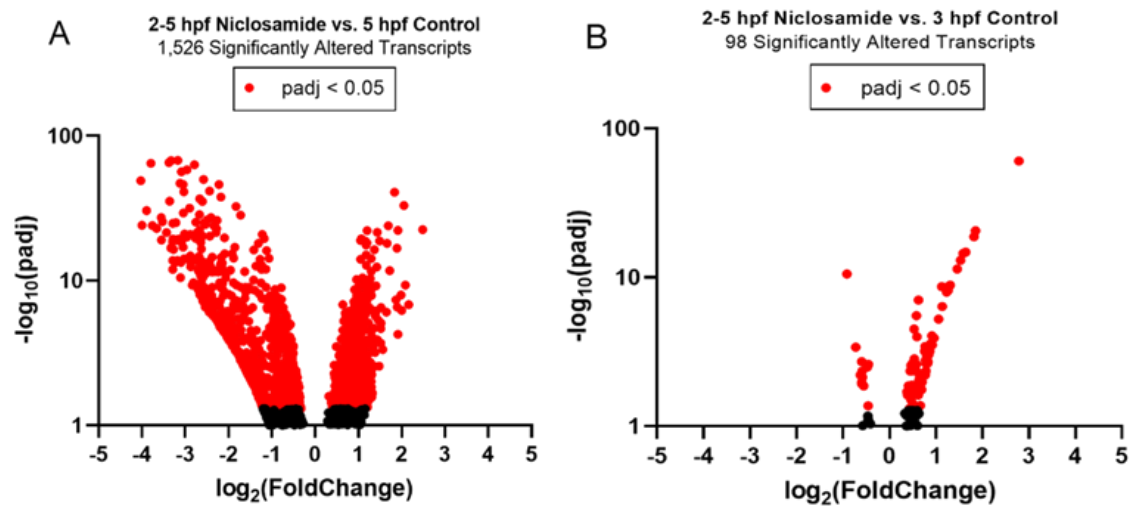


**Figure 24.** Exposure to 0.313  $\mu\text{M}$  niclosamide from 2-5 hpf resulted in widespread alterations to transcript levels relative to time-matched (5 hpf) vehicle controls (A), an impact that was less severe relative to stage-matched (3 hpf) vehicle controls (B).

Of the significantly altered transcripts, 64 were shared between time- and stage-matched comparisons. Interestingly, of these shared transcripts, the majority were decreased and increased when compared to time-matched and stage-matched controls,

respectively. Relative to time-matched (2-5 hpf) vehicle controls, significantly altered transcripts within niclosamide-exposed embryos were grouped within the spliceosome pathway and related to biological processes involved in transcription, phosphorylation, and multicellular development (Figure 25). Relative to stage-matched (2-3 hpf) vehicle controls, significantly altered transcripts were grouped within the ribosome pathways and related to biological processes involved in translation, among other processes (Figure 25).

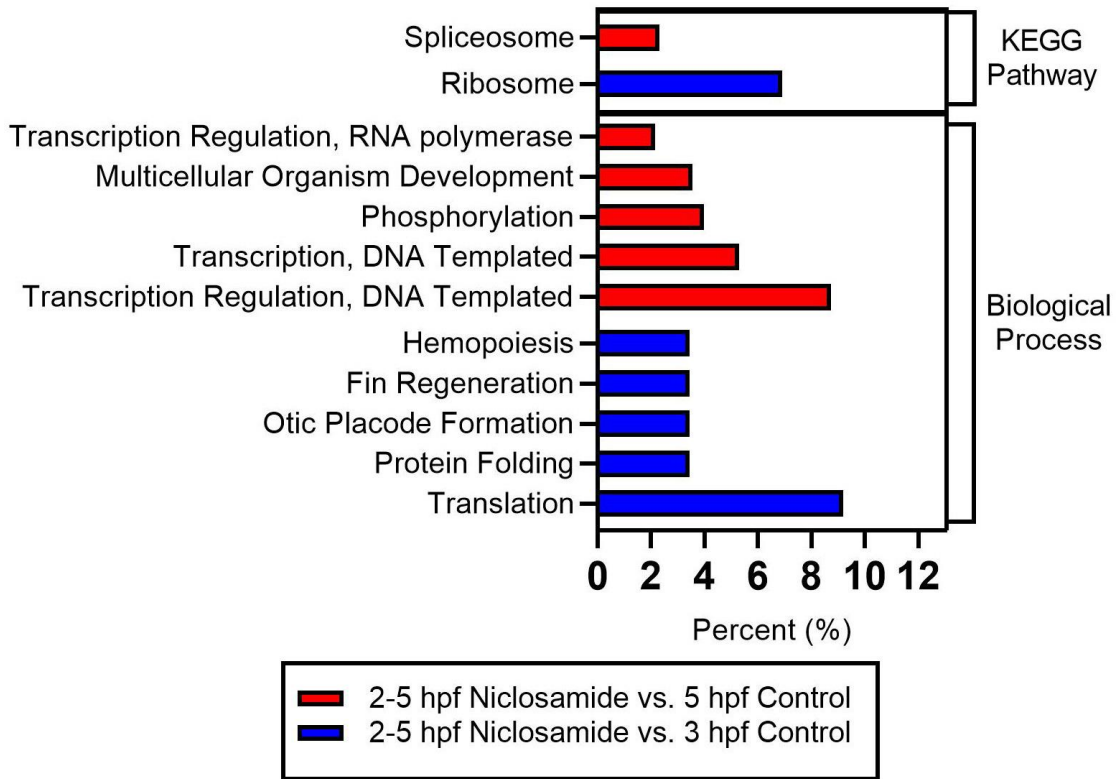


**Figure 25.** Top DAVID biological processes and KEGG pathways identified following time-matched (2-5 hpf niclosamide vs. 2-5 hpf control) and stage-matched (2-5 hpf niclosamide vs. 2-3 hpf control) comparisons. Percent (%) indicates number of genes in data set per total genes in pathway.

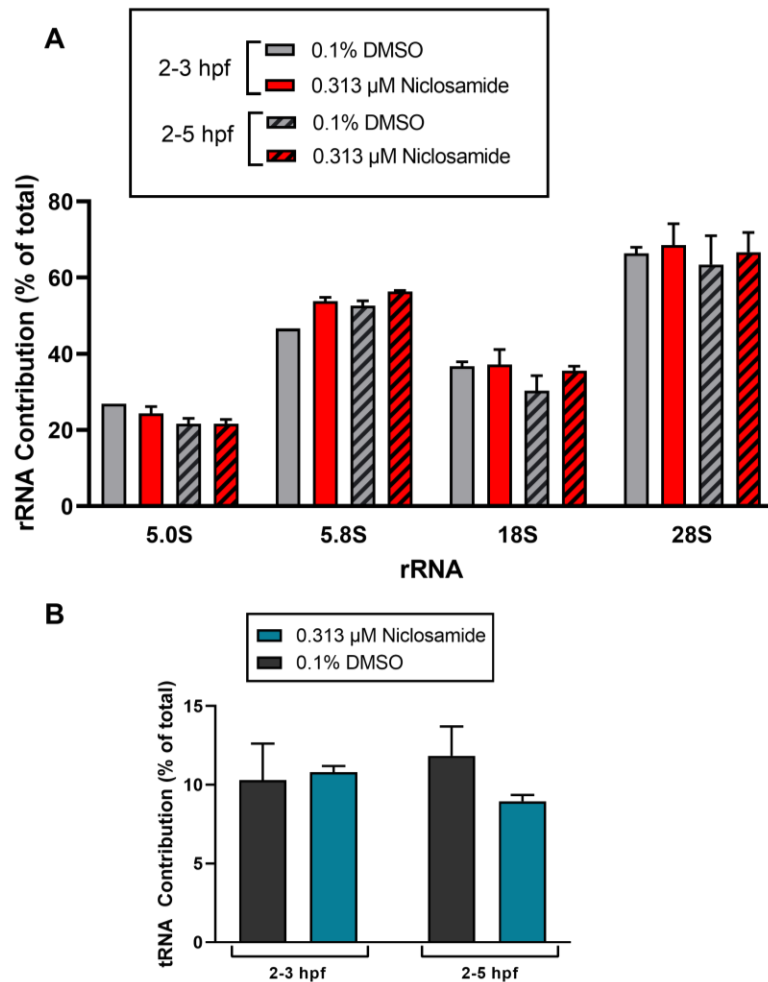


**Figure 26.** Niclosamide exposure from 2-3 and 2-5 hpf does not result in significant alterations to (A) the percent contribution of ribosomal RNA (rRNA) and (B) the percent contribution of transfer RNA (tRNA) in zebrafish embryos. Percent (%) indicates the concentration of rRNA or tRNA relative to the total amount of RNA.

#### 4.3.5 Ribosomal and Transfer RNA

To further understand how niclosamide may potentially be interacting with translational machinery, we quantified levels of ribosomal RNA and transfer RNA within total RNA samples of embryos exposed to either niclosamide (0.313 μM) or vehicle control (0.1% DMSO) from either 2-3 or 2-5 hpf. No significant alterations in the relative

abundance of rRNA or tRNA were observed across either treatment condition or timepoint (Figure 26A and 26B), suggesting that niclosamide is not directly impacting the synthesis or recycling of these RNA species.

#### **4.4 Discussion**

In previous studies, niclosamide has been shown to result in a concentration-dependent delay in epiboly progression during early zebrafish embryogenesis, an effect that may not be a result of OXPHOS disruption (Vliet et al., 2018). Due to the critical role of cytoskeletal networks in epiboly progression and the presence of altered cytoskeleton transcripts following niclosamide exposure (Lepage and Bruce, 2010; Solnica-Krezel and Driever, 1994; Vliet et al., 2018), we initially hypothesized that niclosamide delays epiboly progression through disruption of the embryonic cytoskeleton. Although no alterations in the abundance nor localization of tubulin were previously observed (Vliet et al., 2018), in the present study we demonstrated that exposure to niclosamide during early zebrafish embryogenesis significantly decreased yolk sac integrity relative to vehicle controls. During this stage of zebrafish embryogenesis, the structural integrity of the yolk sac is thought to be supported by a dense area of filamentous actin at the vegetal pole that maintains embryonic morphology (Cheng et al., 2004; Lepage and Bruce, 2010). The presence of this network is important during the late-blastula and early-gastrula stage of development when major cell rearrangements are occurring, and the yolk cell is subjected to a number of forces (Keller et al., 2003). Indeed, we observed a significant decrease in actin staining within the vegetal half of the embryonic yolk sac, suggesting that

niclosamide exposure decreased the ability of the cortical actin network within the yolk sac to properly form – an effect which may have resulted in a loss of yolk sac integrity.

Interestingly, there did not appear to be any effect on actin networks in the cell mass, although there was a significant increase in average cell area following niclosamide exposure. Early cell divisions in the zebrafish embryo are regulated via maternal genes (Abrams and Mullins, 2009), during which the total volume of the embryo remains constant and each cell division results in progressively smaller cells (Kane and Kimmel, 1993; Langley et al., 2014). Therefore, it is possible that niclosamide exposure results in a systemic delay in development that impedes cell division and/or targets maternal transcripts responsible for cell division and yolk sac actin network formation. Given that the presence of the cortical actin network within the yolk sac prior to the MZT has not been well-studied, it is possible that decreased actin levels within the yolk sac were also due to a systemic delay in embryonic development.

As niclosamide is a potential concern for human health, we investigated whether the effects of niclosamide on actin networks were also observed within hESCs. Although niclosamide exposure did result in significant effects on cell viability, these cytotoxic effects occurred at higher nominal concentrations than epiboly-specific effects observed within zebrafish embryos. Therefore, these results suggest that the intact zebrafish embryo may represent a more sensitive model than hESCs to study the developmental consequences of embryonic niclosamide exposure. Finally, no significant effects to actin were observed following exposure of hESCs to niclosamide, suggesting that the observed

decrease in yolk sac actin networks within zebrafish embryos may be due to effects on downstream processes not present within hESCs.

During early zebrafish embryogenesis, energy in the form of ATP is necessary to drive early developmental processes. This is particularly true for the MZT, where a pulse of energy is needed to drive the ATP-dependent degradation of maternal transcripts (DeRenzo and Seydoux, 2004; Dutta and Sinha, 2017). The ATP responsible for driving the MZT is produced through the metabolism of lipid droplets present in the blastodisc (cell-mass), and inhibition of lipolysis results in delays to developmental processes including epiboly and the MZT (Dutta and Sinha, 2017). Interestingly, whole-embryo profiles of non-polar metabolites and lipids within niclosamide-exposed embryos – either before (3 hpf) or after (5 hpf) the initiation of the MZT – were not significantly different relative to vehicle controls. Therefore, these results suggest that niclosamide-induced developmental delay may not be mediated through disruption of lipid metabolism.

During early zebrafish development, the translation of maternally-supplied transcripts is essential to produce proteins involved in early developmental processes, including several transcription factors involved in zygotic genome activation (Abrams and Mullins, 2009; Harvey et al., 2013; Langley et al., 2014; Lee et al., 2013). When maternal transcripts are deposited in the embryo following fertilization, these transcripts are maintained in an inactive state until required for translation. When needed, maternal mRNA is slowly polyadenylated and translated in proteins (Harvey et al., 2013; Langley et al., 2014; Lee et al., 2013). Interestingly, blocking polyadenylation of maternal mRNA prevents the activation of most zygotic genes as well as progression of epiboly (Aanes et

al., 2011). In addition to maternal mRNA, translation also requires ribosomes, amino acids, and nucleotides (Putzer and Laalami, 2013). Following niclosamide exposure, amino acid metabolites relating to the aminoacyl-tRNA biosynthesis pathway were significantly affected within embryos. Aminoacyl-tRNAs act as substrates for translation and consist of tRNAs with an amino acid added at the 3' end (Ibba and Söll, 2004). Given the necessity of aminoacyl-tRNA in translation and the importance of maternal mRNA translation for driving the MZT, epiboly, and embryonic development, niclosamide may interfere with the production of maternal proteins, resulting in a cascade of downstream effects and developmental delays.

When differential expression analysis was performed on embryos with delayed zygotic genome activation (Vliet et al., 2018), we found that exposure to niclosamide resulted in significant and widespread alterations to the embryonic transcriptome. When compared to time-matched vehicle controls (2-5 hpf), 1,529 transcripts were significantly altered (671 and 855 transcripts were increased and decreased, respectively). Interestingly, when niclosamide-exposed embryos were compared to stage-matched vehicle controls (2-3 hpf), only 98 transcripts were significantly altered (86 and 12 transcripts were increased and decreased, respectively). Overall, these transcriptional responses suggest that niclosamide-exposed embryos are transcriptionally more like 3-hpf control embryos, further supporting the hypothesis that niclosamide exposure results in systemic delays to embryonic development. When differentially expressed transcripts were further evaluated by DAVID and KEGG, the spliceosome pathway and transcriptional processes were the most statistically significant groups based on time-matched comparisons, and the

ribosomal pathway and translational processes were the most statistically significant groups for stage-matched comparisons. These results are consistent with the hypothesis that niclosamide exposure may be delaying the MZT and causing a systemic delay in development by disrupting the translation of maternally-supplied mRNAs and preventing the successful transcription of zygotic genes, potentially through inhibition of the ribosomal machinery or disruption of the t-RNA biosynthesis pathway.

The translation of proteins from mRNA requires both functioning ribosomes as well as aminoacyl-tRNA. During translation, tRNA present in the cytosol binds to free amino acids, becoming aminoacyl-tRNA. As the aminoacyl-tRNA biosynthesis pathway was significantly altered following niclosamide exposure, and our mRNA-sequencing results indicated that niclosamide may be altering translation through a ribosomal pathway, we investigated levels of tRNA and rRNA. No significant alterations in the relative abundance of rRNA or tRNA were observed across either treatment condition or timepoint, suggesting that niclosamide is not directly impacting the synthesis or recycling of these RNA species. Instead of directly impacting tRNA or rRNA, these data support the hypothesis that niclosamide may be interfering with the ability of tRNA to bind amino acid and complete protein translation.

In conclusion, this study showed that (1) niclosamide exposure during early zebrafish embryogenesis resulted in a decrease in yolk sac integrity with a concomitant decrease in the presence of yolk sac actin networks and increase in cell size; (2) zebrafish embryos were more sensitive to niclosamide exposure than hESCs; (3) within whole embryos, niclosamide exposure did not alter non-polar metabolites and lipids but did

significantly alter amino acids related to aminoacyl-tRNA biosynthesis; (4) niclosamide significantly altered transcripts related to translation, transcription, and mRNA processing pathways; and (5) niclosamide did not significantly alter levels of rRNA or tRNA. Overall, our collective data suggest that niclosamide may be causing a systemic delay in embryonic development by disrupting the translation of maternally-supplied mRNAs, an effect that may be mediated through disruption the aminoacyl-tRNA biosynthesis pathway. This study highlights the utility of the zebrafish embryo as a model for the identification of novel mechanisms of action, especially considering that these effects may have not been detected using an in utero-based study or hESCs alone. Although we have shown that niclosamide disrupted basic processes of maternal mRNA translation and zygotic genome activation, future studies are needed to (1) confirm the potential target and mechanism of action for niclosamide within zebrafish embryos; (2) determine whether similar effects on the MZT occur within mammalian models following non-oral routes of niclosamide exposure; and (3) examine the effect of non-oral niclosamide exposure on embryo implantation and maternal fertility, as the stages of zebrafish embryos examined in this study represent pre-implantation stages within human populations.

## Chapter 5: Summary and Conclusions

### 5.0 Summary

Zebrafish embryos offer a promising alternative animal model for the identification and investigation of potential developmental toxicants. Their small size, rapid developmental timeline, conservation of early developmental processes, and sequenced genome make them amenable to HCS and HTS applications, as well as in-depth mechanistic and molecular studies. The findings and data presented in this dissertation demonstrate and reinforce the utility of embryonic zebrafish as a physiologically-intact, non-mammalian model for screening and prioritization of chemicals for further mechanistic investigations. Regarding the use of early embryonic zebrafish behavior as a predictive endpoint, the data presented in Chapter 2 demonstrate that background spontaneous activity, at least within the work presented, is affected by a wide range of pharmacologically and structurally diverse compounds. Our data also suggest that spontaneous activity is unable to identify neuroactive compounds and is unable to predict biological targets and discriminate chemical modes of action. In Chapter 3, we demonstrated that, despite the limitations of embryonic behavior as a predictive readout, screening with zebrafish embryos as a whole-animal model was able to detect several potential developmental toxicants, including the anthelmintic compound niclosamide. We demonstrated that exposure to low concentrations of niclosamide during early zebrafish embryogenesis results in a concentration-dependent delay in the early developmental process of epiboly, the spreading of the embryonic cell-mass around the yolk-sac. Our data indicate that niclosamide-induced epiboly delay may be independent of the traditional

mode-of-action for niclosamide – disruption of oxidative phosphorylation – and interferes with the degradation of maternal transcripts, initiation of zygotic genome activation, and results in a concentration-dependent decrease in tubulin polymerization *in vitro*. Finally, in Chapter 4, we demonstrated that early embryonic niclosamide exposure decreased yolk sac integrity while resulting in a simultaneous increase in cell size and decrease in the presence of yolk sac actin networks. Niclosamide-exposed embryos also exhibited altered levels of amino acids specific to aminoacyl-tRNA biosynthesis and altered transcripts related to translation, transcription, and mRNA processing pathways, although no significant alterations to rRNA or tRNA were observed. Overall, these data highlight the power of the zebrafish embryo as a model for chemical screening and demonstrate its capability to facilitate the rapid progression from a large suite of diverse compounds to a specific molecular mechanism that may not have been detected using cell-based assays or mammalian models. Additionally, this work demonstrates the potential of niclosamide to cause systemic delays in embryonic development through the potential interference with the translation of maternally-supplied mRNAs (Figure 28). As niclosamide is currently being discussed widely within the scientific and medical communities, these results are important in understanding the potential toxicity of niclosamide, particularly following off-label uses and non-oral routes of exposure.

## **5.1 Behavioral Screening in Embryonic Zebrafish**

Zebrafish embryos offer a promising and cost-effective alternative vertebrate model to support drug discovery and toxicity testing. This is particularly true for the

detection of neuroactive compounds, for which there has been several zebrafish-based behavioral assays developed to date. Although different forms of larval and adult zebrafish locomotion have been used as endpoints within these assays, spontaneous activity (tail contractions) in the early zebrafish provided a primitive behavioral endpoint for the potential identification of chemicals impacting the developing nervous system. Despite the widespread use of spontaneous activity as an endpoint in toxicity tests and chemical screens, the responsiveness of this behavior is not yet fully understood, and it remains unclear whether spontaneous activity is responsive only to certain compounds with specific mechanisms of action. In Chapter 2, we aimed to address these limitations by establishing the reproducibility of spontaneous activity as a behavioral readout and, using a large chemical library screen, determine which biological targets are detected using spontaneous activity as a behavioral readout. This study demonstrated, despite our initial hypothesis, that background spontaneous activity was (1) affected by a wide range of pharmacologically and structurally diverse compounds; (2) was unable to identify neuroactive compounds; and (3) was unable to predict biological targets and discriminate chemical modes of action.

Despite the non-specificity of spontaneous activity, this work demonstrated an unbiased way of detecting potentially developmentally toxic compounds and identifying unexpected compound hits that may, or may not, have been detected using other chemical screening methods such as *in-vitro*, cell-based, and mammalian assays. We were able to rapidly screen and prioritize a large number of compounds and detect an unexpected compound, niclosamide, with a potentially novel mechanism of developmental toxicity. In

addition, this study also highlighted the importance of understanding the physiochemical characteristics of compounds during aqueous exposures.

Although this was one of the first studies to systematically screen a well-characterized library of compounds using spontaneous activity as a behavioral readout, this work was subject to several limitations. As discussed in Chapter 2, our assay examined background spontaneous activity, as opposed to stimulated behavioral responses that are used in many other current assays. The use of unstimulated spontaneous activity may provide a less sensitive and less specific readout than stimulated behavior, potentially explaining our non-specific results. In addition, the LOPAC<sup>1280</sup> library, while containing a well-characterized and diverse set of chemicals, is based on targets derived primarily from human cell lines. It is a possibility that the compound targets, as described in the library, may not be conserved across zebrafish and may be acting through other pathways within the zebrafish embryo, leading to incorrect conclusions about the relationship of the compound target to spontaneous activity. A third limitation of this study, and a concern among all aqueous immersion exposures, is uncertainty related to compound uptake and distribution. As internal concentrations were not quantified, it is therefore impossible to determine whether compound uptake and distribution were a factor in influencing these results. As waterborne exposures deliver the compound to the embryo by immersing the whole organism, non-targeted systemic uptake is likely to be occurring and may potentially result in differential responses between embryonic zebrafish and other model systems in which the route of exposure is more targeted. There is a strong possibility that, for compounds expected to act as stimulants within the LOPAC<sup>1280</sup> library, waterborne

exposure led to systemic uptake and distribution that overwhelmed the intended target and significantly biased spontaneous activity toward a unidirectional hypoactive response.

Overall, this work raises important questions and implications for the wider scientific community using the zebrafish embryo as a model for chemical screening and toxicity testing. Regarding spontaneous activity, this work served to highlight the uncertainties and limitations that exist regarding spontaneous activity as a behavioral readout. The results of the study issues regarding the predictive power of spontaneous activity as a predictive behavioral readout and highlighted the possibility of differential behavioral responses between life-stages; questions that are essential to the continued use of zebrafish behavior as an endpoint within chemical screens. Additionally, this study highlighted the uncertainties that exist regarding toxicokinetics associated with aqueous immersive exposures. Overall, this study contributes to our understanding of the utility and domain of applicability for the zebrafish embryo as an alternative non-mammalian model within chemical screening applications.

## **5.2 Niclosamide as a Potential Developmental Toxicant**

Within the LOPAC<sup>1280</sup> behavioral screen conducted in Chapter 2, several compounds emerged as hits in both tier I and tier II. Among these compound hits, niclosamide demonstrated potent effects to embryo survival at a limit concentration of 10  $\mu$ M, raising questions regarding the compound's potential developmental toxicity. Niclosamide, a traditional anthelmintic compound used in the treatment of intestinal parasites, is receiving increased attention within the medical community for a range of off-label,

alternative uses. Due to our preliminary toxicity data and the public health concerns associated with new niclosamide applications, we aimed to further investigate the developmental toxicity of niclosamide within early embryonic stages of zebrafish. In Chapter 3, we began the study by characterizing the phenotype resulting from exposure to low concentrations of niclosamide during the blastula period of development, a concentration-dependent delay in the process of epiboly. Due to the traditional mode of action for the compound within invertebrates, inhibition of oxidative phosphorylation, we then investigated whether this could be causing the observed epiboly defects. Our data indicated that niclosamide-induced epiboly delay may be independent of this traditional mode-of-action, and our attention turned towards identifying a potential biological mechanism underlying the observed effects. Overall, this study demonstrated that niclosamide may be preventing the progression of epiboly by disrupting the timing of zygotic genome activation, an effect that may be mediated through disruption of maternal transcription factors and/or microtubule polymerization. In Chapter 4 we expanded on these investigations, further investigating the effects of niclosamide exposure on early embryonic development. Overall, our findings suggest that niclosamide exposure during blastulation alters the normal trajectory of embryogenesis through interference with maternal mRNA translation, an effect that may be mediated through interference with aminoacyl tRNA-biosynthesis and/or the utilization and recycling of amino acids.

Amino-acid biosynthesis is a key process in maintaining the specificity of protein translation and successfully generating cellular proteins from both maternal and zygotic mRNA transcripts (Ibba and Soll, 2000). The aminoacylation of tRNAs with amino acids

is catalyzed by aminoacyl-tRNA synthetases (AARSs), enzymes that are responsible for attaching the correct amino acid to the 3' end of tRNA. Data generated within Chapter 3 and 4 suggest that niclosamide may be interfering with maternal mRNA translation through interference with tRNA-biosynthesis and/or the utilization and recycling of amino acids. Given the key role of AARS in this process, the enzyme provides a potential macromolecular target and molecular initiating event (MIE) for niclosamide within zebrafish embryos (Figure 27, Figure 28). Within vertebrates, several different AARSs are present and the accurate recognition of the correct amino acid and tRNA is different for each enzyme. Since the different amino acids have different functional groups, the enzyme for each amino acid has a different binding pocket (Rajendran et al., 2018). This difference in binding pocket provides a potential explanation as to why alterations in the relative abundance of free amino acids following niclosamide exposure was limited to a few amino acids, however further research is needed to validate this hypothesis.

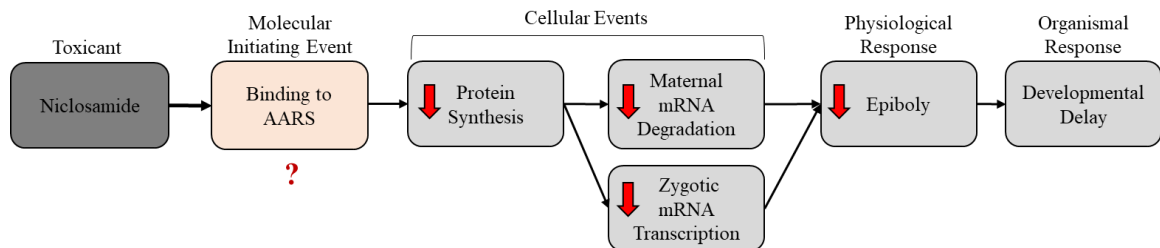


**Figure 27:** Hypothesized Adverse Outcome Pathway for niclosamide during early zebrafish embryogenesis.

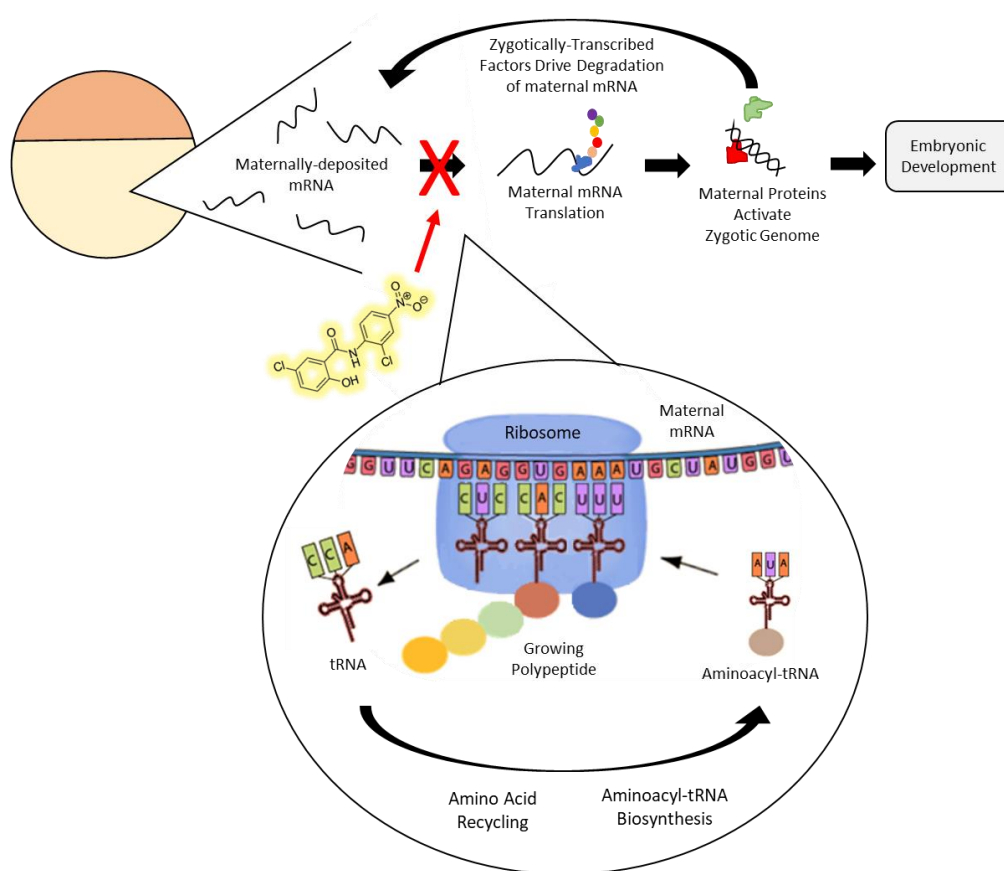


**Figure 28:** Conceptual diagram demonstrating the current hypothesis of niclosamide-induced developmental delay. Data suggest that niclosamide interferes with the translation and subsequent production of maternally-regulated proteins in the early embryo, resulting in systemic developmental delays and inhibition of zygotic genome activation. Metabolomic data suggest that translation may be disrupted through inhibition of aminoacyl-tRNA biosynthesis, an effect that may be mediated through disruptions to amino acid recycling or the enzymes required for amino acid acylation.

Given that the majority of niclosamide toxicity studies use non-modified oral doses, and the developmental toxicity of non-oral niclosamide exposure remains, to a large degree, understudied, this study demonstrated the potential of niclosamide to interfere with developmental processes. The process of epiboly, while not a process occurring during human embryonic development, is a conserved process among many other species. Aside

from the specific process of epiboly, dramatic changes in cell shape and cell migration are occurring during early embryonic development in humans and, as these processes may be potential targets of niclosamide within human populations, this study raises concerns regarding the use of niclosamide in women of reproductive age. Additionally, the hypothesized biological target of niclosamide – maternal mRNA translation and a subsequent disruption of the MZT – are crucial processes conserved within human development (Figure 29), raising further concerns for human use. Within human epidemiological studies, as well as with mammalian *in utero* toxicity studies, there has been little attention given towards the potential developmental toxicity of niclosamide. However, it is important to note that the stages of zebrafish development in which we saw niclosamide-induced toxicity correspond to pre-implantation stages of development within human embryos (Figure 28). Therefore, there is a potential for developmental toxicity within human populations that may be missed, as impacts to embryos at this stage would likely result in the absence of implantation, a lack of pregnancy, and an overall decrease in fertility rates.

Although we demonstrated the ability of niclosamide to disrupt the normal trajectory of embryonic development, our studies are subject to several limitations and uncertainties. As mentioned, the process of epiboly is a key event within early zebrafish development but does not occur during early human embryogenesis. Although there are similar processes of cell migration occurring, and underlying mechanisms may be conserved, it remains unknown whether niclosamide exposure would result in developmental disruptions within human populations. Another key uncertainty in the

extrapolation of these results to human development is compound metabolism. During early zebrafish embryogenesis, xenobiotic metabolism is likely not occurring to an appreciable degree, and the embryo is being exposed to niclosamide in its parent form.

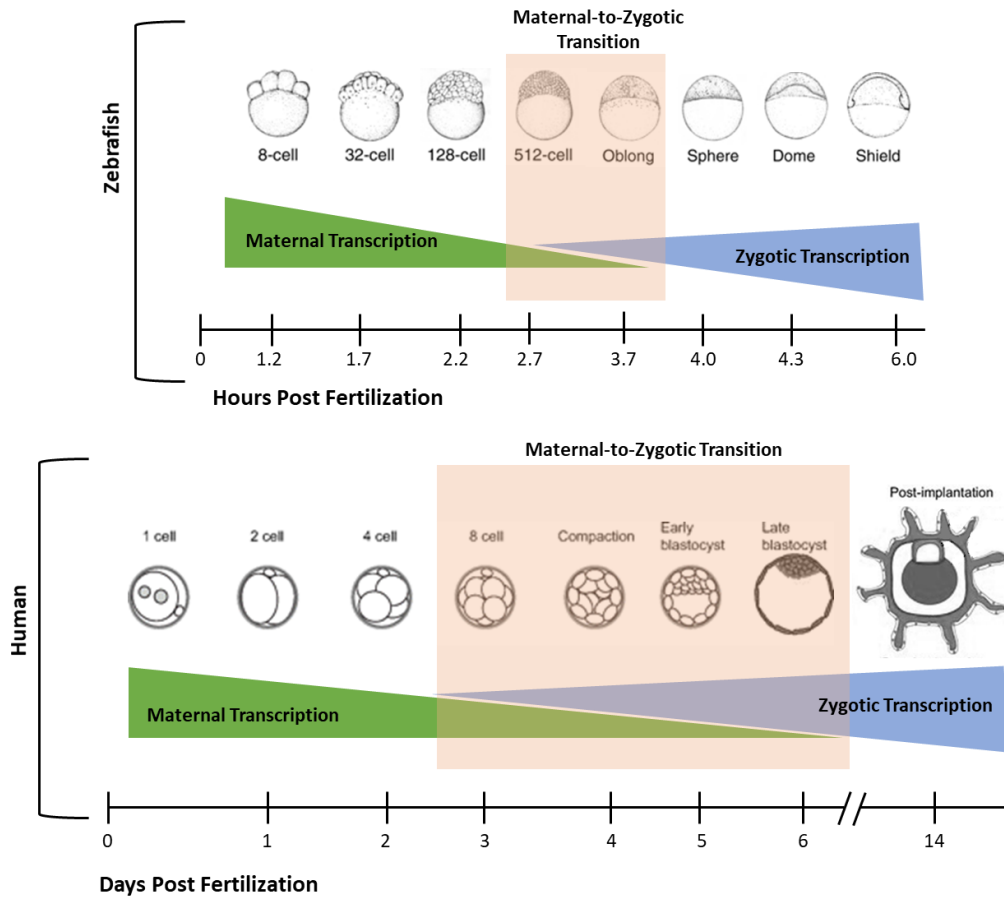


**Figure 29:** The comparative timelines of early embryonic development and the maternal-to-zygotic transition in the zebrafish and human embryo.

In human populations, within human liver microsomes, niclosamide undergoes hydroxylation and glucuronidation, and the reduced form of niclosamide has been detected in rats following oral dosing (Espinosa-Aguirre et al., 1991; Lu et al., 2016). Although it

is unclear how niclosamide may be interacting with biological components to alter the translation of maternal mRNA, the ability of niclosamide to uncouple oxidative phosphorylation has been correlated to the presence of the nitro group. Therefore, it is a possibility that the metabolism of niclosamide within human populations will result in overall detoxification. However, increased developmental toxicity via metabolism to more toxic metabolites is also a possibility.

Overall, the studies carried out in Chapters 2 and 3 demonstrate the potential for niclosamide to disrupt the normal progression of embryonic development in zebrafish embryos; results that may be relevant to human populations. Given the interest in niclosamide for a number of off-label uses (Souza et al., 2019), future studies are needed to (1) confirm the molecular target and MIE for niclosamide within zebrafish embryos; (2) determine whether similar effects on embryonic development occur *in utero* within mammalian models following non-oral routes of niclosamide exposure; and (3) examine the effect of non-oral niclosamide exposure on embryo implantation and maternal fertility within human populations.

### **5.3 The Embryonic Zebrafish Model: Further Directions and Considerations**

As chemical toxicity testing guidelines continue to progress and the concerns over animal testing grow, alternative models will continue to become increasingly more necessary. Due to its small size and rapid development, the zebrafish is a promising vertebrate model for assessing the potential effects of chemical exposure on embryonic development using HCS/HTS methods. As such, the zebrafish embryo model will likely

become increasingly used by developmental toxicologists to screen and prioritize compounds for further testing and examine mechanisms of toxicity. Therefore, in response, it is imperative that the scientific community continue to strive towards greater validation and standardization of zebrafish husbandry methods, assay design, and laboratory techniques. Similar to rodent models, determining the domain of applicability and taking an honest assessment of the limitations of the model is the only way to move the zebrafish embryo forward and gain acceptance in the regulatory environment.

In its current state, the predictability and reproducibility of assays utilizing zebrafish embryos are subject to a suite of limitations, some of which have been previously mentioned. Arguably the greatest of these limitations is the large degree of uncertainty surrounding chemical uptake and distribution. In most assays, the embryo is exposed to the compound via immersion in aqueous media. As such, it becomes challenging to determine where the chemical is partitioning within the organism. This challenge is magnified when working with hydrophobic compounds that may preferentially partition into the embryonic yolk sac or larger molecules that may not easily cross the embryonic chorion. Although most early developmental processes are conserved across vertebrate species, it cannot be assumed that the biological target for a given chemical will be present in both zebrafish and mammalian models, generating uncertainty when extrapolating across species. To further complicate these issues, as was demonstrated in Chapter 2, different life-stages of zebrafish likely contain different sets of pathways and targets, potentially leading to differential phenotypes and behavioral responses.

In addition to biological concerns, zebrafish assays are also subject to a suite of

logistical issues that can influence biological readouts and result in decreased assay reproducibility. Within embryonic assays, for example, ambient temperature can result in slower or faster rates of development and, due to the rapid developmental timeline of zebrafish, can result in comparisons occurring between embryos of different stages. Zebrafish husbandry, while not often discussed regarding the predictability of the model, can be highly variable. For example, fish diet, fish rearing conditions, reproductive age, water quality parameters, and genetic background are all factors that can influence how embryos respond to chemical exposure and warrant standardization.

In conclusion, the zebrafish embryo holds great promise as an alternative testing model and has the potential to transform the field of toxicology and chemical screening. The ability to rapidly progress through thousands of chemicals, easily assess developmental malformations, and conduct trans-generational studies in a relatively quick time-frame is precisely what the field of toxicology needs to narrow the many data gaps that exist regarding chemical safety. Despite this promise and the rapid increase of zebrafish work being conducted around the world, there are clear limitations to the model that need to be addressed to enable the broader adoption of zebrafish for toxicological screening.

## References

- Aanes, H., Winata, C.L., Lin, C.H., Chen, J.P., Srinivasan, K.G., Lee, S.G.P., Lim, A.Y.M., Hajan, H.S., Collas, P., Bourque, G., et al. (2011). Zebrafish mRNA sequencing deciphers novelties in transcriptome dynamics during maternal to zygotic transition. *Genome Res.* *21*, 1328–1338.
- Abrams, E.W., and Mullins, M.C. (2009). Early zebrafish development: It's in the maternal genes. *Curr. Opin. Genet. Dev.* *19*, 396–403.
- Al-Hadiya, B. (2005). Niclosamide: Comprehensive Profile. *32*, 67–96.
- Andrews, P., Thyssen, J., and Lorke, D. (1982). The biology and toxicology of molluscicides, Bayluscide. *Pharmacol. Ther.* *19*, 245–295.
- Arora, T., Mehta, A.K., Joshi, V., Mehta, K.D., Rathor, N., Mediratta, P.K., and Sharma, K.K. (2011). Substitute of animals in drug research: an approach towards fulfillment of 4Rs. *Indian J. Pharm. Sci.* *73*, 1.
- Balgi, A.D., Fonseca, B.D., Donohue, E., Tsang, T.C.F., Lajoie, P., Proud, C.G., Nabi, I.R., and Roberge, M. (2009). Screen for Chemical Modulators of Autophagy Reveals Novel Therapeutic Inhibitors of mTORC1 Signaling. *PLOS ONE* *4*, e7124.
- Bal-Price, A.K., Coecke, S., Costa, L., Crofton, K.M., Fritsche, E., Goldberg, A., Grandjean, P., Lein, P.J., Li, A., Lucchini, R., et al. (2012). Advancing the science of developmental neurotoxicity (DNT): testing for better safety evaluation. *ALTEX* *29*, 202–215.
- Bang, P.I., Yelick, P.C., Malicki, J.J., and Sewell, W.F. (2002). High-throughput behavioral screening method for detecting auditory response defects in zebrafish. *J. Neurosci. Methods* *118*, 177–187.
- Behra, M., Cousin, X., Bertrand, C., Vonesch, J.-L., Biellmann, D., Chatonnet, A., and Strähle, U. (2002). Acetylcholinesterase is required for neuronal and muscular development in the zebrafish embryo. *Nat. Neurosci.* *5*, 111–118.
- Bestman, J.E., Stackley, K.D., Rahn, J.J., Williamson, T.J., and Chan, S.S.L. (2015). The cellular and molecular progression of mitochondrial dysfunction induced by 2,4-dinitrophenol in developing zebrafish embryos. *Differentiation* *89*, 51–69.
- Boehmler, W., Obrecht-Pflumio, S., Canfield, V., Thisse, C., Thisse, B., and Levenson, R. (2004). Evolution and expression of D2 and D3 dopamine receptor genes in zebrafish. *Dev. Dyn.* *230*, 481–493.

- Boehmler, W., Carr, T., Thisse, C., Thisse, B., Canfield, V.A., and Levenson, R. (2007). D4 Dopamine receptor genes of zebrafish and effects of the antipsychotic clozapine on larval swimming behaviour. *Genes Brain Behav.* 6, 155–166.
- Bovard, D., Iskandar, A., Luettich, K., Hoeng, J., and Peitsch, M.C. (2017). Organs-on-a-chip: A new paradigm for toxicological assessment and preclinical drug development. *Toxicol. Res. Appl.* 1, 2397847317726351.
- Brockerhoff, S.E., Hurley, J.B., Janssen-Bienhold, U., Neuhauss, S.C., Driever, W., and Dowling, J.E. (1995). A behavioral screen for isolating zebrafish mutants with visual system defects. *Proc. Natl. Acad. Sci.* 92, 10545–10549.
- Broeckling, C.D., Afsar, F.A., Neumann, S., Ben-Hur, A., and Prenni, J.E. (2014). RAMClust: A Novel Feature Clustering Method Enables Spectral-Matching-Based Annotation for Metabolomics Data.
- Cairns, D.M., Boorgu, D.S.S.K., Levin, M., and Kaplan, D.L. (2018). Niclosamide rescues microcephaly in a humanized in vivo model of Zika infection using human induced neural stem cells. *Biol. Open* 7.
- CEHTRA (2012). ECHA Report on Survey of Worldwide CROs: Costs and Practicalities of Two New OECD Guidelines for Testing Chemical Substances.
- Center For Drug Evaluation and Research, F. (1997). Guidance for Industry.
- Chen, M., Wang, J., Lu, J., Bond, M.C., Ren, X.-R., Lysterly, H.K., Barak, L.S., and Chen, W. (2009). The Anti-Helminthic Niclosamide Inhibits Wnt/Frizzled1 Signaling. *Biochemistry* 48, 10267–10274.
- Chen, W., Mook, R.A., Premont, R.T., and Wang, J. (2017). Niclosamide: Beyond an antihelminthic drug. *Cell. Signal.* 41, 89–96.
- Cheng, J.C., Miller, A.L., and Webb, S.E. (2004). Organization and function of microfilaments during late epiboly in zebrafish embryos. *Dev. Dyn.* 231, 313–323.
- Coecke, S., Goldberg, A.M., Allen, S., Buzanska, L., Calamandrei, G., Crofton, K., Hareng, L., Hartung, T., Knaut, H., Honegger, P., et al. (2007). Workgroup Report: Incorporating In Vitro Alternative Methods for Developmental Neurotoxicity into International Hazard and Risk Assessment Strategies. *Environ. Health Perspect.* 115, 924–931.
- Crofton, K.M., Mundy, W.R., Lein, P.J., Bal-Price, A., Coecke, S., Seiler, A.E., Knaut, H., Buzanska, L., and Goldberg, A. (2011). Developmental neurotoxicity testing: recommendations for developing alternative methods for the screening and prioritization of chemicals. *Altex* 28, 9–15.

- Crofton, K.M., Mundy, W.R., and Shafer, T.J. (2012). Developmental neurotoxicity testing: A path forward. *Congenit. Anom.* 52, 140–146.
- Dennis, G., Sherman, B.T., Hosack, D.A., Yang, J., Gao, W., Lane, H.C., and Lempicki, R.A. (2003). DAVID: Database for Annotation, Visualization, and Integrated Discovery. *Genome Biol.* 4, R60.
- DeRenzo, C., and Seydoux, G. (2004). A clean start: degradation of maternal proteins at the oocyte-to-embryo transition. *Trends Cell Biol.* 14, 420–426.
- Domalaon, R., Silva, P.M.D., Kumar, A., Zhanel, G.G., and Schweizer, F. (2019). The Anthelmintic Drug Niclosamide Synergizes with Colistin and Reverses Colistin Resistance in Gram-Negative Bacilli. *Antimicrob. Agents Chemother.* 63, e02574-18.
- Duffié, R., and Bourc'his, D. (2013). Chapter Nine - Parental Epigenetic Asymmetry in Mammals. In *Current Topics in Developmental Biology*, E. Heard, ed. (Academic Press), pp. 293–328.
- Dutta, A., and Sinha, D.K. (2017). Zebrafish lipid droplets regulate embryonic ATP homeostasis to power early development. *Open Biol.* 7.
- Egan, R.J., Bergner, C.L., Hart, P.C., Cachat, J.M., Canavello, P.R., Elegante, M.F., Elkhayat, S.I., Bartels, B.K., Tien, A.K., Tien, D.H., et al. (2009). Understanding behavioral and physiological phenotypes of stress and anxiety in zebrafish. *Behav. Brain Res.* 205, 38–44.
- Espinosa-Aguirre, J.J., Reyes, R.E., and Cortinas de Nava, C. (1991). Mutagenic activity of 2-chloro-4-nitroaniline and 5-chlorosalicylic acid in *Salmonella typhimurium*: two possible metabolites of niclosamide. *Mutat. Res. Lett.* 264, 139–145.
- European Chemical Industry Council (2018). *Facts & Figures*.
- FDA (2015). *The Drug Development Process*.
- FDA, C. for D.E. and (2018). *Guidance, Compliance, & Regulatory Information*.
- Fernandes, T.G., Diogo, M.M., Clark, D.S., Dordick, J.S., and Cabral, J.M.S. (2009). High-throughput cellular microarray platforms: applications in drug discovery, toxicology and stem cell research. *Trends Biotechnol.* 27, 342–349.
- Gallicano, G.I. (2001). Composition, Regulation, and Function of the Cytoskeleton in Mammalian Eggs and Embryos. *Front. Biosci.* 6, 1089–1108.
- Goodarzi, O.D. and M. (2012). In Silico Quantitative Structure Toxicity Relationship of Chemical Compounds: Some Case Studies.

- Grunwald, D.J., and Eisen, J.S. (2002). Headwaters of the zebrafish — emergence of a new model vertebrate. *Nat. Rev. Genet.* *3*, 717–724.
- Gustafson, A.-L., Stedman, D.B., Ball, J., Hillegass, J.M., Flood, A., Zhang, C.X., Panzica-Kelly, J., Cao, J., Coburn, A., Enright, B.P., et al. (2012). Inter-laboratory assessment of a harmonized zebrafish developmental toxicology assay – Progress report on phase I. *Reprod. Toxicol.* *33*, 155–164.
- Gwisai, T., Hollingsworth, N.R., Cowles, S., Tharmalingam, N., Mylonakis, E., Fuchs, B.B., and Shukla, A. (2017). Repurposing niclosamide as a versatile antimicrobial surface coating against device-associated, hospital-acquired bacterial infections. *Biomed. Mater. Bristol Engl.* *12*, 045010.
- Harvey, S.A., Sealy, I., Kettleborough, R., Fenyes, F., White, R., Stemple, D., and Smith, J.C. (2013). Identification of the zebrafish maternal and paternal transcriptomes. *Dev. Camb. Engl.* *140*, 2703–2710.
- Hill, A.J. (2005). Zebrafish as a Model Vertebrate for Investigating Chemical Toxicity. *Toxicol. Sci.* *86*, 6–19.
- Huang, D.W., Sherman, B.T., and Lempicki, R.A. (2009a). Bioinformatics enrichment tools: paths toward the comprehensive functional analysis of large gene lists. *Nucleic Acids Res.* *37*, 1–13.
- Huang, D.W., Sherman, B.T., and Lempicki, R.A. (2009b). Systematic and integrative analysis of large gene lists using DAVID bioinformatics resources. *Nat. Protoc.* *4*, 44–57.
- Ibba, M., and Soll, D. (2000). Aminoacyl-tRNA synthesis. *Annu. Rev. Biochem.* *69*, 617–650.
- Ibba, M., and Söll, D. (2004). Aminoacyl-tRNAs: setting the limits of the genetic code. *Genes Dev.* *18*, 731–738.
- Imperi, F., Massai, F., Pillai, C.R., Longo, F., Zennaro, E., Rampioni, G., Visca, P., and Leoni, L. (2013). New Life for an Old Drug: the Anthelmintic Drug Niclosamide Inhibits *Pseudomonas aeruginosa* Quorum Sensing. *Antimicrob. Agents Chemother.* *57*, 996–1005.
- Irons, T.D., Kelly, P.E., Hunter, D.L., MacPhail, R.C., and Padilla, S. (2013). Acute administration of dopaminergic drugs has differential effects on locomotion in larval zebrafish. *Pharmacol. Biochem. Behav.* *103*, 792–813.
- Jedrzejczak-Silicka, M. (2017). History of Cell Culture. *New Insights Cell Cult. Technol.*

Jesuthasan, S., and Strähle, U. (1997). Dynamic microtubules and specification of the zebrafish embryonic axis. *Curr. Biol.* *7*, 31–42.

Jin, Y., Lu, Z., Ding, K., Li, J., Du, X., Chen, C., Sun, X., Wu, Y., Zhou, J., and Pan, J. (2010). Antineoplastic Mechanisms of Niclosamide in Acute Myelogenous Leukemia Stem Cells: Inactivation of the NF- $\kappa$ B Pathway and Generation of Reactive Oxygen Species. *Cancer Res.* *70*, 2516–2527.

Johnson, M.A., Vidoni, S., Durigon, R., Pearce, S.F., Rorbach, J., He, J., Brea-Calvo, G., Minczuk, M., Reyes, A., Holt, I.J., et al. (2014). Amino Acid Starvation Has Opposite Effects on Mitochondrial and Cytosolic Protein Synthesis. *PLOS ONE* *9*, e93597.

Kane, D., and Adams, R. (2002). Life at the Edge: Epiboly and Involution in the Zebrafish. In *Pattern Formation in Zebrafish*, (Springer, Berlin, Heidelberg), pp. 117–135.

Kane, D.A., and Kimmel, C.B. (1993). The zebrafish midblastula transition. *Development* *119*, 447–456.

Kane, D.A., Hammerschmidt, M., Mullins, M.C., Maischein, H.M., Brand, M., van Eeden, F.J., Furutani-Seiki, M., Granato, M., Haffter, P., Heisenberg, C.P., et al. (1996). The zebrafish epiboly mutants. *Dev. Camb. Engl.* *123*, 47–55.

Keller, R., Davidson, L.A., and Shook, D.R. (2003). How we are shaped: the biomechanics of gastrulation. *Differ. Res. Biol. Divers.* *71*, 171–205.

Kimelman, D., and Schier, A.F. (2002). Mesoderm induction and patterning. *Results Probl. Cell Differ.* *40*, 15–27.

Kimmel, C.B., Warga, R.M., and Schilling, T.F. (1990). Origin and organization of the zebrafish fate map. *Dev. Camb. Engl.* *108*, 581–594.

Kimmel, C.B., Ballard, W.W., Kimmel, S.R., Ullmann, B., and Schilling, T.F. (1995). Stages of embryonic development of the zebrafish. *Dev. Dyn.* *203*, 253–310.

King-Heiden, T.C., Mehta, V., Xiong, K.M., Lanham, K.A., Antkiewicz, D.S., Ganser, A., Heideman, W., and Peterson, R.E. (2012). Reproductive and Developmental Toxicity of Dioxin in Fish. *Mol. Cell. Endocrinol.* *354*, 121–138.

Kirla, K.T., Groh, K.J., Steuer, A.E., Poetzsch, M., Banote, R.K., Stadnicka-Michalak, J., Eggen, R.I.L., Schirmer, K., and Kraemer, T. (2016). Zebrafish Larvae Are Insensitive to Stimulation by Cocaine: Importance of Exposure Route and Toxicokinetics. *Toxicol. Sci.* *154*, 183–193.

- K. Nasrallah, G., Al-Asmakh, M., Rasool, K., and A. Mahmoud, K. (2018). Ecotoxicological assessment of Ti<sub>3</sub>C<sub>2</sub>T<sub>x</sub> (MXene) using a zebrafish embryo model. *Environ. Sci. Nano* 5, 1002–1011.
- Knogler, L.D., and Drapeau, P. (2014). Sensory gating of an embryonic zebrafish interneuron during spontaneous motor behaviors. *Front. Neural Circuits* 8.
- Knogler, L.D., Ryan, J., Saint-Amant, L., and Drapeau, P. (2014). A Hybrid Electrical/Chemical Circuit in the Spinal Cord Generates a Transient Embryonic Motor Behavior. *J. Neurosci.* 34, 9644–9655.
- Kokel, D., Bryan, J., Laggner, C., White, R., Cheung, C.Y.J., Mateus, R., Healey, D., Kim, S., Werdich, A.A., Haggarty, S.J., et al. (2010). Rapid behavior-based identification of neuroactive small molecules in the zebrafish. *Nat. Chem. Biol.* 6, 231–237.
- Kokel, D., Dunn, T.W., Ahrens, M.B., Alshut, R., Cheung, C.Y.J., Saint-Amant, L., Bruni, G., Mateus, R., Ham, T.J. van, Shiraki, T., et al. (2013). Identification of Nonvisual Photomotor Response Cells in the Vertebrate Hindbrain. *J. Neurosci.* 33, 3834–3843.
- de Koning, C., Beekhuijzen, M., Tobor-Kaplon, M., de Vries-Buitenweg, S., Schoutsen, D., Leeijen, N., van de Waart, B., and Emmen, H. (2015). Visualizing Compound Distribution during Zebrafish Embryo Development: The Effects of Lipophilicity and DMSO: COMPOUND DISTRIBUTION IN THE ZEBRAFISH EMBRYO. *Birth Defects Res. B. Dev. Reprod. Toxicol.* 104, 253–272.
- Kuhlmann, J. (1999). Alternative strategies in drug development: clinical pharmacological aspects. *Int. J. Clin. Pharmacol. Ther.* 37, 575–583.
- Kuhlmann, J. (2000). Responsibilities of clinical pharmacology in the early phase of drug development. *Med. Klin. Munich Ger.* 1983 95, 31–40.
- Lai, K., Selinger, D.W., Solomon, J.M., Wu, H., Schmitt, E., Serluca, F.C., Curtis, D., and Benson, J.D. (2013). Integrated Compound Profiling Screens Identify the Mitochondrial Electron Transport Chain as the Molecular Target of the Natural Products Manassantin, Sesquicillin, and Arctigenin. *ACS Chem. Biol.* 8, 257–267.
- Langley, A.R., Smith, J.C., Stemple, D.L., and Harvey, S.A. (2014). New insights into the maternal to zygotic transition. *Development* 141, 3834–3841.
- Lawson, N.D., and Weinstein, B.M. (2002). In Vivo Imaging of Embryonic Vascular Development Using Transgenic Zebrafish. *Dev. Biol.* 248, 307–318.

- Lee, J., and Freeman, J.L. (2014). Zebrafish as a Model for Developmental Neurotoxicity Assessment: The Application of the Zebrafish in Defining the Effects of Arsenic, Methylmercury, or Lead on Early Neurodevelopment. *Toxics* 2, 464–495.
- Lee, M.T., Bonneau, A.R., Takacs, C.M., Bazzini, A.A., DiVito, K.R., Fleming, E.S., and Giraldez, A.J. (2013). Nanog, Pou5f1 and SoxB1 activate zygotic gene expression during the maternal-to-zygotic transition. *Nature* 503, 360–364.
- Lee, S., Son, A.-R., Ahn, J., and Song, J.-Y. (2014). Niclosamide enhances ROS-mediated cell death through c-Jun activation. *Biomed. Pharmacother.* 68, 619–624.
- Legradi, J., Dahlberg, A.-K., Cenijn, P., Marsh, G., Asplund, L., Bergman, Å., and Legler, J. (2014). Disruption of Oxidative Phosphorylation (OXPHOS) by Hydroxylated Polybrominated Diphenyl Ethers (OH-PBDEs) Present in the Marine Environment. *Environ. Sci. Technol.* 48, 14703–14711.
- Lepage, S.E., and Bruce, A.E.E. (2010). Zebrafish epiboly: mechanics and mechanisms. *Int. J. Dev. Biol.* 54, 1213–1228.
- Li, L., Lu, X., and Dean, J. (2013). The Maternal to Zygotic Transition in Mammals. *Mol. Aspects Med.* 34, 919–938.
- Li, P., Shah, S., Huang, L., Carr, A.L., Gao, Y., Thisse, C., Thisse, B., and Li, L. (2007). Cloning and spatial and temporal expression of the zebrafish dopamine D1 receptor. *Dev. Dyn.* 236, 1339–1346.
- Li, Y., Li, P.-K., Roberts, M.J., Arend, R.C., Samant, R.S., and Buchsbaum, D.J. (2014). Multi-targeted therapy of cancer by niclosamide: A new application for an old drug. *Cancer Lett.* 349, 8–14.
- Li, Z., Brecher, M., Deng, Y.-Q., Zhang, J., Sakamuru, S., Liu, B., Huang, R., Koetzner, C.A., Allen, C.A., Jones, S.A., et al. (2017). Existing drugs as broad-spectrum and potent inhibitors for Zika virus by targeting NS2B-NS3 interaction. *Cell Res.* 27, 1046–1064.
- Locke, P.A., and Bruce Myers, D. (2010). Implementing the National Academy’s Vision and Strategy for Toxicity Testing: opportunities and challenges under the U.S. Toxic Substances Control Act. *J. Toxicol. Environ. Health B Crit. Rev.* 13, 376–384.
- Low, L., and Tagle, D. (2017). Microphysiological Systems (“Organs-on-Chips”) for Drug Efficacy and Toxicity Testing. *Clin. Transl. Sci.* 10, 237–239.
- Lu, D., Ma, Z., Zhang, T., Zhang, X., and Wu, B. (2016). Metabolism of the anthelmintic drug niclosamide by cytochrome P450 enzymes and UDP-glucuronosyltransferases: metabolite elucidation and main contributions from CYP1A2 and UGT1A1. *Xenobiotica* 46, 1–13.

- MacLean, B., Tomazela, D.M., Shulman, N., Chambers, M., Finney, G.L., Frewen, B., Kern, R., Tabb, D.L., Liebler, D.C., and MacCoss, M.J. (2010). Skyline: an open source document editor for creating and analyzing targeted proteomics experiments. *Bioinforma. Oxf. Engl.* *26*, 966–968.
- MacRae, C.A., and Peterson, R.T. (2015). Zebrafish as tools for drug discovery. *Nat. Rev. Drug Discov.* *14*, 721–731.
- McGee, S.P., Cooper, E.M., Stapleton, H.M., and Volz, D.C. (2012). Early zebrafish embryogenesis is susceptible to developmental TDCPP exposure. *Environ. Health Perspect.* *120*, 1585–1591.
- Mendelsohn, B.A., and Gitlin, J.D. (2008). Coordination of development and metabolism in the pre-midblastula transition zebrafish embryo. *Dev. Dyn.* *237*, 1789–1798.
- Möller, C., and Slack, M. (2010). Impact of new technologies for cellular screening along the drug value chain. *Drug Discov. Today* *15*, 384–390.
- Mook, R.A., Wang, J., Ren, X.-R., Piao, H., Lysterly, H.K., and Chen, W. (2019). Identification of novel triazole inhibitors of Wnt/ $\beta$ -catenin signaling based on the Niclosamide chemotype. *Bioorg. Med. Chem. Lett.* *29*, 317–321.
- National Academies Press (2007). *Toxicity Testing in the 21st Century: A Vision and a Strategy* (Washington, D.C.: National Academies Press).
- Newton, P.T. (2019). New insights into niclosamide action: autophagy activation in colorectal cancer. *Biochem. J.* *476*, 779–781.
- Pampaloni, F., and Stelzer, E. (2010). Three-dimensional cell cultures in toxicology. *Biotechnol. Genet. Eng. Rev.* *26*, 117–138.
- Pan, J.-X., Ding, K., and Wang, C.-Y. (2012). Niclosamide, an old antihelminthic agent, demonstrates antitumor activity by blocking multiple signaling pathways of cancer stem cells. *Chin. J. Cancer* *31*, 178–184.
- Park, J.P., and Fioravanti, C.F. (2006). Catalysis of NADH $\rightarrow$ NADP $^+$  transhydrogenation by adult *Hymenolepis diminuta* mitochondria. *Parasitol. Res.* *98*, 200.
- Pelka, K.E., Henn, K., Keck, A., Sapel, B., and Braunbeck, T. (2017). Size does matter – Determination of the critical molecular size for the uptake of chemicals across the chorion of zebrafish (*Danio rerio*) embryos. *Aquat. Toxicol.* *185*, 1–10.
- Persson, M., and Hornberg, J.J. (2016). Advances in Predictive Toxicology for Discovery Safety through High Content Screening. *Chem. Res. Toxicol.* *29*, 1998–2007.

- Peterson, R.T., Nass, R., Boyd, W.A., Freedman, J.H., Dong, K., and Narahashi, T. (2008). USE OF NON-MAMMALIAN ALTERNATIVE MODELS FOR NEUROTOXICOLOGICAL STUDY. *Neurotoxicology* 29, 546–555.
- Prather, G.R., MacLean, J.A., Shi, M., Boadu, D.K., Paquet, M., and Hayashi, K. (2016). Niclosamide As a Potential Nonsteroidal Therapy for Endometriosis That Preserves Reproductive Function in an Experimental Mouse Model. *Biol. Reprod.* 95, 74–74.
- Putzer, H., and Laalami, S. (2013). Regulation of the Expression of Aminoacyl-tRNA Synthetases and Translation Factors (Landes Bioscience).
- Raftery, T.D., and Volz, D.C. (2015). Abamectin induces rapid and reversible hypoactivity within early zebrafish embryos. *Neurotoxicol. Teratol.* 49, 10–18.
- Raftery, T.D., Isales, G.M., Yozzo, K.L., and Volz, D.C. (2014). High-content screening assay for identification of chemicals impacting spontaneous activity in zebrafish embryos. *Environ. Sci. Technol.* 48, 804–810.
- Raheem, K.A., El-Gindy, H., and Al-Hassan, J. (1980). Interrelationship of molluscicidal concentration and temperature on the respiration of *Bulinus truncatus*. *Hydrobiologia* 74, 11–15.
- Raies, A.B., and Bajic, V.B. (2016). In silico toxicology: computational methods for the prediction of chemical toxicity. *Wiley Interdiscip. Rev. Comput. Mol. Sci.* 6, 147–172.
- Rajamuthiah, R., Fuchs, B.B., Conery, A.L., Kim, W., Jayamani, E., Kwon, B., Ausubel, F.M., and Mylonakis, E. (2015). Repurposing Salicylanilide Anthelmintic Drugs to Combat Drug Resistant *Staphylococcus aureus*. *PLOS ONE* 10, e0124595.
- Rajendran, V., Kalita, P., Shukla, H., Kumar, A., and Tripathi, T. (2018). Aminoacyl-tRNA synthetases: Structure, function, and drug discovery. *Int. J. Biol. Macromol.* 111, 400–414.
- Reif, D.M., Truong, L., Mandrell, D., Marvel, S., Zhang, G., and Tanguay, R.L. (2015). High-throughput characterization of chemical-associated embryonic behavioral changes predicts teratogenic outcomes. *Arch. Toxicol.* 1–12.
- Ren, X., Duan, L., He, Q., Zhang, Z., Zhou, Y., Wu, D., Pan, J., Pei, D., and Ding, K. (2010). Identification of Niclosamide as a New Small-Molecule Inhibitor of the STAT3 Signaling Pathway. *ACS Med. Chem. Lett.* 1, 454–459.
- Richmond, J. (2002). Refinement, Reduction, and Replacement of Animal Use for Regulatory Testing: Future Improvements and Implementation Within the Regulatory Framework. *ILAR J.* 43, S63–S68.

- Rihel, J., and Schier, A.F. (2012). Behavioral screening for neuroactive drugs in zebrafish. *Dev. Neurobiol.* *72*, 373–385.
- Rossini, G.P., and Hartung, T. (2012). Towards tailored assays for cell-based approaches to toxicity testing. *ALTEX* *29*, 359–372.
- Rusche, B. (2003). The 3Rs and Animal Welfare – Conflict or the Way Forward? *ALTEX* 63–76.
- Rusyn, I., and Daston, G. (2010). Computational Toxicology: Realizing the Promise of the Toxicity Testing in the 21st Century. *Environ. Health Perspect.*
- Sachidanandan, C., Yeh, J.-R.J., Peterson, Q.P., and Peterson, R.T. (2008). Identification of a Novel Retinoid by Small Molecule Screening with Zebrafish Embryos. *PLoS ONE* *3*, e1947.
- Saint-Amant, L., and Drapeau, P. (1998). Time course of the development of motor behaviors in the zebrafish embryo. *J. Neurobiol.* *37*, 622–632.
- Saint-Amant, L., and Drapeau, P. (2000). Motoneuron Activity Patterns Related to the Earliest Behavior of the Zebrafish Embryo. *J. Neurosci.* *20*, 3964–3972.
- Saint-Amant, L., and Drapeau, P. (2001). Synchronization of an Embryonic Network of Identified Spinal Interneurons Solely by Electrical Coupling. *Neuron* *31*, 1035–1046.
- Schymanski, E.L., Jeon, J., Gulde, R., Fenner, K., Ruff, M., Singer, H.P., and Hollender, J. (2014). Identifying Small Molecules via High Resolution Mass Spectrometry: Communicating Confidence.
- Sha, Q.-Q., Zhang, J., and Fan, H.-Y. A story of birth and death: mRNA translation and clearance at the onset of maternal-to-zygotic transition in mammals. *Biol. Reprod.*
- Solnica-Krezel, L. (2002). *Pattern Formation in Zebrafish* (Springer Science & Business Media).
- Solnica-Krezel, L. (2005). Conserved Patterns of Cell Movements during Vertebrate Gastrulation. *Curr. Biol.* *15*, R213–R228.
- Solnica-Krezel, L., and Driever, W. (1994). Microtubule arrays of the zebrafish yolk cell: organization and function during epiboly. *Development* *120*, 2443–2455.
- Souza, I.N.O., Barros-Aragão, F.G.Q., Frost, P.S., Figueiredo, C.P., and Clarke, J.R. (2019). Late Neurological Consequences of Zika Virus Infection: Risk Factors and Pharmaceutical Approaches. *Pharmaceuticals* *12*, 60.

Stackley, K.D., Beeson, C.C., Rahn, J.J., and Chan, S.S.L. (2011). Bioenergetic Profiling of Zebrafish Embryonic Development. *PLOS ONE* 6, e25652.

Strahle, U., and Jesuthasan, S. (1993). Ultraviolet irradiation impairs epiboly in zebrafish embryos: evidence for a microtubule-dependent mechanism of epiboly. *Development* 119, 909–919.

Suliman, M.A., Zhang, Z., Na, H., Ribeiro, A.L.L., Zhang, Y., Niang, B., Hamid, A.S., Zhang, H., Xu, L., and Zuo, Y. (2016). Niclosamide inhibits colon cancer progression through downregulation of the Notch pathway and upregulation of the tumor suppressor miR-200 family. *Int. J. Mol. Med.* 38, 776–784.

Sumner, L.W., Amberg, A., Barrett, D., Beale, M.H., Beger, R., Daykin, C.A., Fan, T.W.-M., Fiehn, O., Goodacre, R., Griffin, J.L., et al. (2007). Proposed minimum reporting standards for chemical analysis. *Metabolomics* 3, 211–221.

Tao, H., Zhang, Y., Zeng, X., Shulman, G.I., and Jin, S. (2014). Niclosamide ethanolamine-induced mild mitochondrial uncoupling improves diabetic symptoms in mice. *Nat. Med.* 20, 1263–1269.

Tharmalingam, N., Port, J., Castillo, D., and Mylonakis, E. (2018). Repurposing the anthelmintic drug niclosamide to combat *Helicobacter pylori*. *Sci. Rep.* 8, 3701.

Tran, U.T., and Kitami, T. (2019). Niclosamide activates the NLRP3 inflammasome by intracellular acidification and mitochondrial inhibition. *Commun. Biol.* 2, 2.

Truong, L., Gonnerman, G., Simonich, M.T., and Tanguay, R.L. (2016). Assessment of the developmental and neurotoxicity of the mosquito control larvicide, pyriproxyfen, using embryonic zebrafish. *Environ. Pollut.* 218, 1089–1093.

US EPA (2017). Annual Report Risk Evaluations.

US EPA (2018). Annual Risk Evaluation Plan.

US EPA, O. (2013a). Federal Insecticide, Fungicide, and Rodenticide Act (FIFRA) and Federal Facilities.

US EPA, O. (2013b). Summary of the Toxic Substances Control Act.

US EPA, O. (2013c). Data Requirements for Pesticide Registration.

US EPA, O. (2015a). About the TSCA Chemical Substance Inventory.

US EPA, O. (2015b). Series 870 - Health Effects Test Guidelines.

US EPA, O. (2016). The Frank R. Lautenberg Chemical Safety for the 21st Century Act.

- Vliet, S.M., Ho, T.C., and Volz, D.C. (2017). Behavioral screening of the LOPAC1280 library in zebrafish embryos. *Toxicol. Appl. Pharmacol.* 329, 241–248.
- Vliet, S.M., Dasgupta, S., and Volz, D.C. (2018). Niclosamide Induces Epiboly Delay During Early Zebrafish Embryogenesis. *Toxicol. Sci.*
- van Vliet, E. (2011). Current standing and future prospects for the technologies proposed to transform toxicity testing in the 21st century. *Altex-Altern. Anim. Exp.* 28, 17.
- Wambaugh, J.F., Hughes, M.F., Ring, C.L., MacMillan, D.K., Ford, J., Fennell, T.R., Black, S.R., Snyder, R.W., Sipes, N.S., Wetmore, B.A., et al. (2018). Evaluating In Vitro-In Vivo Extrapolation of Toxicokinetics. *Toxicol. Sci.* 163, 152–169.
- Weinbach, E., and Garbus, J. (1969). Mechanism of action of reagents that uncouple oxidative phosphorylation. *Nature* 221, 1016–1018.
- WHO (2002). WHO Specifications and Evaluations for public Health Pesticides: Niclosamide.
- Wilson, D.F., Rumsey, W.L., Green, T.J., and Vanderkooi, J.M. (1983). The Oxygen Dependence of Mitochondrial Oxidative Phosphorylation Measured by a New Optical Method for Measuring Oxygen Concentration. *J. Biol. Chem.* 263, 2712–2718.
- Wolpert, L., Tickle, C., and Arias, A.M. (2015). *Principles of Development* (Oxford University Press).
- Xu, M., Lee, E.M., Wen, Z., Cheng, Y., Huang, W.-K., Qian, X., Tcw, J., Kouznetsova, J., Ogden, S.C., Hammack, C., et al. (2016). Identification of small-molecule inhibitors of Zika virus infection and induced neural cell death via a drug repurposing screen. *Nat. Med.* 22, 1101–1107.
- Yartseva, V., and Giraldez, A.J. (2015). The maternal-to-zygotic transition during vertebrate development: a model for reprogramming. *Curr. Top. Dev. Biol.* 113, 191–232.
- Yorke, R.E., and Turton, J.A. (1974). Effects of fasciolicidal and anti-cestode agents on the respiration of isolated *Hymenolepis* mitochondria. *Z. Für Parasitenkd.* 45, 1–10.
- Yozzo, K.L., McGee, S.P., and Volz, D.C. (2013). Adverse outcome pathways during zebrafish embryogenesis: A case study with paraoxon. *Aquat. Toxicol.* 126, 346–354.
- Zakaria, Z.Z., Benslimane, F.M., Nasrallah, G.K., Shurbaji, S., Younes, N.N., Mraiche, F., Da'as, S.I., and Yalcin, H.C. (2018). Using Zebrafish for Investigating the Molecular Mechanisms of Drug-Induced Cardiotoxicity. *BioMed Res. Int.* 2018.

Zanella, F., Lorens, J.B., and Link, W. (2010). High content screening: seeing is believing. *Trends Biotechnol.* 28, 237–245.

Zhu, H., Zhang, J., Kim, M.T., Boison, A., Sedykh, A., and Moran, K. (2014). Big Data in Chemical Toxicity Research: The Use of High-Throughput Screening Assays To Identify Potential Toxicants. *Chem. Res. Toxicol.* 27, 1643–1651.

Zon, L.I., and Peterson, R.T. (2005). In vivo drug discovery in the zebrafish. *Nat. Rev. Drug Discov.* 4, 35–44.